SYSTEMS ANALYSIS OF CARDIOVASCULAR REGULATION

Teză destinată obţinerii
titlului ştiinţific de doctor inginer
la
Universitatea Politehnica Timişoara
în domeniul INGINERIA SISTEMELOR
de către

Ing. Alexandru Codrean

Conducător ştiinţific:	prof.univ.dr.ing. Toma-Leonida Dragomir
Referenţi ştiinţifici:	prof.univ.dr.ing. Ioan Dumitrache
	conf.univ.dr.ing. Levente Kovács
	prof.univ.dr.ing. Adina Aştilean

Ziua susţinerii tezei: 13.05.2015

Seriile Teze de doctorat ale UPT sunt:

1. Automatică
2. Chimie
3. Energetică
4. Ingineria Chimică
5. Inginerie Civilă
6. Inginerie Electrică
7. Inginerie Electronică şi Telecomunicaţii
8. Inginerie Industrială
9. Inginerie Mecanică
10. Ştiinţa Calculatoarelor
11. Ştiinţa şi Ingineria Materialelor
12. Ingineria sistemelor
13. Inginerie energetică
14. Calculatoare şi tehnologia informaţiei
15. Ingineria materialelor
16. Inginerie şi Management

Universitatea Politehnica Timişoara a iniţiat seriile de mai sus în scopul diseminării expertizei, cunoştinţelor şi rezultatelor cercetărilor întreprinse în cadrul Şcolii doctorale a universităţii. Seriile conţin, potrivit H.B.Ex.S Nr. 14 / 14.07.2006, tezele de doctorat susţinute în universitate începând cu 1 octombrie 2006.

România, 300159 Timişoara, Bd. Republicii 9,
Tel./fax 0256 403823
e-mail: editura@edipol.upt.ro

ACKNOWLEDGMENTS

As a chapter of my life closes, I would like to thank all the people who have helped and supported me over the years, and therefore made this work possible.

First and foremost I would like to thank my thesis supervisor Professor Toma-Leonida Dragomir, who has inspired me both scientifically and pedagogically. Professor Dragomir has supported me all the way throughout my work, through constructive ideas and feedback, as well as solutions to the problems where I got stuck. Through his meticulous and rigorous approach, he has pushed me continuously to improve my work. Overall, Professor Dragomir has showed me by example what thoroughly means to be a member of an academic community.

Next, I would like to express my appreciation to Professor Ioan Silea, Head of the Department of Automation and Applied Informatics, who always helped me to overcome each problem that I faced during my stay at the University.

Through Professor Dragomir, I had the fortunate chance to meet Octavian Stefan - a teaching assistant. Over the years, he became my colleague and close friend. During all this time (before and during my PhD studies), we worked together on some problems concerning Networked Control Systems. For this very fruitful scientific collaboration, for his support during my own research studies, and especially for his sincere friendship, I am very grateful to him.

I am grateful to several colleagues from the Department of Automation and Applied Informatics, with whom I had the opportunity to engage in many technical and beyond technical discussions over the years: Bogdan Radac, Cosmin Koch-Ciobotaru, Adrian Korodi, Ana Maria Dan, Alexandra Stinean, Flavius Petcut.

I would like to thank the members of my Ph.D. Committee for accepting to review my thesis and for their help and suggestions concerning my research.

A special thank you goes to my high school mathematics Professor Mihai Big (classus dominus), who guided my professional and personal development during that important period of my life. Professor Big inspired me with a certain work style (even beyond mathematics), and stands out as a role model - both as a professional and as a human being.

Last but not least, I would like to thank my parents Ioan Codrean and Adriana Codrean for their unconditional love and support, my cousin Marius Todoran and his wife Cristina Todoran, and to one of my best friends Vlad Ghise.

This work was partially supported by the strategic grant POSDRU/159/1.5/S/137070 (2014) of the Ministry of National Education, Romania, co-financed by the European Social Fund – Investing in People, within the Sectorial Operational Programme Human Resources Development 2007-2013.

Timisoara, May 2015 Alexandru Codrean

This thesis is dedicated to my parents.

Codrean, Alexandru

Systems analysis of cardiovascular regulation

Teze de doctorat ale UPT, Seria 12, Nr. 15, Editura Politehnica, 2015, 100 pagini, 27 figuri, 4 tabele.

ISSN: 2068-7990

ISBN: 978-606-554-951-7

Cuvinte cheie:

cardiovascular system, cardiovascular regulation, averaged system, nonlinear system, time delays, stability, robustness.

Rezumat,

The PhD thesis is focused on systems analysis of cardiovascular regulation. In the first part of the thesis, an averaged model of cardiovascular regulation on short term (i.e. for the cardiovascular system along with its nervous control loop) is derived. A weighted averaging approach is proposed for the cardiovascular system, and the obtained averaged model is coupled with a simplified model for the baroreflex control mechanism. In the second part of the thesis, the averaging approach is generalized for a class of nonlinear systems - pulse-frequency modulated systems with constant duty ratios- whose trajectories exhibit a moving average dependent on the modulation period. The proposed averaging method leads to a period-dependent averaged model, simpler than the original one. The cardiovascular system, regarded as a pulse-frequency modulated system, is considered as a case study. The third part of the thesis addresses the stability analysis problem for the qualitative averaged model of cardiovascular regulation, focusing on deriving new insights on the role of time delays in generating stability or instability, along with assuring some global properties, like trajectory convergence and boundedness. Finally, all results are tested through simulations.

TABLE OF CONTENTS

TABLE OF FIGURES

LIST OF SYMBOLS AND NOTATIONS

$\mathbf{I}$	identity matrix
$\mathbf{0}$	zero matrix
$\mathbf{x}$	state vector
$\mathbf{u}$	input vector
$\mathbf{y}$	output vector
$\mathbf{x}_e$	equilibrium point
τ	time delay
V	Lyapunov function
$\|\| \cdot \|\|$	norm of a vector
Re(z)	real part of a complex variable z
Im(z)	imaginary part of a complex variable z
$O(\cdot)$	order of magnitude notation
sup	supremum
T	heart period
HR	hear rate
P_{sa}	systemic arterial pressure
det(A)	determinant of a matrix A
rank(A)	rank of a matrix A
D	discriminant
R	resultant
s	complex operational variable
t	time

1. INTRODUCTION

Medicine has historically evolved from art to science, and from data or knowledge accumulation to decrypting and understanding the complexity of living organisms. In this quest, interdisciplinary and multidisciplinary is no longer just an option, but a requirement - different other scientific branches interfere (besides the classical ones - chemistry, physics, biology), like engineering and mathematics. Concomitantly, the problem of arriving at a holistic view becomes more and more pressing, thus leading to the use of notions and tools from systems theory for understanding how an organism functions as a whole[1].

Thus clinical medicine, chemical and physical experiments, mathematical modeling, biomedical instrumentation (done by engineers), are no longer enough – the need of an integrative approach has started to be felt more and more – from diagnosis to treatments, from epidemics to genetics. Systems theory makes use of experimental data, pure theories, instrumentation, and wraps them together in functional interpretations of how a living organism acts as a system, with inputs and outputs, controls and disturbances, a given role, and finally tries to give predictions of how the systems will behave (dynamically) in time and how it will react in certain scenarios.

It is in human nature that once something is analyzed and understood (to a certain degree) to further try to control it. Thus, as a natural continuation to systems theory, control theory provides a theoretical framework with tools for controlling different types of systems. Of course that the problem of controlling biomedical systems is more delicate (e.g. sometimes it is not ethical or simply not possible), but it still an important chapter, for example in treatment options - from drugs to surgery. An alternative approach is to do some kind of reverse engineering, that is to study the existing (biological/physiological) control mechanisms (homeostasis), and to understand how they function (work), which eventually not only helps in deriving better diagnosis and treatments, but it also permits engineers to develop so called 'biologically inspired' algorithms for technical systems (man made systems).

The present research study takes a few first steps in this direction, more exactly in the systems analysis of biomedical systems.

1.1. Motivation and Aims

Contemporary medicine is dealing with more and more problems which have reach a level of complexity that imposes an interdisciplinary approach. Such an approach should integrate - for example - aspects from natural science and biological sciences with exact sciences and engineering. This is how the birth of biomedical engineering[2] occurred. Because of the high potential it has in improving

[1] It should be mentioned that we assume that a systems approach to living organism is possible in the simplifying circumstances where one ignores free will and any type of consciousness intervention.

[2] A comprehensive book on the main areas of biomedical engineering is [23].

the quality of human life, the field has been regarded as one with high priority in the framework of different international research strategies – in Europe through the program *Virtual Physiological Human* (*VPH*) ([9]), at a global level through *IUPS Physiome Project* ([10]), or other programs in Biotechnologies etc.

Because for understanding the dynamics of (patho-) physiological or biological phenomena, on one hand, different mathematical models have been developed and used over the years, and on the other hand, for understanding homeostasis mechanisms of living organisms elements from systems theory and control theory have been addressed, in the field of (automatic) control a new applicative area has emerged: modeling and control of biomedical systems. An increasing interest in this research direction has been pointed out in reports of important scientific communities (societies) like the *Society of Industrial and Applied Mathematics* (SIAM) - [6] - and the *Control Systems Society of the Institute of Electrical and Electronics Engineers (IEEE CSS)* - [7]. Additionally, at the *International Federation of Automatic Control* (IFAC), there exists a technical committee exactly on this domain of research - *IFAC Technical Committee 8.2 Biological and Medical Systems* – which organizes international conferences exclusively on this topic. Finally, different highly regarded control conferences (like the *IFAC World Congress*, *IEEE Control and Decision Conference*), or high impact control journals (like *Control Engineering Practice*, *IEEE Transactions on Control Systems Technology, IEEE Transactions on Automatic Control, Automatica*) have scientific sessions, respectively special issues or articles, dedicates to this research area.

One problem of prime interest in biomedical engineering refers to understanding the control mechanisms of the cardiovascular system (especially on short term, but also on long term), because cardiovascular diseases still represent the main cause of mortality in the world ([22]). Over the last two decades, an increasing number of research groups focus on the development of mathematical models for the cardiovascular system, along with its associated nervous control mechanisms, in order to improve the understanding of physiological and pathological phenomena.

In this context, the present study aims to bring an important contribution to the understanding of the control mechanism that act on the cardiovascular system, based on the systems analysis of the closed loop dynamics of cardiovascular regulation in respect with different disturbance scenarios. Such a study implies the use of mathematical models as simple as possible, stability analysis studies in connections with different (possible) pathologies, and robustness analysis. Furthermore, we will focus especially on the role of (multiple) time delays in generating stability or instability (local and global perspective)[3].

Systems analysis of cardiovascular regulation represents a complex task, due to the strong nonlinearities, large dimensionality and high variability of the models proposed in the literature. So, although there are a large number of models

[3] Time delay systems have been studied intensively in the last decades. Although the role of time delays in physiological systems has been pointed out relatively early (e.g. [28], [29]), such studies – which can also be connected to practice - are still in an incipient phase. For a recent review on the analysis and modeling of time delays in physiological systems see [32].

used in the literature, most analysis studies resume only to simulation results[4] (and comparisons with experimental data), which can not give but a particular image of the dynamic behavior. In order to get a more complete picture of the dynamics of cardiovascular regulation, (quasi-) analytical analysis studies are imperiously needed. Such studies lead not only to better understanding and prediction, but open the door to model based synthesis or design studies – like the design of model based nonlinear state observers which estimate physiological variables that are not measurable non-invasively (thus providing possible new clinical indicator for diagnosis)[5], or the design of (artificial) controllers for different types of assisting devices[6].

1.2. Biomedical systems and cardiovascular regulation

The connections between systems theory and control theory with biological (physiological) systems and biotechnology can be traced back to the early works of Claude Bernard (the milieu interieur), Walter Cannon (homeostasis) and Norbert Wiener (cybernetics) - ([7], pp. 57-67). The filed that encompasses the modeling, analysis and control of biomedical systems has emerged as one of high priority, while the (potential) impact on healthcare is only recently noticed and highlighted ([14] - Part H *Automation in Medical and Healthcare System*)[7]. From all the particularities of biomedical systems, in respect with the systems usually encountered in classical process control, that make the research to evolve on a gentle slope, we can mention: high variability between physical (biological) systems from the same class (species), complex and high dimensional systems that are only partially known and understood (structural uncertainty), difficult process of translating theoretical results to clinical practice (time and cost demanding clinical trials), communication difficulties between engineers and medical doctors (or control scientists and theoretical biologists), ethical issues (e.g. organ donation, artificial life support), and so on. Needless to say that, due to the possible (high & wide) impact on human life, the filed of biomedical systems is reporter as a grand challenge in many scientific communities (e.g. National Academy of Engineering [37]).

In our present study, we are not such much interest in analyzing the artificial (external) control of biomedical systems, but in the intrinsic control that biological (physiological) systems already posses. Such control mechanisms, that make homeostasis possible, have been put forward by scientists several decades ago (e.g. [18], [21])[8]. It is now generally accepted that the human body has many physiological control mechanisms that make sure that the organism is maintained under certain physiological limits, which ensure a stable behavior, around a certain equilibrium point or on a stable limit cycle. Of course all these control mechanisms

[4] As far as we know, the only exceptions are the works of [30] and [31]. However, the analysis from [30] uses an oversimplified model, while both studies consider only the single delay case (local analysis). In contrast, our study makes uses of a more realistic qualitative model, approaches the multiple delays case, along with determining some global properties of cardiovascular regulation. Additionally, the methods used in our analysis study are easily scalable to more complex (complete) models of cardiovascular regulation.
[5] See for example [24], [25], [26].
[6] E.g. a controller for a left ventricle assisting device (LVAD) – [27].
[7] The need for more systems and control theory in medicine has been pointed out also in [33], [34] and [35].
[8] And more recently in [11].

interact with each other, but because the entire human organism is very hard to grasp as a single complex model, most mechanisms are studied independently, usually being studied only for certain well defined scenarios ([36]). That means an implicit separability based approach that is not generally true.

One of the most studied systems of the human body is the cardiovascular system, as it plays a crucial role in complex living organisms, explaining also the high mortality rate encountered in cardiovascular diseases. Global control mechanisms of the cardiovascular system act on short-term (minutes) or long-term (hours, days) on the entire system (human body) to maintain appropriate blood flow, while these mechanisms are supplemented by local mechanisms in each vascular region[9]. Finally, hierarchical supervisory control also interferes and adapts the function of the lower level control mechanisms, making the entire system even more complicated to analyze.

Long-term control of the cardiovascular system refers primary to hormonal control mechanisms, while short-term control refers to nervous control mechanisms ([38], [5]). Here, we will resume only to nervous control mechanisms, which are more deeply understood. The main control strategies encountered in general in physiological systems, and in particular in cardiovascular regulation, can be synthesized schematically as in Fig. 1.1 ([12]). The controlled system (or process) has a control input, a disturbance input[10] and a controlled output. Although not depicted in the figure, the controlled system can possess local auto-regulation mechanisms[11]. Usually, the principal control mechanism is thorough feedback, but there can be multiple feedback mechanisms that act simultaneously with different strength of impact on the overall control[12]. The feedforward controller detects an external stimulus or disturbance, and influences the feedback controller accordingly, in order to somehow compensate the effect of the disturbance[13]. Finally, an adaptive controller intervenes and changes the way the other controllers operate, as dictated by (higher) nervous centers[14]. The higher nervous centers in turn can change the reference input in relation to numerous other factors.

Despite this hierarchical overview of physiological control (and in particular cardiovascular regulation), the entire "design" operates optimally in a certain sense, by ensuring a trade off between stability, performance and robustness. For example it may be more important to have robust stability than to impose a small control

[9] The complexity of cardiovascular regulation is thus given by the presence of multiple control mechanisms that act simultaneously on different time scales ([13]).
[10] The disturbance can refer to the action of an external stimulus (ex. work, movement), to a pathological agent (e.g. virus, injury), or even the interconnection with other systems within the human body (e.g. the interconnection between the respiratory system and the cardiovascular system).
[11] In particular, for the cardiovascular system, this refers to the intrinsic or local control of peripheral blood flow ([8], pp. 383–386).
[12] For the cardiovascular system, the baroreflex is the most important (short-term) feedback control mechanism, but other feedback control mechanisms are present, like the cardiopulmonary reflex ([17]).
[13] Sometimes the feedforward action is directly on the controlled system, bypassing the feedback controller, as it is in the case of the vestibular sympathetic reflex, which responds to orthostatic stress ([17]).
[14] Such adaptive response can be caused, for example, by an emotional response of the subject (like extreme fear), and can be depicted systemically only for a priori fixed scenarios.

error. Additionally, energy factors are included through multiple limitations on the control signals.

Next, although cardiovascular regulation, as any other physiological control system, has multiple control mechanisms (as previously discussed), throughout our study we will restrict our analysis to the main feedback control mechanism acting on short term: the baroreflex mechanism. Consequently, our control loop reduces to the one from Fig. 1.2.

The baroreflex mechanism acts as an output feedback controller, by measuring the systemic arterial pressure (the output or controlled variable), and commanding the heart rate, heart contractility, systemic peripheral resistance and venous unstressed volume ([39]). Thus, we are dealing with a single input – multiple output feedback controller.

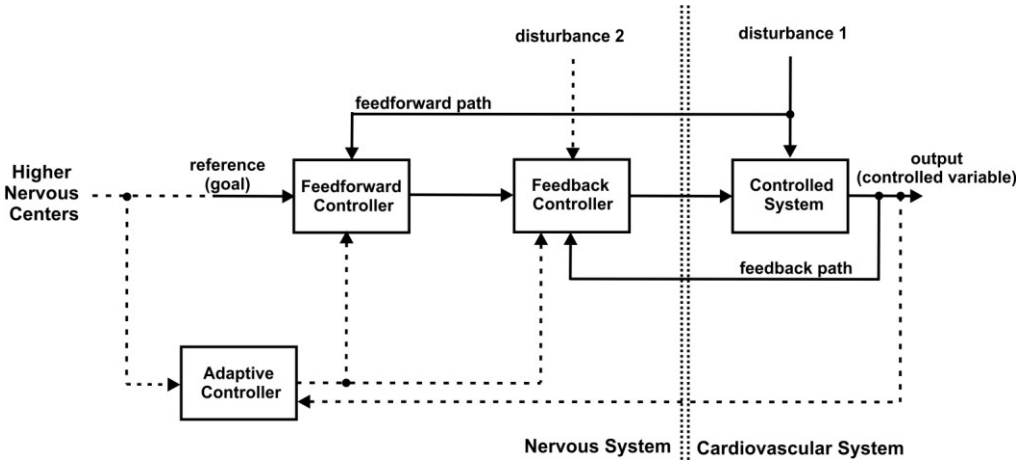

Fig.1.1. Control strategies in physiological systems (in particular cardiovascular regulation) – adapted from [12].

The measurements are done by the baroreceptors (stretch receptors placed on the arteries), which transmit nervous impulses (signal modulation) to the nervous system (more exactly to the medulla oblongata). The generated control signals are then sent (again as nervous impulses) thorough the peripheral nervous system[15] (divided into a sympathetic and parasympathetic subsystem) to the cardiovascular system. Through the expression – baroreflex feedback mechanism – we will further refer to all this components.

The controlled system (process) for the baroreflex feedback mechanism is the cardiovascular system. The cardiovascular system is composed out of the heart system and the circulatory system (schematically depicted in Fig. 1.3).

[15] Here is where time delays (transport delays) appear on each control path. Different pathologies at the level of the peripheral nervous system can alter these time delays: Autonomic peripheral neuropathy ([41]), Guillain-Barré syndrome ([40]), Diabetic neuropathy ([42]).

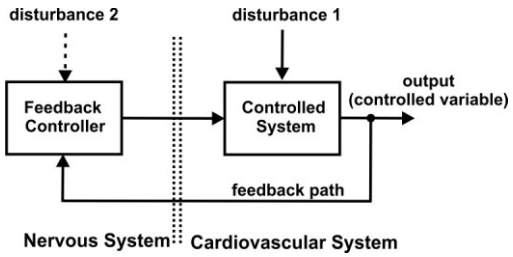

Fig.1.2. Simplified view of cardiovascular regulation (baroreflex feedback control mechanism).

The heart is composed out of a left side (which pumps blood into the systemic circulation) and a right side (pumps blood into the pulmonary circulation). Each side presumes an atrium, a valve, a ventricle and a final output valve. The blood accumulates in the atrium, and when the atrioventricular valve opens it fills the ventricle (the period of the cardiac cycle called diastole). After the atrioventricular valve closes, the ventricle starts contracting, the output valve opens and the blood is ejected into the arteries (the period of the cardiac cycle called systole)[16].

The heart pumps the blood through the circulation. The circulation transports nutrients to body tissues and gets rid of waste product ([4]), and it is divided into the systemic circulation and the pulmonary circulation (Fig. 1.3). Each circulation in turn is composed out of arteries (large high pressure vessels), capillaries (small low pressure vessels), and veins (large high volume vessels)[17]. The systemic circulation ensures appropriate blood flow to all the tissues except the lungs (at the capillary level oxygen is transferred to the tissue). The pulmonary circulation transport blood the lungs and back to the heart (at the capillary level carbon dioxide is transferred to the tissue).

Although both the systemic and pulmonary circulations are clearly distributed systems, usually a compartmental (lumped) approach is used in describing the part of each circulation: arterial compartment (large arteries), peripheral compartment (small arteries, capillaries, small veins), and venous compartment (large veins).[18]

[16] See [5] for a more detailed physiological description, along with suggestive graphical illustrations.
[17] Each side of the heart (left, right) pumps the blood received from the main veins into the main arteries through repeated, rhythmic contractions (cardiac cycle).
[18] Similarly with many other studies from the literature which focus on short term control mechanisms for the cardiovascular system, in the present study, our main interest is what happens at the heart level.

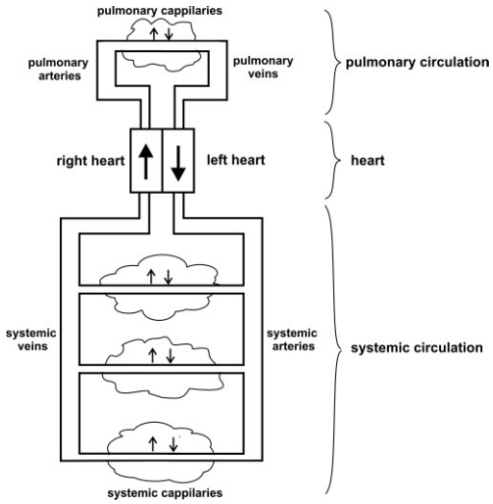

Fig.1.3. The cardiovascular system (heart and circulation) – schematic physiological representation

Finally, throughout the thesis, we considered as reference textbooks in matters of basic physiology the works of Berne & Levy ([8]), Guyton ([4]), respectively Silbernagl & Despopoulos ([5]).

1.3. Analysis of nonlinear systems

A *system* represents an ensemble of interconnected objects with a clear given role, and well defined in respect with the exterior environment ([16]). The systems dynamics may be reported to time *(time driven systems*) or events (*event driven systems*)[19]. Let us focus further on time driven systems, which can be further divided into *discrete time systems* and *continuous time systems*. If for (control) design, a discrete time approach can be adopted, for systems analysis, the continuous time domain approach is the most common[20]. In continuous time, dynamics systems are described quantitatively through mathematical models, more exactly through systems of differential equations.

The principle of superposition tells us if a dynamical system is linear or nonlinear. *Linear systems* respect the superposition principle, and can be characterized by a system of linear differential equations, which is usually represented under the canonical form[21] ([15], [16])

$$\begin{cases} \dot{\boldsymbol{x}}(t) = \boldsymbol{A}\boldsymbol{x}(t) + \boldsymbol{B}\boldsymbol{u}(t) \\ \boldsymbol{y}(t) = \boldsymbol{C}\boldsymbol{x}(t) + \boldsymbol{D}\boldsymbol{u}(t) \end{cases}, \tag{1.1}$$

[19] The presents study deals only with lumped parameters systems, as a simplified approach to what in reality are distributed parameters systems (like the cardiovascular system) – i.e. systems dynamics dependes on a certain space distribution also.
[20] Most real (physical) systems are continuous in nature. However, when the nature of the real systems is discrete (e.g. digital electronics, computer networks), the analysis has to be done also in discrete time.
[21] Such a system is called a linear time invariant continuous time system.

where **u** is the input of the system, **y** is the output, and **x** are referred to as states[22] of the systems. **A**, **B**, **C** and **D** are constant matrices with appropriate dimensions. However, most real (physical) systems are nonlinear in nature[23], and do not respect the principle of superposition. *Nonlinear systems* can only be rigorously depicted as systems of nonlinear differential equations of the general form ([1])

$$\begin{cases} \dot{\boldsymbol{x}}(t) = \boldsymbol{f}\big(t, \boldsymbol{x}(t), \boldsymbol{u}(t)\big) \\ \boldsymbol{y}(t) = \boldsymbol{h}\big(t, \boldsymbol{x}(t), \boldsymbol{u}(t)\big) \end{cases}, \tag{1.2}$$

with **f** and **h** as vector functions[24]. A nonlinear system can exhibit different types of complex dynamic behaviors, that a linear systems can not – like *finite escape time*, *multiple equilibrium points*, *limit cycles*, bifurcations, *chaos*, and so on ([1]).

For linear systems, the main exception of systems which can not be embedded to the form (1.1), are linear time delay systems – which may have the form ([43])

$$\begin{cases} \dot{\boldsymbol{x}}(t) = \boldsymbol{A}\boldsymbol{x}(t) + \boldsymbol{A}_d\boldsymbol{x}(t-\tau) + \boldsymbol{B}\boldsymbol{u}(t) \\ \boldsymbol{y}(t) = \boldsymbol{C}\boldsymbol{x}(t) + \boldsymbol{D}\boldsymbol{u}(t) \end{cases}, \tag{1.3}$$

where τ is the time delay. If there are more than one time delays (τ_1,τ_2,…), we have more than one matrix $\mathbf{A}_d$ (i.e. $\mathbf{A}_{d1}$, $\mathbf{A}_{d2}$…). For nonlinear systems, although there are several classes of dynamical systems that can not be framed by (1.2), we will mention just two exceptions (which are more relevant to our present study): non-autonomous nonlinear time delay systems of the form

$$\begin{cases} \dot{\boldsymbol{x}}(t) = \boldsymbol{f}\big(t, \boldsymbol{x}(t), \boldsymbol{x}(t-\tau), \boldsymbol{u}(t)\big) \\ \boldsymbol{y}(t) = \boldsymbol{h}\big(t, \boldsymbol{x}(t), \boldsymbol{u}(t)\big) \end{cases}, \tag{1.4}$$

and non-autonomous switched systems of the form

$$\begin{cases} \dot{\boldsymbol{x}}(t) = \boldsymbol{f}_{\sigma(t)}\big(t, \boldsymbol{x}(t), \boldsymbol{u}(t)\big) \\ \boldsymbol{y}(t) = \boldsymbol{h}\big(t, \boldsymbol{x}(t), \boldsymbol{u}(t)\big) \end{cases}, \tag{1.5}$$

where σ is the (exogenous) switching signal[25]. Again, if there are more than one time delays, we have additional terms in the function **f** from (1.4) – $\mathbf{x}(t-\tau_1)$, $\mathbf{x}(t-\tau_2)$, and so on.

Let us move on to analysis methods, with a focus on *stability*[26]. The analysis of linear systems of the form (1.1) is well known (classical). In short, the stability is

---

[22] Usually denote accumulation of energy.
[23] Engineers most often use linear systems as approximations of the nonlinear systems near nominal operating points.
[24] As a common notation convention, we will in the future drop the time dependency of the variables, in order to ease readability. It will result from context if a variable varies in time or not.
[25] The switching signal can take positive natural values 1, 2, 3,…,n, corresponding to the selection of a particular function $\mathbf{f}_1$, $\mathbf{f}_2$, $\mathbf{f}_3$…,$\mathbf{f}_n$. Thus, we are dealing actually with a variable structure system.
[26] A system is considered stable in respect with an equilibrium point (or nominal trajectory) if when the system starts near this point (or trajectory) it remains nearby (in its vicinity), despite possible perturbations.

dictated by the location of the eigenvalues of the matrix **A** in respect with the complex plane: instability occurs if there are eigenvalues in the right half plane.

The analysis of linear time delays systems of the form (1.3) already introduces significant complications. For the single delay case, several techniques have been proposed in the literature, from distribution of characteristic roots[27] (analytical or numerical methods) and Nyquist plots (or other types of frequential approaches), to matrix pencils and algebraic transformations, and even to Lyapunov (like) approaches (see [44], [46], [45], [43], along with the reference therein). Current research directions focus on the case when the time delay is time varying (e.g. [47]), or on the multiple delay case (e.g. [43]), but most methods proposed are either conservative (only sufficient stability conditions) or computationally demanding (even infeasible at the present computational capabilities). In respect with multiple delay linear systems, there are relatively few methods that provide feasible (practical) necessary and sufficient conditions (like in [48]).

If classical systems theory has set forth the tools for analyzing linear systems, modern systems theory is mainly concerned with nonlinear systems. However, for nonlinear systems analysis there are no general methods, i.e. methods that work on all types of nonlinear systems. Instead, the tools from nonlinear systems analysis work on certain classes of nonlinear systems. Moreover, in contrast to linear systems, these tools usually lead to sufficient only stability conditions, and thus the results can be quite conservative[28]. If one is interested in the local behavior of the nonlinear system around an equilibrium point, the linearization method (also called Lyapunov's indirect method) is often used for obtaining a linear system that approximates the nonlinear systems near the equilibrium point. As an example, for a nonlinear system described by the state equations

$$\dot{\boldsymbol{x}} = \boldsymbol{f}(\boldsymbol{x}, \boldsymbol{u}), \tag{1.6}$$

and an equilibrium point $\mathbf{x}_e=\mathbf{0}$ (i.e. $\mathbf{f}(\mathbf{0},\mathbf{0})=\mathbf{0}$), the state equation of the linearized system is

$$\dot{\boldsymbol{x}} = \underbrace{\left(\left. \frac{\partial \boldsymbol{f}}{\partial \boldsymbol{x}} \right|_{\boldsymbol{x}=\boldsymbol{0},\boldsymbol{u}=\boldsymbol{0}} \right)}_{\boldsymbol{A}} \boldsymbol{x} + \underbrace{\left(\left. \frac{\partial \boldsymbol{f}}{\partial \boldsymbol{u}} \right|_{\boldsymbol{x}=\boldsymbol{0},\boldsymbol{u}=\boldsymbol{0}} \right)}_{\boldsymbol{B}} \boldsymbol{u} . \tag{1.7}$$[29]

When linearization is not possible ([1]), or one is interested in the global behavior of the nonlinear system, Lyapunov's direct method is most often employed. For an autonomous nonlinear system of the form

$$\dot{\boldsymbol{x}} = \boldsymbol{f}(\boldsymbol{x}), \tag{1.8}$$

---

[27] The characteristics roots of (1.1), respectively (1.3), are the solutions of the equation $\det(s\mathbf{I}-\mathbf{A})=0$, respectively $\det(s\mathbf{I}-\mathbf{A}-\mathbf{A}_d e^{-\tau s})=0$, with s as a complex variable and $\mathbf{I}$ as the unitary matrix.

[28] In most cases, if a certain analysis method fails or can not conclude that the system is stable, this does not imply that the system is unstable. Moreover, even when one knows a domain in which the system is stable, he can not know how this domain relates to the real stability domain – which can be larger than the one found (and thus the conservative results).

[29] First order Taylor series.

the method implies the use of a Lyapunov function (scalar energy-like function) $V(\mathbf{x})$ [30]: if this positive definite function decreases in time (negative semi-definite time derivative), then the equilibrium point is stable in the sense of Lyapunov ([2], [1]). If $V(\mathbf{x})$ is radially unbounded (i.e. $V(\mathbf{x})\rightarrow\infty$ as $||\mathbf{x}||\rightarrow\infty$), then the stability is global ([1]). The entire problem is how to find such a function for a given nonlinear system. Although some approaches for finding Lyapunov functions have been proposed (see [2]-ch. 3, [1]-ch4), these work only on certain classes of nonlinear systems[31]. There are no general ways of finding Lyapunov functions that work for all categories of nonlinear systems.[32]

An alternative to the internal (Lyapunov) stability based approaches is to focus on the input-output dynamics, and ignore what happens to the states of the systems (black box approach). A systems is stable in the input-output sense if small inputs lead to correspondingly small outputs ([3]-vol. 3-ch. 44). Passivity theory, finite gain stability (L_2), bounded-input-bounded-output and the small gain theorem: all these provide valuable tools for input-output stability analysis (see [1]-ch 5, [3]-vol. 3-ch. 44). The possibility of separating the linear part from the nonlinear part (usually static or memoryless) leads to particular stability criteria like the Circle Criterion and Popov Criterion. Either way, in many cases one eventually makes use of Lyapunov-like arguments[33].

More recently, the input-to-state stability paradigm has been developed, which sits at the intersection of internal stability and input-output stability ([3]-vol. 3-ch. 45). Such an approach is useful when, for a nonlinear system like (1.6), we want to determine stability in respect with the input **u**. Ultimately, such methods resume again to Lyapunov functions, but this time the stability conditions are dependent on the domain of variation of the input **u** (see [3]-vol. 3-ch. 45 and [1]-ch. 4.9**)**.[34]

The stability of nonlinear time delay systems – of the form (1.4) for example - is extremely complex. There are very few stability methods in the literature which address such systems, capable of global results. Of course, there are extensions of Lyapunov theory even here – Lyapunov functionals: Krasovskii or Razumikhin type ([45]) - but this makes the task of finding an appropriate Lyapunov functional for a specific nonlinear system even more difficult. Most analysis studies resume to local stability analysis via linearization[35]. An exception is

---

[30] For non-autonomous systems, i.e. when $\dot{\boldsymbol{x}} = \boldsymbol{f}(t, \boldsymbol{x})$, more complex function have to be used - $V(\mathbf{x},t)$, and the stability conditions are more restrictive: uniformity in respect with an initial time t_0 ([1]), V must be decrescent (i.e. dominated by a time-invariant positive definite function: $V(\mathbf{x},t)\leq V_1(\mathbf{x})$) - [2].

[31] As a more recent example, a computational approach has been proposed in [50] to finding Lyapunov functions for a class of nonlinear systems called polynomial systems.

[32] Of course that a physical insight of the system can help (guide) in finding a Lyapunov function ([2]-ch 9, [51])

[33] Passivity theory makes use of so called storage functions, which represent generalizations of Lyapunov functions.

[34] Although in applied mathematics one can also find other stability approaches, our presentation revolves around Lyapunov-like approaches because, according to our knowledge, these are the most often encountered in control engineering practice.

[35] Especially in fields like mathematical biology, where models can not easily fit into a standard class of nonlinear systems.

the recent work from [49], which developed a computational approach to finding such Lyapunov functionals for polynomial time delays systems.

Switched systems of the from (1.5) are encountered in practice when, along the continuous dynamics, discrete events appear (e.g. a valve, a thermostat, a power switch) - [53]. This complicates the analysis by introducing discontinuities[36]. However, a particular class of switched systems – switched linear systems – has been intensively studied in the last two decades due to its high applicability and efficient computational tools for analysis ([52]). As example, for (1.5) one can use multiple Lyapunov function V_i (one for each subsystem selected by the switching function σ) – [3]-vol. 3-ch.30, and if (1.5) is reduced to a switched linear system of the form

$$\dot{\boldsymbol{x}} = \boldsymbol{A}_{\sigma(t)}\boldsymbol{x}\,, \tag{1.9}$$

then the stability can be assed through a piecewise quadratic Lyapunov function $V_i=\mathbf{x}^T\mathbf{P}_i\mathbf{x}$, with *i* as the index of given subsystem selected by the switching function σ ([3]-vol. 3-ch.30, [52]). The stability conditions for (1.9) can be expressed as linear matrix inequalities (LMIs), for which efficient computational tools already exist.[37]

Finally, throughout the thesis, we considered as reference textbooks in matters of linear systems theory the works from [15] and [16], for nonlinear systems theory the works from [1] and [2], and for control theory in general the extensive handbook [3]. The computational part of the theoretical methods used and the numerical results obtained, were all done in Matlab ([19]) and/or Maple ([20]).

1.4. Thesis organization

The thesis is structures in five chapters. The current chapter - Chapter 1 – has provided a short introduction into the motivation of the study, features of biomedical systems and in particular cardiovascular regulation, and presented some of the main categories of nonlinear systems along with the tools to study (analyze) them.

In Chapter 2 a model for cardiovascular regulation is built based on cardiovascular and baroreflex models from the literature, and a simplified averaged model is finally derived. At the end of Chapter 2 the obtained model is validated on a pathological scenario in comparison with experimental data from the literature.

Because the averaging method used in Chapter 2 is new, Chapter 3 provides a theoretical framework for the averaging method. The theoretical framework extends the applicability of the new averaging method to an entire class of nonlinear systems.

---

[36] In some cases, switched systems are used to approximate more complicated nonlinear systems: switching behavior can be viewed as an approximation of a more complex dynamics, but which occurs on a very small time span in respect with the dynamics of the whole system (so small that it can be neglected).

[37] LMIs can be solved thorough convex optimization ([54]).

The stability analysis of cardiovascular regulation is the object of Chapter 4. The first part of the chapter deals with the local analysis via linearization, with the focus on the role of multiple time delays. The second part of the chapter deals with global analysis via contraction theory, with a focus on robustness. Each part of Chapter 4 ends with some numerical results and a discussion.

The final chapter – chapter 5 – points out some final conclusions, highlights the main contributions of the thesis, and presents some oportunities for future work.

1.5. Publications

The publications during my PhD studies consist in the following published and submitted articles:

- Stefan O., **Codrean A.**, Dragomir T.-L., "A Network Control Structure with a Switched PD Delay Compensator and a Nonlinear Network Model", American Control Conference (ACC), Washington, USA, 2013, pp. 758-764. (IEEE Xplore, ISI).
- **Codrean A.**, Dragomir T.-L., "Averaged modeling of the cardiovascular system", IEEE 52nd Annual Conference on Decision and Control (CDC), Florence, Italy, 2013, pp. 2066-2071. (IEEE Xplore, ISI)
- **Codrean A.**, Dragomir T.-L., "Period dependent averaging of a class of pulse modulated systems. Application to the cardiovascular system", Journal of Control Engineering an Applied Informatics (CEAI), vol. 17, no. 1, 2015, pp. 91-98. (ISI, Scopus)
- **Codrean A.**, Dragomir T.-L., "Delay effect on cardiovascular regulation - a systems analysis approach", European Control Conference (ECC), Linz, Austria, 2015, in press. (IEEE Xplore, ISI)
- **Codrean A.**, Dragomir T.-L., "Stability analysis of cardiovascular regulation", 23rd Mediterranean Conference on Control and Automation (MED), Torremolinos, Spain, 2015, accepted. (IEEE Xplore, Scopus)

2. ON MODELING CARDIOVASCULAR REGULATION

2.1. Introduction

The use of mathematical models in medicine has become a very active area of research, given its potential applicability in both design problems (e.g. medical devices, surgery) and analysis problems (e.g. diagnosis). A particular focus is on aspects regarding the functioning of the cardiovascular system, due to its crucial physiological role – that of providing supplies for maintaining vital functions of different organs and getting rid of waste material, and also because cardiovascular diseases are among the leading cause of mortality in the world. Over the past decades, a very wide range of models of the cardiovascular system have been proposed in the literature, from distributed models which characterize both the spatial and temporal proprieties of blood flow through the circulatory system (a network of blood vessels), to lumped-parameter models which focus more on the functioning of the heart (and its interaction with large vessels), and finally to models of cardiovascular regulation (with a focus on certain control loops).

Despite the fact that detailed models of the cardiovascular system may be useful for studying specific physiological or pathophysiological scenarios ([55]), the high complexity of such models usually obscures the basic functional principles of the system. Moreover, control mechanisms acting on the cardiovascular system (which are still poorly understood) are hard to grasp, due to the overall complexity of the closed loop system. Thus, if we want to gain insight into the dynamics of physiological control ([11]), we have to resort to models which are as simple as possible (as it has been done in control engineering).

On short-term, cardiovascular regulation is done through nervous control mechanisms, among which the most important is the baroreflex mechanism ([56]). Although the cardiovascular system has a periodic (pulsatile) dynamic behavior (due to the dynamics of cardiac contraction), the baroreflex feedback control loop deals mainly with time averaged state variables, and thus acting on a slower time scale ([57], [58], [59], [60]-ch.1). This indicates that the transient behavior of the overall control loop could be represented through simpler models. Also, in many practical cases, only short-term average values of the corresponding variables are of interest (in response to certain perturbations), and not their instantaneous values or their specific waveform (during a heart period) – [61], [62]. All these together provide a strong motivation for addressing (cycle-) averaged models of the cardiovascular system.

Averaging theory has been widely used in approximating nonlinear systems. Over the years, several averaging methods have been proposed, ranging from rather heuristic or application oriented methods to theoretical methods for specific classes of systems ([63], [64], [65], [66], [67], [1]-ch.10, [60]-ch.1). Recent interests are in extending the averaging theory to hybrid systems, and in particular

to switched systems ([68]), due to their ability to model (in a simple and straightforward manner) a wide variety of complex systems ([52]). Averaging of switched systems can be regarded as a process of dehybridization ([69]), which aims in further simplifying the analysis and design phases for the considered system. Naturally, such an approach plays an important role in periodic (or quasi-periodic) switched systems, and in particular in pulse-modulated switched systems. As in the case of averaging pulse modulated systems ([70]), averaging of pulse-modulated switched systems is equivalent with the averaging of the pulse modulation (switching) signal over the modulation period ([68]).

The cardiovascular system can also be regarded as a hybrid system, due to the heart valves, which open and close very fast, thus approximating a switching behavior ([71], [72]). Moreover, we shall show here that simple models of the cardiovascular system can be brought to the form of switched linear systems or switched affine systems. By taking into account the influence of the nervous control on the mechanism of cardiac contraction, as an idealization, the cardiovascular system can be further regarded as actually a pulse-modulated switched system. However, similar to other cases of pulse modulation in biological systems ([73]), we are dealing here with pulse-frequency modulation. For pulse-frequency modulated systems with constant duty ratio (e.g. the cardiovascular system), most conventional averaging methods (which were mostly used for pulse-width modulated systems) fail, resulting in an averaged model invariant to the modulation frequency (which would lead to very large errors as the frequency varies). In addressing this issue, this study presents an extension to a weighted averaging approach, which leads to a frequency dependent averaged model, while maintaining the averaged model as simple as possible.

While the cardiovascular system can be considered to play to the role of a controlled process, the baroreflex mechanism plays the role of a nonlinear controller, with one measured input – (mean) arterial pressure and multiple control outputs - heart rate, contractility, peripheral systemic resistance, and unstressed venous volume. The nonlinearity is mainly due to nonlinear static characteristics presented on each control pathway. In this study we derive also a simplified version of a well known model for the baroreflex mechanism ([39]).

Finally, the main objective of this study is reached by obtaining the closed loop averaged model of cardiovascular regulation, through the coupling of the averaged model of the cardiovascular system with the simplified model of the baroreflex mechanism. A comparison between the dynamic behavior of the closed loop averaged model and the original closed loop pulsatile model is further done through simulations. [38]

2.2. Modeling the cardiovascular system

The cardiovascular system is characterized by a very complex dynamic behavior, mainly due to time-varying nonlinearities which are hard to model mathematically in a quantitative manner. Numerous models have been proposed in the literature. Although the system is with distributed parameters, in most cases it is approximated through lumped parameter models, with varying degrees of complexity, ranging from detailed high order models (e.g. 21st –order, in [57]), to

[38] Some of the results of this chapter have been published in [74].

medium order models (e.g. 14th –order, in [39]), and finally to low order models (e.g. 3rd –order, in [61]) which capture just the basic dynamic phenomena of the whole system. Although detailed models can capture a wide palette of physiological and pathophysiological aspects, it is usually very difficult to use them in practice. In this context, for modeling the cardiovascular system, a qualitative approach is adopted, focusing on insight, rather than accuracy.

2.2.1 A simple model of the cardiovascular system

As a starting point, the simple pulsatile lumped-parameter model (Windkessel type) of the cardiovascular system from [61] is considered. The model captures only the dynamics of the left ventricle and the systemic circulation, and it is considered to be sufficient in order to approximate basic hemodynamic waveforms[39]. Similar low-order models have also been used throughout the literature (e.g. [71], [75], [76], [77]).

The cardiovascular system is predominantly of a hydraulic nature, but for modeling, due to basic isomorphisms, conceptual electrical circuits type models are used, with the following analogies: voltage represents pressure, current represent flow, charge represents volume, electrical resistance represents hydraulic resistance, capacitance represents compliance, and diode represent heart valve. The circuit diagram corresponding to the model of the cardiovascular system is shown in Fig. 2.1.

The model is composed out of 3 coupled differential equations:

$$\begin{cases} \frac{d}{dt}\left[C(t)V_0(t)\right] = i_2(t) - i_0(t) \\ \frac{d}{dt}\left[C_1 V_1(t)\right] = i_0(t) - i_1(t) \\ \frac{d}{dt}\left[C_2 V_2(t)\right] = i_1(t) - i_2(t) \end{cases}, \tag{2.1}$$

with initial values

$$C(t_0) = C_0,\ V_0(t_0) = V_{00},\ V_1(t_0) = V_{10},\ V_2(t_0) = V_{20} \tag{2.2}$$

and where the currents are given by

$$\begin{aligned} i_0(t) &= \frac{1}{R_0}\left[V_{out}(t) - V_1(t)\right] \\ i_1(t) &= \frac{1}{R_1}\left[V_1(t) - V_2(t)\right] \\ i_2(t) &= \frac{1}{R_2}\left[V_2(t) - V_{in}(t)\right] \end{aligned} \tag{2.3}$$

The voltages V_0, V_1 and V_2 correspond to left ventricular pressure, systemic arterial

[39] From a more rigorous perspective, the venous compartment actually incorporates, besides the systemic veins, also the right ventricle and the pulmonary circulation - which are considered to have a rather passive role ([75]). With this in mind, the model captures in a pertinent manner only the hemodynamic response of the left ventricle and systemic arteries (i.e. it focuses on the variations of pressures P_{lv} and P_{sa}).

pressure and venous pressure (further on denoted as P_{lv}, P_{sa}, P_v).

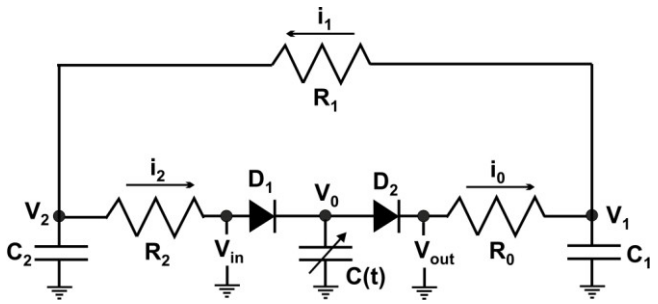

Fig.2.1. Pulsatile model of the cardiovascular system (adapted from [61])

The pulsatile nature of the model is given by the time-varying compliance (capacitance) *C(t)*, which is the inverse of an time-varying elastance *C(t)=1/E(t).* The elastance[40] has a periodic waveform, with period T (heart period, i.e. duration of the cardiac cycle), and its analytical expression, determined from experimental data, can be given by a piecewise linear form ([61])

$$E(t)=\begin{cases}(E_s-E_d)\dfrac{3t}{T}+E_d & ,\ nT\le t<nT+\dfrac{T}{3}\\ (E_s-E_d)\left(2-\dfrac{6t}{T}\right)+E_s & ,\ nT+\dfrac{T}{3}\le t<nT+\dfrac{T}{2}\\ E_d & ,\ nT+\dfrac{T}{2}\le t<(n+1)T\end{cases}\quad ,\quad n\in N \tag{2.4}$$

where E_s and E_d are the maximum and minimum elastance value, also called end-systolic elastance and end diastolic elastance. The waveforms of the elastance and compliance for a heart period of T= 1 sec is shown in Fig. 2.2.

As a further simplification, the time-varying compliance is approximated in [61] as a piecewise constant function (Fig. 2.3):

$$C_a(t)=\begin{cases}C_s, & nT\le t<nT+\tau\\ C_d, & nT+\tau\le t<(n+1)T\end{cases}\quad ,\quad n\in N, \tag{2.5}$$

where the first interval is considered to be the duration of the systole (which can be approximated as τ=T/3 – [61]), the second interval is the duration of the diastole, while C_s and C_d are the minimum, respectively maximum, values of the compliance.

[40] For a detailed description of the elastance concept see [17].

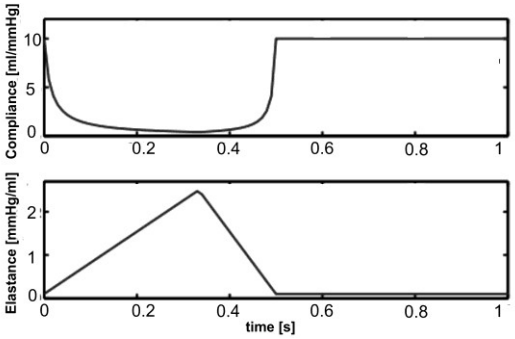

Fig.2.2. Time-varying compliance and elastance (adapted from [78])

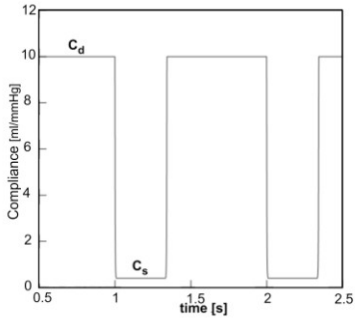

Fig.2.3. Approximation of the time-varying compliance (adapted from [61])

Next, the commutation of the two diodes is modeled in a manner similar as in [61], by introducing a periodic switching function q, which takes the value q=1 when the diode D_1 is conducting and D_2 is non-conducting, and the value q=0 in the opposite situation[41]. In the case of the square-wave time-varying compliance (Fig. 2.3), the switching function can be defined as[42]:

$$q(t) = \begin{cases} 0 & , \quad nT \le t < nT + \tau \\ 1 & , \quad nT + \tau \le t < (n+1)T \end{cases} , \quad n \in \mathcal{N}. \tag{2.6}$$

The equations of the voltages V_{out} and V_{in} (which were additionally introduced) can now be written as:

$$\begin{aligned} V_{out}(t) &= [1 - q(t)]\, V_0(t) + q(t)\, V_1(t) \\ V_{in}(t) &= [1 - q(t)]\, V_2(t) + q(t)\, V_0(t) \end{aligned} \tag{2.7}$$

Finally, based on equation (2.1)-(2.3) and (2.5)-(2.7), and by defining the states as $x_0(t)=C_a(t)V_0(t)$, $x_1(t)=C_1V_1(t)$, $x_2(t)=C_2V_2(t)$[43], and the input $u(t)=E_a(t)$ (with $E_a=1/C_a$), the model can be written in the following nonlinear state space form:

[41] This means that the isovolumic contraction/relaxation phases are ignored.
[42] When using the piecewise linear elastance function instead, q has to be defined in a more elaborate manner, because the elastance is defined on 3 subintervals instead of two, and an issue of synchronization appears between these subintervals and the intervals in which the diodes commute. Moreover, the manner in which the switching signal q appears in the model has to be reanalyzed, because (2.7) can no longer be used.
[43] The new states now represent stressed volumes, in their hydraulic interpretation.

$$\begin{cases} \dot{x}_0(t) = -\left[\frac{1}{R_2}q(t) + \frac{1}{R_0} - \frac{1}{R_0}q(t)\right]x_0(t)u(t) + \frac{1}{R_0C_1}\left[1-q(t)\right]x_1(t) + \frac{1}{R_2C_2}q(t)x_2(t) \\ \dot{x}_1(t) = \frac{1}{R_0}\left[1-q(t)\right]x_0(t)u(t) - \left[-\frac{1}{R_0C_1}q(t) + \frac{1}{R_0C_1} + \frac{1}{R_1C_1}\right]x_1(t) + \frac{1}{R_1C_2}x_2(t) \\ \dot{x}_2(t) = \frac{1}{R_2}q(t)x_0(t)u(t) + \frac{1}{R_1C_1}x_1(t) - \left[\frac{1}{R_1C_2} + \frac{1}{R_2C_2}q(t)\right]x_2(t) \end{cases} \tag{2.8}$$

The compressed form of the model is given by

$$\dot{\boldsymbol{x}}(t) = \boldsymbol{f}\left(\boldsymbol{x}(t), u(t), q(t)\right) \quad , \quad \boldsymbol{x}(t_0) = \boldsymbol{x}_{00} \tag{2.9}$$

with the state vector $\boldsymbol{x}(t) = [x_0(t)\ x_1(t)\ x_2(t)]^T$, and where states and the input signals are of periodic nature, i.e. $\boldsymbol{x}(t)=\boldsymbol{x}(t+T)$, $u(t)=u(t+T)$ and $q(t)=q(t+T)$.

The output equations can be also written as

$$\boldsymbol{y}(t) = \boldsymbol{h}\left(\boldsymbol{x}(t)\right) = diag\left(\frac{1}{C_a(t)}, \frac{1}{C_1}, \frac{1}{C_2}\right)\boldsymbol{x}(t) \tag{2.10}$$

where the output vector is $\boldsymbol{y}(t)=[y_0(t)\ y_1(t)\ y_2(t)]^T$, with $y_0=V_0$, $y_1=V_1$ and $y_2=V_2$.

A final remark: for a future coupling of model (2.9)-(2.10) with a model of the nervous control system (composed mainly of the baroreflex control mechanism), only the output V_1 is needed, corresponding to arterial pressure (P_{sa}).

2.2.2 The cardiovascular system as a hybrid system

The cardiovascular system can be regarded as a hybrid system, in which the ideal diodes may induce time based or state based switching. The switching denotes the transition from one heart regime to the other (e.g. from systole to diastole). Because the switching is periodic, and is actually induced by the elastance function which acts as an external signal (mechanism of contraction), the cardiovascular system falls into the category of pulse modulated switched systems. Moreover, because the switching frequency (heart rate) can change under the influence of nervous control (as a result to different types of perturbations), we are actually dealing with a pulse frequency modulation.

Although most studies consider the cardiovascular system as a hybrid system with state based switching (e.g. [71], [72]), we will show here that under certain simplifying assumptions (mainly in respect with the expression the time-varying elastance/compliance), the cardiovascular system can be regarded also as a time-based switched system. Indeed, it has been shown in the general case, that under certain conditions, a state based switched system can be equivalent with a time based switched system ([53]-ch.1)[44].

[44] If an exogenous time dependent switching function can be identified which assures a one-to-one correspondence with the operating regions of the state space, so that the state and time dependent switched systems have a common trajectory (solution), the system can be reduced to a time dependent switched system.

2.2.2.1 Time based switched system

For model (2.9)-(2.10) of the cardiovascular system, with the input $u=E_a=1/C_a$, consider that the switching of the two diodes D_1 and D_2 is synchronized with the intervals in which the square-wave compliance changes. Based on the switching signal q defined in (2.6), the input u can be written as

$$u(t)=\frac{1}{C_d}\,q(t)+\frac{1}{C_s}\,\left[1-q(t)\right]=E_d\;q(t)+E_s\;\left[1-q(t)\right] \tag{2.11}$$

This means that instead of the two inputs q and u, we can consider the single input q, in which case the model (2.9) can be recasted to the standard from of a switched linear system (with time based switching):

$$\begin{aligned}\dot{\boldsymbol{x}}(t)&=\boldsymbol{A}_{q(t)}\,\boldsymbol{x}(t)\\ \boldsymbol{y}(t)&=\boldsymbol{C}_{q(t)}\,\boldsymbol{x}(t)\end{aligned} \tag{2.12}$$

where the switching function q:[0,∞)→{0,1}, defined as in (2.6), provides the index of the active mode, i.e. it selects the appropriate matrices $\boldsymbol{A}$ and $\boldsymbol{C}$ from the sets $\{\boldsymbol{A_0},\ \boldsymbol{A_1}\}$ and $\{\boldsymbol{C_0},\ \boldsymbol{C_1}\}$, according to the specific regime in which the system is operating ($\boldsymbol{A_0,C_0}$ - systole, $\boldsymbol{A_1,C_1}$ - diastole). In accordance with (2.9)-(2.12), these matrices are given by

$$\boldsymbol{A}_0=\begin{bmatrix}-\frac{E_s}{R_0} & \frac{1}{R_0C_1} & 0\\ \frac{E_s}{R_0} & -\frac{R_0+R_1}{R_0R_1C_1} & \frac{1}{R_1C_2}\\ 0 & \frac{1}{R_1C_1} & -\frac{1}{R_1C_2}\end{bmatrix},\ \boldsymbol{A}_1=\begin{bmatrix}-\frac{E_d}{R_2} & 0 & \frac{1}{R_2C_2}\\ 0 & -\frac{1}{R_1C_1} & \frac{1}{R_1C_2}\\ \frac{E_d}{R_2} & \frac{1}{R_1C_1} & -\frac{R_1+R_2}{R_1R_2C_2}\end{bmatrix} \tag{2.13}$$

$$\boldsymbol{C}_0=diag\left(E_s,\frac{1}{C_1},\frac{1}{C_2}\right),\boldsymbol{C}_1=diag\left(E_d,\frac{1}{C_1},\frac{1}{C_2}\right).$$

2.2.2.2 Model order reduction

Model (2.8) is non-minimal, because of the linear dependence $x_0(t)+x_1(t)+x_2(t)=x_T$ - conservation of charge, respectively conservation of volume; x_T represent the total stressed volume (i.e. total volume minus total unstressed/zero-pressure volume). This means that the state x_2 can be determined as $x_2(t)=x_T-x_1(t)-x_0(t)$. Consequently, model (2.8) can be reduced from a 3rd order model to a 2nd order one:

$$\begin{cases}\dot{x}_0(t)=-\left\{\left[\frac{q(t)}{R_2}+\frac{1}{R_0}-\frac{q(t)}{R_0}\right]u(t)+\frac{q(t)}{R_2C_2}\right\}x_0(t)+\left[\frac{1-q(t)}{R_0C_1}-\frac{1}{R_2C_2}q(t)\right]x_1(t)+\frac{q(t)}{R_2C_2}x_T\\ \dot{x}_1(t)=\left[\frac{1-q(t)}{R_0}u(t)-\frac{1}{R_1C_2}\right]x_0(t)-\left[-\frac{1}{R_0C_1}q(t)+\frac{1}{R_0C_1}+\frac{1}{R_1C_1}+\frac{1}{R_1C_2}\right]x_1(t)+\frac{1}{R_1C_2}x_T\end{cases} \tag{2.14}$$

Based on similar arguments with those from chapter 2.2.1, model (2.14) can be recasted as a switched affine system:

$$\begin{aligned}\dot{\tilde{\boldsymbol{x}}}(t) &= \tilde{\boldsymbol{A}}_{q(t)}\,\tilde{\boldsymbol{x}}(t) + \tilde{\boldsymbol{b}}_{q(t)}\\ \tilde{\boldsymbol{y}}(t) &= \tilde{\boldsymbol{C}}_{q(t)}\,\tilde{\boldsymbol{x}}(t)\end{aligned} \tag{2.15}$$

with the states $\tilde{\boldsymbol{x}}(t) = [x_0(t)\ x_1(t)]^T$, the outputs $\tilde{\boldsymbol{y}}(t) = [y_0(t)\ y_1(t)]^T$, and with the matrices and vectors

$$\begin{aligned}\tilde{\boldsymbol{A}}_0 &= \begin{bmatrix} -\frac{E_s}{R_0} & \frac{1}{R_0C_1} \\ \frac{E_s}{R_0} - \frac{1}{R_1C_2} & -\frac{1}{R_0C_1} - \frac{1}{R_1C_1} - \frac{1}{R_1C_2} \end{bmatrix},\ \tilde{\boldsymbol{b}}_0 = \begin{bmatrix} 0 \\ \frac{x_T}{R_1C_2} \end{bmatrix}\\ \tilde{\boldsymbol{A}}_1 &= \begin{bmatrix} -\frac{E_d}{R_2} - \frac{1}{R_2C_2} & -\frac{1}{R_2C_2} \\ -\frac{1}{R_1C_2} & -\frac{1}{R_1C_1} - \frac{1}{R_1C_2} \end{bmatrix},\ \tilde{\boldsymbol{b}}_1 = \begin{bmatrix} \frac{x_T}{R_2C_2} \\ \frac{x_T}{R_1C_2} \end{bmatrix},\\ \tilde{\boldsymbol{C}}_0 &= diag\left(E_s, \frac{1}{C_1}\right), \tilde{\boldsymbol{C}}_1 = diag\left(E_d, \frac{1}{C_1}\right).\end{aligned} \tag{2.16}$$

As a remark, it is important to point out that now x_T appears explicitly in the model, which would facilitate a future integration with the nervous (baroreflex) feedback loop which controls the unstressed volume ([79]).

2.3. Modeling the nervous control system

The nervous control system is composed out of several nervous reflex mechanisms which act on the cardiovascular system, among which the most important is the baroreflex mechanism ([56]). In this section we focus on modeling aspects of the baroreflex feedback control loop, which will be further coupled with the model of the cardiovascular system in the next section.

2.3.1. Initial baroreflex model

The baroreflex model from [39] is considered as a starting point, which is regarded as one of the most well established models, derived from experimental data and thoroughly validated. The model is divided into three parts: afferent part (corresponding to the baroreceptors), central part (central nervous system) and efferent part (peripheral autonomous nervous system). Due to the large number of nonlinearities and parameters/variables, and for a more intuitive and simple presentation, the model will be further described only in a graphical manner (through block diagrams) and with brief comments; the detailed equations, along with the parameter values, can be found in [39].

The afferent part is modeled as a series connection between a linear first-order filter and a sigmoid-type static nonlinearity – Fig. 2.4. The input represents the arterial pressure (P_{sa}), and corresponds to the signal V_1 from model (2.9)-(2.10), while the output represents the firing rate of the baroreceptors - n_{br}.

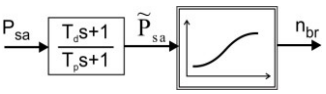

Fig.2.4. Afferent part of the baroreflex model

The central part captures two parallel nervous pathways, a sympathetic (excitatory) and a parasympathetic (inhibitory) pathway, modeled by an exponential-type static nonlinearity, respectively a sigmoid-type static nonlinearity – Fig. 2.5. The two outputs represent the firing rates of the sympathetic and parasympathetic pathways – n_s and n_p.

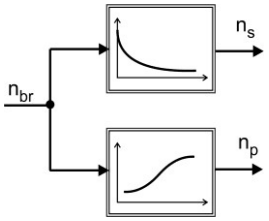

Fig.2.5. Central part of the baroreflex model

The efferent part is composed out several nervous pathways: a sympathetic pathway which controls the maximum amplitude of the elastance E_s, a sympathetic pathway which controls the peripheral (systemic) resistance R_p, a sympathetic pathway which controls the (systemic) venous unstressed volume V_{uv}, a sympathetic pathway and a parasympathetic pathway which control the heart period (in an antagonistic manner)[45]. The sympathetic pathways which control E_s, R_p and V_{uv}[46], are modeled as series connections between a time delay, a logarithmic type static nonlinearity, a first order low pass filter dynamics and a summation with a nominal value of the output. The sympathetic and parasympathetic pathways which control the heart period T are modeled as a summation between: a series connection of a time delay, logarithmic type static nonlinearity and a first order low pass filter dynamics (sympathetic part); a series connection between a time delay, a static gain and a first order low pass filter dynamics (parasympathetic part); along with a nominal value of the corresponding output. Fig. 2.6 shows the block diagram of this part of the model (T_E, T_R, T_V, T_{Ts}, T_{Tp} are the time constants; τ_E, τ_R, τ_V, τ_{Ts}, τ_{Tp} are the time delays; $E_{s,0}$, $R_{p,0}$, $V_{uv,0}$, T_0 represents the nominal values).

[45] For simplicity, we will not distinguish between the efferent variables of the left and right part of the heart, nor between the splanchnic and extrasplanchnic circulation. It is considered that the main features of the models are still conserved, while condensing the presentation as much as possible.

[46] It will be shown in the subsequent chapter how these variables relate to those of the cardiovascular model presented in chapter 2.2.

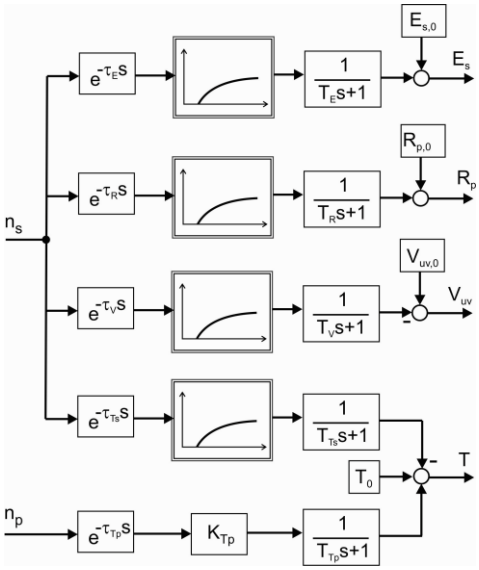

Fig.2.6. Efferent part of the baroreflex model

2.3.2. Simplified baroreflex model

The baroreflex model presented so far appears relatively complex. From a practical point of view, it is of interest to simplify the model as much as possible in order to permit a deeper understanding of its dynamic behavior. In this direction, we have managed to arrive at a simpler model - Fig. 2.7 (equivalent from an input-output perspective), by making the following operations:

- the time delay elements where moved after the logarithmic-type static nonlinearities. Such an operation is allowed due to the static nature of the nonlinearities;
- equivalent nonlinearities for the central and efferent sympathetic pathway is determined: the series connection of the exponential-type static nonlinearity and the logarithmic-type static nonlinearities lead to a affine-type static nonlinearities;
- equivalent nonlinearity for the entire sympathetic pathway are determined: the series connection of the afferent sigmoid-type static nonlinearity and the affine-type static nonlinearities (previously determined) lead to a sigmoid-type static nonlinearities (monotonically decreasing);
- an equivalent nonlinearity for the entire parasympathetic pathway is determined: the series connection of the afferent sigmoid-type static nonlinearity and the central sigmoid-type static nonlinearity leads to a sigmoid-type static nonlinearity (monotonically increasing);
- the summations with the nominal values of the outputs of the efferent part are incorporated in the sigmoid-type static nonlinearities determined for the sympathetic and parasympathetic pathways.

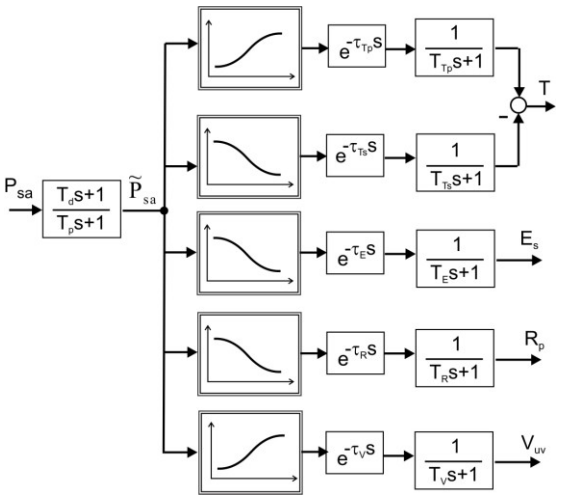

Fig.2.7. Simplified baroreflex model

Based on the above considerations, we can now give the full set of equations of the simplified baroreflex model:

$$
\begin{aligned}
&T_p\,\dot{\tilde{P}}_{sa}(t)+\tilde{P}_{sa}(t)=T_d\,\dot{P}_{sa}(t)+P_{sa}(t)\\
&\dot{T}_{\Delta p}(t)=-\frac{1}{T_{Tp}}T_{\Delta p}(t)+\frac{1}{T_{Tp}}f_{sig,Tp}\left(\tilde{P}_{sa}(t-\tau_{Tp})\right)\\
&\dot{T}_{\Delta s}(t)=-\frac{1}{T_{Ts}}T_{\Delta s}(t)+\frac{1}{T_{Ts}}f_{sig,Ts}\left(\tilde{P}_{sa}(t-\tau_{Ts})\right)\\
&T(t)=T_{\Delta p}(t)-T_{\Delta s}(t)\\
&\dot{E}_s(t)=-\frac{1}{T_E}E_s(t)+\frac{1}{T_E}f_{sig,E}\left(\tilde{P}_{sa}(t-\tau_E)\right)\\
&\dot{R}_p(t)=-\frac{1}{T_R}R_p(t)+\frac{1}{T_R}f_{sig,R}\left(\tilde{P}_{sa}(t-\tau_R)\right)\\
&\dot{V}_{uv}(t)=-\frac{1}{T_V}V_{uv}(t)+\frac{1}{T_V}f_{sig,V}\left(\tilde{P}_{sa}(t-\tau_V)\right)
\end{aligned}
\qquad (2.17)
$$

where the functions f_{sig} have the sigmoid form

$$
f_{sig,i}\left(\tilde{P}_{sa}(t-\tau_i)\right)=\frac{j^{min}+j^{max}\,e^{\left(\tilde{P}_{sa}(t-\tau_i)-P_{san}\right)/k_i}}{1+e^{\left(\tilde{P}_{sa}(t-\tau_i)-P_{san}\right)/k_i}},
\qquad (2.18)
$$

$$
(j,i)\in\{(T_{\Delta p},Tp),(T_{\Delta s},Ts),(E_s,E),(R_p,R),(V_{uv},V)\}.
$$

Furthermore, the functions f_{sig} can be written under the simpler form:

$$
f_{sig,i}\left(\tilde{P}_{sa}(t-\tau_i)\right)=\frac{j^{\Delta}}{1+\gamma_i\,e^{\tilde{P}_{sa}(t-\tau_i)k_{ii}}}+j^{max},
\qquad (2.19)
$$

$$
k_{ii}=1/k_i\,,\ j^{\Delta}=j^{min}-j^{max},\ \gamma_i=e^{-P_{san}k_{ii}}.
$$

2.4. Closed loop model of cardiovascular regulation

This section presents the closed loop model obtained by coupling the cardiovascular model and the baroreflex model presented in the previous two sections. The coupling involves an analysis of the interactions which appear between the two models, and ways of modeling them in an intuitive and simple manner.

Before proceeding any further, it is important to explain how the variables of the baroreflex control loop and the cardiovascular model are related, in the context in which each part has been adapted from different studies. The problem is twofold: first the input and output variables should be uniquely clarified, second the parameters should be calibrated in order to reproduce normal hemodynamic behavior of the overall closed loop model (the control loop should have the effect on the controlled systems as in [39]).

In addressing the first aspect, it's important to note that the cardiovascular model presented so far uses electrical variables (based on the analogy between electrical and hydraulic circuits), while the baroreflex model deals with hydraulic variables. From this point further we will consider all the variables in their hydraulic interpretation. This means that, for models (2.9)-(2.10) and (2.15), the outputs $\{y_0, y_1, y_2\}$ will now represent the pressures $\{P_{lv}, P_{sa}, P_v\}$ and the states $\{x_0, x_1, x_2\}$ will now become stressed volumes $\{V_{lv}^S, V_{sa}^S, V_v^S\}$[47]. The inputs variables remain the same- $\{T, E_s, R_1, x_T\}$, but will now represent heart period, hydraulic elastance, hydraulic resistance, and total stressed volume. Finally, the outputs of the baroreflex model (2.17) will change from $\{T, E_s, R_p, V_{uv}\}$ to $\{T, E_s, R_1, x_T\}$.

In order to obtain a homogenous closed loop model capable of reproducing normal hemodynamic results, the second step involves a parameter calibration phase. Moreover, because for the baroreflex model, the old control output V_{uv} (unstressed venous volume) was replaced by the new control output x_T (total stressed volume), an additional output constraint needs to be added (which will be integrated in the sigmoid function of the corresponding output path).

Further on, we will adopt this change of variables, while the parameter calibration of the baroreflex loop will be pursued in chapter 2.6.2.

2.4.1. Interactions between the baroreflex model and the cardiovascular model

The interactions between the cardiovascular model and the baroreflex model appear at the afferent and efferent levels of the baroreflex control loop. Let the cardiovascular system be considered as a controlled process, and the baroreflex mechanism as the control structure. In such a case, the afferent path corresponds to a feedback path in which the sensors (baroreceptors) transmit information to the controller (central nervous system), and the efferent path corresponds to a direct path in which the controller transmits the control signals to the process, via an actuator. So we are actually dealing with a physiological control system ([11]).

[47] As consequence, P_{sa} will be the input to the baroreflex model instead of V_1.

2.4.1.1 Feedback Path

On the feedback path, we have a filter (Fig. 2.4), which extracts the information needed for the baroreflex control loop. However, the precise information which is actually extracted by the baroreceptors is still not well understood – whether it is the average pressure, the instantaneous pressure, or a combination of both ([58]). Depending on the modeling objective, several variations can be found in the literature.

For example, in ([58]), the rate of change of an average arterial pressure (P_{sa1}) defined as

$$P_{sa1}(t) = \alpha \int_{-\infty}^{t} P_{sa}(s)\, e^{-\alpha(t-s)} ds \tag{2.20}$$

is considered as input to the baroreflex control loop (α is a weighting factor). The model can be written in transfer function form as

$$H_b(s) = \frac{P_{sa1}^{p}(s)}{P_{sa}(s)} = \frac{s}{\frac{1}{\alpha}s + 1} \tag{2.21}$$

with the block diagram from Fig. 2.8 (P_{sa1}^{p} stands for the rate of change of the average pressure). Based on comparisons of the frequency response, it can be shown that the model approximates the first-order filter given in ([39]) – see Fig. 2.4 – for a sufficiently high frequency band.

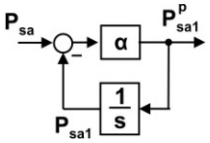

Fig.2.8. Block diagram of the linear part of the baroreceptor model from [58]

Alternatively, if we consider that the average pressure is obtained through a low pass filter (this is possible when the time constant is large enough in respect with the signal period), then the parallel connection from Fig. 2.9a, with $K=1/T_p$ and $\alpha=1/T_p$, may correspond to the filter (2.21), while the parallel connection from Fig. 2.9b, with $K=1/(1-K_1)$ and $T_d=K\cdot T_p$, may correspond to the filter from Fig. 2.4.

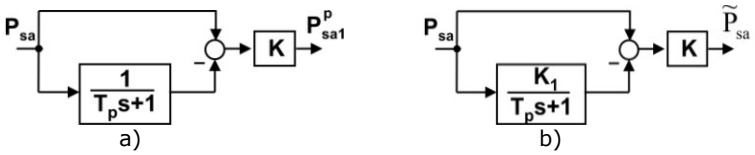

Fig.2.9. Alternative block diagrams for the linear part of the baroreceptor model

Other approaches, like the ones from [57], [59], [60]-ch.1 or [30], consider as input for the baroreflex control loop simply the average arterial pressure.

An interesting interpretation is proposed in [80], where the pulsatility effect on the baroreflex observed in experiments ([39]) is regarded as a dither effect, lowering the gains of the baroreflex control loop[48]. This however sustains the view that whether or not one takes the instantaneous pressure into account, the average pressure is the predominant component.

Finally, for our purpose of coupling the cardiovascular model with the baroreflex control loop, it seems that the baroreceptor model from [39] is a suitable choice, by capturing the response of the baroreceptors to both an average pressure and an instantaneous pressure. On the other hand, when coupling the baroreflex control loop with an averaged cardiovascular model (chapter 2.5.4), we will we will consider only the averaged pressure as input to the baroreflex control loop – but with lower central point slopes for the sigmoids (see the calibration from chapter 2.6.2).

2.4.1.2 Direct Path

For the direct path, we need to model how to generate the elastance function from the "prescribed" heart period (by the baroreflex model). From a mathematical point of view, we need a nonlinear operator M which maps an input function $f_T(t)=1/T(t)$ to an output function $E(t)$: $M: f_T \mapsto E$. A model of this type can be regarded as a Pulse Modulator ([70]).The input of the Pulse Modulator is the continuous signal $f_T(t)$, while the output consists of a series of pulses, which have the shape given by $E(t)$. Because in our particular case, the input of the Pulse Modulator is actually the frequency of the output $E(t)$, and by considering also that we want to preserve the shape of each pulse as the period changes, we are dealing with a combination of pulse-frequency and pulse-width modulation. Such a Pulse Modulator is referred to as a Pulse-frequency-width Modulator (PFWM) or as a Combined Pulse Modulator (CPM)[49].

Using the mathematical framework from [70], the model for CPM with rectangular output pulses can be written as:

---

[48] Consider the output of the structure from Fig. 2.9b as the input of the baroreflex control loop, and regard the pressure P_{sa} as composed out of an average component (the same one extracted by the low pass filter from the lower pathway) and a zero mean variation component. Then it results that the input to the baroreflex control loop actually consists in a slow varying signal (the average of P_{sa}) and a superimposed high frequency signal – dither (the zero mean variation of P_{sa} multiplied by K). Both signals are then at the input of a static nonlinearity (sigmoid). The theory regarding dithering ([67], [80]) states that this scheme is equivalent to one where we have as input only the slow varying signal, in series with an equivalent static nonlinearity. Additionally, because in our case the dither signal is of triangular form (idealized waveform of arterial pressure), the equivalent nonlinearity has a lower central point slope than the original one.

[49] Depending on the modeling objectives (e.g. shape of the elastance function), in some studies an Integral Pulse-Frequency Modulator is used instead (IPFM) – see the last paragraph of Appendix 1 for a discussion on the equivalence between a relay-hysteresis model and an IPFM. At last, when using a simple elastance function like the one corresponding to Fig. 2.3, a CPM is enough, while when using a more elaborated elastance function like the one from Fig. 2.2, and IPFM is needed.

$$E(t)=\begin{cases} E_s & , \quad t_n \le t < t_n+\tau_n \\ E_d & , \quad t_n+d_n \le t < t_{n+1} \end{cases}$$
$$t_{n+1}=t_n+T(t_n), \quad \tau_n=\frac{1}{3}T(t_n), \tag{2.22}$$

where the time moments $t_0=0<t_1<t_2<\ldots<t_n<t_{n+1}<\ldots$ are considered sampling moments, and with T as the sampling period. By further considering an inverse operation of the type $C(t)=1/E(t)$, we arrive at the compliance function given in Fig. 2.3 ($C_s=1/E_s$ and $C_d=1/E_d$).

2.4.2. Relay-hysteresis model of a combined pulse modulator

The CPM model given by (2.22) describes a nonlinear sample-data system. However, models of Pulse Modulators may be analyzed also in the continuous-time domain ([70], [81]). In fact, several studies can be found in the literature, which propose relay type models for different types of Pulse Modulators ([70]-ch.1.7, [82], [83], [84], [85]).

Such an approach is also followed in [81], where it is stated that many Pulse Modulators can be regarded as relay systems which operate in a sliding mode with finite switching frequency (see [81]-ch.3, ch.12). In particular, for PFMs, a relay-hysteresis model is proposed in [81]-ch.13. The model consists in a feedback loop, with an integrator, a gain, and a relay component on the direct path, respectively a gain of the feedback path – Fig. 2.10[50]. The output of the model consists in a train of rectangular pulses with unity amplitude and frequency given by the input signal.

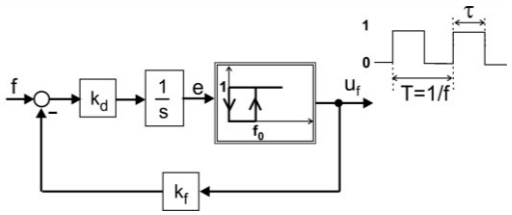

Fig.2.10. Relay-hysteresis model for a PFM

In the case of CPMs, the model from Fig. 2.10 does no longer hold. This is mainly due variations of duration of the modulated pulses - τ_n from (2.22). Because in the initial model the feedback gain k_f is directly correlated to this duration, a natural extension is to consider this parameter variable, as opposed to being constant. Moreover, because the duration τ_n actually changes as the modulation frequency changes, k_f can be continuously adapted according to the variations of the input frequency signal. The block diagram of the new model is shown in Fig. 2.11. In order to generate an elastance function like the one corresponding to Fig. 2.3, as model (2.22) does, we would simply have to add an output component which adapts the output through the mapping $u_f \mapsto u_f \cdot (E_s - E_d) + E_d$. Finally, for

[50] In [81]-ch.3, the relay component presents also a dead zone (useful in changing the basal sliding frequency of the relay system) and symmetry in respect with the origin (needed for the case of double-sign modulation).

a detailed analysis on how these relay systems behave as Pulse Modulators see Appendix 1.

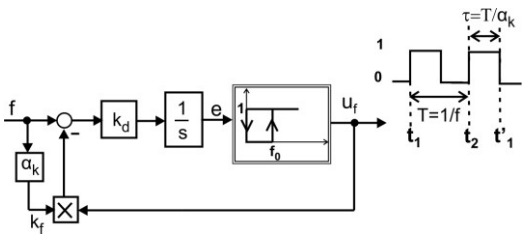

Fig.2.11. Relay-hysteresis model for a CPM

2.4.3. The closed loop model

By coupling the cardiovascular model (2.15), with the simplified baroreflex model (2.17), and with the relay-hysteresis model of the CPM from Fig. 2.11, we arrive at the closed loop model of cardiovascular regulation illustrated through the block diagram from Fig. 2.12. Notice that an additional inversion element is introduced at the input of the CPM so we obtain the heart frequency (f) instead of the heart period (T). Also, as a change of notation, the output u_f of the CPM is now changed with q, the input switching signal for the cardiovascular system.

As an overall interpretation of the model, it can be said that we are dealing with a physiological control system, with the following components:

- a nonlinear "plant" - the cardiovascular system - controlled through multiple input signals,

- sensors – (part of) the baroreceptors – witch act as linear filters,

- a nonlinear static controller - the central nervous system - with multiple outputs (antagonistic outputs for the heart period T),

- and a direct pathway which consists in time delays (due to transmission through the autonomic peripheral nervous system), first-order lag elements (probably due to chemical reactions that take place near the cardiovascular system), and a Pulse Modulator which acts as an actuator (mechanism of cardiac contraction).

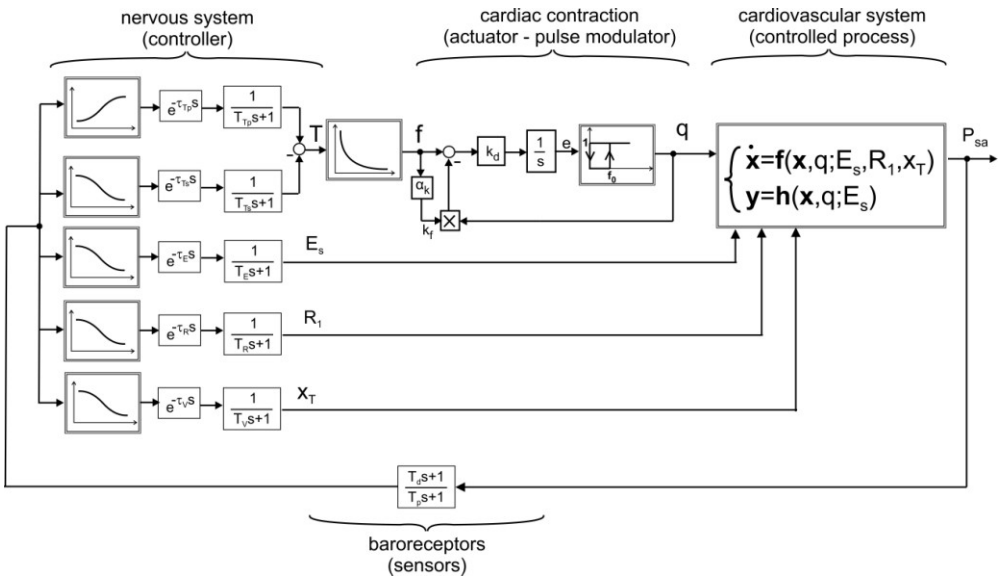

Fig.2.12. Closed loop model of cardiovascular regulation

2.5. Averaged closed loop model of cardiovascular regulation

Averaging theory provides important approximation methods, which are used in the analysis of nonlinear systems. Especially for the class of periodic (quasi-periodic) systems, averaging methods permit one to obtain a simpler non-periodic system, which approximates to a certain degree the original system.

In power electronics, the circuit averaging and state space averaging methods were among the first to be used in applications. The circuit averaging method involves averaging the waveforms of the signals and manipulations of the circuit diagram (different circuit parts are replaced with equivalent ones), which requires a physical insight of the system ([65]). The state space averaging method provides a more general framework, with a simpler a more straightforward methodology, by averaging directly the equations of the state space model associated to the system ([65]). The results obtained with the state space averaging method are identical with those obtained by averaging based on perturbation theory ([1]-ch.10) or through the KBM averaging method of 1st order ([63]). Moreover, the approach was recently adapted to the framework of switched systems ([68]). In order to increase the accuracy of the approximation (with the price of increased complexity), a multifrequency averaging method was proposed in [64], which implies the use of a generalized average defined based on Fourier series. Other approaches were that of the dithering technique (the switching signal is associated to some high-frequency dither signal) – [66], or the incremental-input describing function (an extension of the describing function method) – [67], which both finally lead to replacing the original nonlinearity by an equivalent (averaged) nonlinearity.

Due to the pulsatile (periodic) nature of the cardiovascular system, some attempts were to derive a non-pulsatile (averaged) and simpler model. In [60]-ch.1, a somehow heuristic averaging was done implicitly during the model building step,

which eventually affects the physical interpretability of the model. The circuit averaging method was used in [61], while the multifrequency approach was used in [62], but the resulted models are not simpler than the original ones (when considering the overall closed loop system with cardiovascular regulation). Finally, the dithering technique was used in [80], but the study is still in an incipient stage – the results refer only to a specific part of cardiovascular regulation.

This section presents besides the conventional averaging method, an extension that can provide a simpler (averaged) model for the cardiovascular system, which is further coupled with the nervous (baroreflex) feedback loop.

2.5.1. Conventional Averaging Method

The conventional averaging method for pulsed-modulated switched systems, as it derives from [68], consists in applying an averaging operator M to each equation of the state space model. The operator M associates to each periodic function $\xi(t)$ an averaged function $\xi_a(t)$, defined as

$$\xi_a(t) = M\{\xi(t)\} = \frac{1}{T}\int_{t-T}^{t} \xi(s)\, ds, \tag{2.23}$$

where T is the period of $\xi(t)$. Practically, $\xi_a(t)$ is the moving average of $\xi(t)$. Also, an important propriety of M, which can be easily proved using Leibniz's integral rule, is that

$$\frac{d}{dt}\xi_a(t) = M\left\{\frac{d}{dt}\xi(t)\right\}, \tag{2.24}$$

Next, by applying the averaging operator M to the switched affine system (2.15), we obtain

$$\begin{aligned}
\dot{\tilde{\boldsymbol{x}}}_a(t) &= \frac{\tau}{T}\tilde{\boldsymbol{A}}_0 \underbrace{\frac{1}{\tau}\int_{t-T}^{t-T+\tau} \tilde{\boldsymbol{x}}(s)\, ds}_{\approx \tilde{\boldsymbol{x}}_a} + \frac{T-\tau}{T}\tilde{\boldsymbol{A}}_1 \underbrace{\frac{1}{T-\tau}\int_{t-T+\tau}^{t} \tilde{\boldsymbol{x}}(s)\, ds}_{\approx \tilde{\boldsymbol{x}}_a} + \\
&+ \tilde{\boldsymbol{b}}_0 \frac{1}{T}\int_{t-T}^{t-T+\tau} ds + \tilde{\boldsymbol{b}}_1 \frac{1}{T}\int_{t-T+\tau}^{t} ds \\
\tilde{\boldsymbol{y}}_a(t) &= \frac{\tau}{T}\tilde{\boldsymbol{C}}_0 \underbrace{\frac{1}{\tau}\int_{t-T}^{t-T+\tau} \tilde{\boldsymbol{x}}(s)\, ds}_{\approx \tilde{\boldsymbol{x}}_a} + \frac{T-\tau}{T}\tilde{\boldsymbol{C}}_1 \underbrace{\frac{1}{T-\tau}\int_{t-T+\tau}^{t} \tilde{\boldsymbol{x}}(s)\, ds}_{\approx \tilde{\boldsymbol{x}}_a}
\end{aligned} \tag{2.25}$$

The above marked expressions refer to the approximation of the average over a certain subinterval of the whole period (τ or T-τ), with the average over the entire period (T); this is specific to the state space averaging approach. By further calculating the remaining integral terms, it results that

$$\begin{aligned}
\dot{\tilde{\boldsymbol{x}}}_a(t) &= \tilde{\boldsymbol{A}}_a \tilde{\boldsymbol{x}}_a(t) + \tilde{\boldsymbol{b}}_a, \\
\tilde{\boldsymbol{y}}_a(t) &= \tilde{\boldsymbol{C}}_a \tilde{\boldsymbol{x}}_a(t)
\end{aligned} \tag{2.26}$$

with

$$\tilde{\boldsymbol{A}}_a = d_0\tilde{\boldsymbol{A}}_0 + d_1\tilde{\boldsymbol{A}}_1,\ \tilde{\boldsymbol{b}}_a = d_0\tilde{\boldsymbol{b}}_0 + d_1\tilde{\boldsymbol{b}}_1,\ \tilde{\boldsymbol{C}}_a = d_0\tilde{\boldsymbol{C}}_0 + d_1\tilde{\boldsymbol{C}}_1, \tag{2.27}$$

and where $d_0=\tau/T$ and $d_1=(T-\tau)/T$ are duty ratios ($d_0+d_1=1$). In particular, by considering that $\tau=T/3$, we arrive at the constant duty ratios $d_0=1/3$ and $d_1=2/3$.

The main problem with this result is that for the case of pulse-frequency modulation with constant duty ratios (which, as mention in chapter 2.2, is also the case of the cardiovascular system), the averaged model is invariant in respect with the modulation period T. Because the dynamics of the original (pulsatile) model is implicitly dependent on the period T, this means that such an averaged model can not be used in practice (for this class of pulse modulated systems).

2.5.2. Weighted averaging method

In order to address the above mentioned issue, a weighted averaging operator M_w is further defined as

$$\xi_{wa}(t) = M_w\{\xi(t)\} = \frac{1}{T}\int_{t-T}^{t} \xi(s)\ \ m(s,t)\,ds\ , \tag{2.28}$$

where the weighting function $m(s,t)$ is adopted as the exponential function

$$m(s,t) = e^{a\,(s-t+T)}, \tag{2.29}$$

with a as a tuning parameter (for $a=0$, the operator M_w reduces to the operator M). Notice that the function $m(s,t)$ moves as the moving average moves, on a given interval $[t\text{-}T,\ t)$, providing an monotonic increasing or decreasing weight (from value 1 to e^{aT}) which depends on the parameter T. Moreover, because the function is exponential, the operator M_w also has the propriety that

$$\frac{d}{dt}\xi_{wa}(t) = M_w\left\{\frac{d}{dt}\xi(t)\right\}. \tag{2.30}$$

By now applying the averaging operator M_w to the switched affine system (2.15), we obtain

$$\begin{aligned}
\dot{\tilde{\boldsymbol{x}}}_{wa}(t) = {} & \frac{\tau}{T}\tilde{\boldsymbol{A}}_0 \underbrace{\frac{1}{\tau}\int_{t-T}^{t-T+\tau} \tilde{\boldsymbol{x}}(s)\,m(s,t)\,ds}_{\approx\ \tilde{\boldsymbol{x}}_{wa}} + \frac{T-\tau}{T}\tilde{\boldsymbol{A}}_1 \underbrace{\frac{1}{T-\tau}\int_{t-T+\tau}^{t} \tilde{\boldsymbol{x}}(s)\,m(s,t)\,ds}_{\approx\ \tilde{\boldsymbol{x}}_{wa}} \\
& + \tilde{\boldsymbol{b}}_0\,\frac{1}{T}\int_{t-T}^{t-T+\tau} m(s,t)\,ds + \tilde{\boldsymbol{b}}_1\,\frac{1}{T}\int_{t-T+\tau}^{t} m(s,t)\,ds \\
\tilde{\boldsymbol{y}}_{wa}(t) = {} & \frac{\tau}{T}\tilde{\boldsymbol{C}}_0 \underbrace{\frac{1}{\tau}\int_{t-T}^{t-T+\tau} \tilde{\boldsymbol{x}}(s)\,m(s,t)\,ds}_{\approx\ \tilde{\boldsymbol{x}}_{wa}} + \frac{T-\tau}{T}\tilde{\boldsymbol{C}}_1 \underbrace{\frac{1}{T-\tau}\int_{t-T+\tau}^{t} \tilde{\boldsymbol{x}}(s)\,m(s,t)\,ds}_{\approx\ \tilde{\boldsymbol{x}}_{wa}}
\end{aligned} \tag{2.31}$$

The above marked approximations are similar with those for the conventional averaging approach – (2.25). After calculating the remaining integral terms, it results that

$$\begin{aligned}\dot{\tilde{\boldsymbol{x}}}_{wa}(t) &= \tilde{\boldsymbol{A}}_a\ \tilde{\boldsymbol{x}}_{wa}(t) + \tilde{\boldsymbol{b}}_{wa},\\ \tilde{\boldsymbol{y}}_{wa}(t) &= \tilde{\boldsymbol{C}}_a\ \tilde{\boldsymbol{x}}_{wa}(t)\end{aligned} \tag{2.32}$$

with

$$\tilde{\boldsymbol{b}}_{wa} = \theta_0\tilde{\boldsymbol{b}}_0 + \theta_1\tilde{\boldsymbol{b}}_1,\ \theta_0 = \frac{1}{aT}\left(e^{a\tau}-1\right),\ \theta_1 = \frac{1}{aT}\left(e^{aT}-e^{a\tau}\right). \tag{2.33}$$

The weighted averaged model (2.32) differs from the averaged model (2.26) through the terms θ_0 and θ_1, which are functions of T (recall that also τ=T/3). Thus, the dynamics of the averaged model is now dependent on T.

In some situations it could prove useful to further approximate θ_0 and θ_1 through linear interpolation as - $\theta_0 \approx \alpha_0+\beta_0 T$, $\theta_1 \approx \alpha_1+\beta_1 T$ - which are now affine functions in T. The approximation holds if T varies in a sufficiently small range.

2.5.3. Preliminary analysis and corrections

Until now, all the parameters of the pulse modulated switched system (2.15) were considered constant. In reality, some of them can vary, acting more like slow varying control inputs. From the point of view of the interaction between the cardiovascular system and the baroreflex feedback control loop, {T, E_s, R_1, x_T} play the role of control inputs for the cardiovascular system. The manner of obtaining the averaged models is still valid, under the hypothesis that these variations are slow enough such that these inputs can be considered constant during a modulation period T.

A generic issue reported in the literature for most averaging methods, refers to an offset error between the state trajectories of the averaged system and the evolution of the moving averages (real averages) of the state trajectories of the original (periodic) system. This offset error, which usually can not be expressed in an analytical manner, is dependent of the mentioned slow varying inputs, and has been pointed out and analyzed mostly in applications specific to the power electronics domain (e.g. [63], [64]). However, theoretical studies usually ignore this problem, due to the fact that they address only the issue of how close the state trajectory of the averaged systems is to the state trajectory of the original system (and not their moving average) - [1]-ch.10, [68]. We have found no general systematic solution for dealing with this offset error, without substantially increasing the complexity of the averaged model (as would results by applying the KBM method – additional 2nd order nonlinear terms - [63], or the multyfrequency method – additional states - [64]).

In this context, for addressing the offset error issue, we consider a multiplicative type correction of the system matrix for the weighted averaged model (2.32):

$$\begin{aligned}\dot{\tilde{\boldsymbol{x}}}_{wa}(t) &= \tilde{\boldsymbol{A}}_a\boldsymbol{M}_c\ \tilde{\boldsymbol{x}}_{wa}(t) + \tilde{\boldsymbol{b}}_{wa},\\ \tilde{\boldsymbol{y}}_{wa}(t) &= \tilde{\boldsymbol{C}}_a\ \tilde{\boldsymbol{x}}_{wa}(t)\end{aligned} \tag{2.34}$$

where the correction matrix is diagonal: $\mathbf{M}_c$= diag (ρ_0, ρ_1), with ρ_0 and ρ_1 as tuning parameters. By applying this correction to the weighted averaging method, we arrive at the following tuning parameters: a, ρ_0 and ρ_1. Considering that the slow varying inputs have some constant nominal values (except T), the tuning parameters could be determined by minimizing the following two errors:

$$\boldsymbol{\varepsilon}_{\Delta y} = \left| \Delta \tilde{\boldsymbol{y}}^{s}_{na} - \Delta \tilde{\boldsymbol{y}}^{s}_{wa} \right|, \quad \Delta \tilde{\boldsymbol{y}}^{s}_{na} = \tilde{\boldsymbol{y}}^{s1}_{na} - \tilde{\boldsymbol{y}}^{s2}_{na}, \; \Delta \tilde{\boldsymbol{y}}^{s}_{wa} = \tilde{\boldsymbol{y}}^{s1}_{wa} - \tilde{\boldsymbol{y}}^{s2}_{wa}, \tag{2.35}$$

$$\boldsymbol{\varepsilon}_{y} = \left| \tilde{\boldsymbol{y}}^{s}_{na} - \tilde{\boldsymbol{y}}^{s}_{wa} \right|, \tag{2.36}$$

The first error ($\varepsilon_{\Delta y}$) refers to a scenario involving a step variation of the input T from a value T_1 to another value T_2. The upper indexes s_1 and s_2 denote steady state (permanent periodic) regimes corresponding to T_1 and T_2, the lower index *wa* refers to values calculated analytically based on the an averaged model, while the index *na* refers to values determined numerically, as moving averages for the original periodic system (2.15). The second error (ε_y) refers to a steady state scenario with nominal values of the inputs (including T), where again, the lower index *wa* refers to the analytical value of the average, while *na* refers to the numerical value.

These two criteria can be used in different manners. For example, by following two steps:

Step 1. Determine the parameter a which minimizes the error $\varepsilon_{\Delta y}$, in the situation where the averaged model (2.32) is used.

Step 2. Determine the parameters ρ_0 and ρ_1 which minimize the error ε_y, in the situation where the averaged model (2.34) is used.

2.5.4. Averaged closed loop model

An averaged closed loop model of cardiovascular regulation, associated to the original (periodic) closed loop model given through Fig. 2.12, can be obtained by coupling the averaged model of the cardiovascular system (2.34) with the simplified model of the baroreflex system (2.17).

First we define the states $x_{Tp}(t) \triangleq T_{\Delta p}(t)$, $x_{Ts}(t) \triangleq T_{\Delta s}(t)$, $x_E(t) \triangleq E_s(t)$, $x_R(t) \triangleq R_1(t)$ and $x_V(t) \triangleq x_T(t)$[51]. This settles the situation on the direct path. For the feedback path, we will consider - as mentioned in section 2.4.1.1 - that the input to the baroreflex control loop is simply the averaged arterial pressure (average of P_{sa}), given by y_{wa1} from model (2.34).

Next, the averaged closed loop model is obtained as

[51] The considerations from the beginning of chapter 2.4- where R_p was replaced by R_1 and V_{uv} was replaced by x_T - apply here also. Moreover, for avoiding confusions with the states x_{Tp} and x_{Ts}, the state x_T is redefined as x_V.

$$
\begin{aligned}
\dot{x}_{wa0}(t) &= a_{00}\left(x_E(t)\right) x_{wa0}(t) + a_{01}\, x_{wa1}(t) + b_0\left(x_V(t), x_{Ts}(t), x_{Tp}(t)\right)\\
\dot{x}_{wa1}(t) &= a_{10}\left(x_E(t), x_R(t)\right) x_{wa0}(t) + a_{11}\left(x_R(t)\right) x_{wa1}(t) + b_1\left(x_V(t), x_{Ts}(t), x_{Tp}(t), x_R(t)\right)\\
\dot{x}_{Tp}(t) &= -\frac{1}{T_{Tp}} x_{Tp}(t) + \frac{1}{T_{Tp}} f_{sig,Tp}\left(C_1^{-1}\, x_{wa1}(t-\tau_{Tp})\right)\\
\dot{x}_{Ts}(t) &= -\frac{1}{T_{Ts}} x_{Ts}(t) + \frac{1}{T_{Ts}} f_{sig,Ts}\left(C_1^{-1}\, x_{wa1}(t-\tau_{Ts})\right)\\
\dot{x}_{E}(t) &= -\frac{1}{T_{E}} x_{E}(t) + \frac{1}{T_{E}} f_{sig,E}\left(C_1^{-1}\, x_{wa1}(t-\tau_{E})\right)\\
\dot{x}_{R}(t) &= -\frac{1}{T_{R}} x_{R}(t) + \frac{1}{T_{R}} f_{sig,R}\left(C_1^{-1} x_{wa1}(t-\tau_{R})\right)\\
\dot{x}_{V}(t) &= -\frac{1}{T_{V}} x_{V}(t) + \frac{1}{T_{V}} f_{sig,V}\left(C_1^{-1}\, x_{wa1}(t-\tau_{V})\right)
\end{aligned}
\qquad (2.37)
$$

with

$$
a_{00}\left(x_E(t)\right) = -\frac{\rho_0 d_0}{R_0} x_E(t) - \frac{\rho_0 d_1 E_d}{R_2} - \frac{\rho_0 d_1}{R_2 C_2},\ a_{01} = \frac{\rho_1 d_0}{R_0 C_1} - \frac{\rho_1 d_1}{R_2 C_2}
$$

$$
a_{10}\left(x_E(t), x_R(t)\right) = \frac{\rho_0 d_0}{R_0} x_E(t) - \frac{\rho_0}{C_2}\frac{1}{x_R(t)},
$$

$$
a_{11}\left(x_R(t)\right) = -\frac{\rho_1 d_0}{R_0 C_1} - \frac{\rho_1 C_1 + \rho_1 C_2}{C_1 C_2}\frac{1}{x_R(t)},
$$

$$
b_0\left(x_V(t), x_{Ts}(t), x_{Tp}(t)\right) = \frac{\alpha_1}{R_2 C_2} x_V(t) + \frac{\beta_1}{R_2 C_2} x_V(t)\left(-x_{Ts}(t) + x_{Tp}(t)\right),
$$

$$
\begin{aligned}
b_1\left(x_V(t), x_{Ts}(t), x_{Tp}(t), x_R(t)\right) = {} & \frac{\alpha_0 + \alpha_1}{C_2} x_V(t)\frac{1}{x_R(t)} + \\
& + \frac{\beta_0 + \beta_1}{C_2}\frac{1}{x_R(t)} x_V(t)\left(-x_{Ts}(t) + x_{Tp}(t)\right),
\end{aligned}
$$

$$
f_{sig,i}\left(C_1^{-1}\, x_{wa1}(t-\tau_i)\right) = \frac{x_i^{\Delta}}{1+\gamma_i\, e^{C_1^{-1} x_{wa1}(t-\tau_i) k_{ii}}} + x_i^{max},
$$

$$
k_{ii} = 1/k_i\ ,\ x_i^{\Delta} = x_i^{min} - x_i^{max}\ ,\ \gamma_i = e^{-P_{san} k_{ii}}\ ,\ i \in \{Tp, Ts, E, R, V\}.
$$

Since often we are interested in the outputs y_{wa0} and y_{wa1}[52], we can add the following output equations

$$
\begin{aligned}
y_{wa0}(t) &= d_0 x_E(t) x_{wa0}(t) + d_1 E_d x_{wa0}(t)\\
y_{wa1}(t) &= C_1^{-1} x_{wa1}(t)
\end{aligned}
\qquad (2.38)
$$

Finally, by defining the state vector $\boldsymbol{x_{ac}}(t)=[x_{wa0}(t)\ x_{wa1}(t)\ x_{wa1}(t-\tau_{Tp})\ x_{wa1}(t-\tau_{Ts})\ x_{wa1}(t-\tau_E)\ x_{wa1}(t-\tau_R)\ x_{wa1}(t-\tau_V)\ x_{Tp}(t)\ x_{Ts}(t)\ x_E(t)\ x_R(t)\ x_V(t)]^T$, and the output

[52] I.e. pressures Plv and Psa instead of the stressed volumes V_{lv}^S and V_{sa}^S.

vector $\boldsymbol{y_{ac}}(t)=[y_{wa0}(t)\ y_{wa1}(t)]^T$, the closed loop model can be written in condensed form as a nonlinear autonomous system

$$\begin{aligned}\dot{\boldsymbol{x}}_{ac} &= \boldsymbol{f}(\boldsymbol{x}_{ac})\\ \boldsymbol{y}_{ac} &= \boldsymbol{g}(\boldsymbol{x}_{ac})\end{aligned} \tag{2.39}$$

Notice that although the model is still strongly nonlinear and complex, it is considerably simpler than the one derived based on Fig. 2.12.

2.6. Simulations

This section will present simulation results with the original periodic models and the averaged models of the cardiovascular system – both in open loop and closed loop. In open loop, the control inputs for the cardiovascular system will change sequentially, in a certain predefined range. In closed loop, all the control inputs will change simultaneously, according to a predefined pathological scenario (induced by a disturbance signal acting on the control loop). This will give a comparative perspective of cardiovascular regulation, described through the averaged and non-averaged models, in both open loop and closed loop conditions.

2.6.1. Open loop simulations

For open loop evaluation of the obtained weighted averaged model (2.34), all the parameter values for the original pulsatile model (2.15) were taken from [61] - see Table 2.1, the duty ratios are $d_0=1/3$ and $d_1=2/3$, while the tuning parameters were determined as: a=-0.7, ρ_0=0.6 and ρ_1=1.0. Through linear interpolation, we obtain reasonable good approximations for θ_0 and θ_1 - $\theta_0\approx$0.33-0.03·T and $\theta_1\approx$0.61-0.18·T, on a physiological domain for T between 0.33 s and 2 s. The results are illustrated in Fig. 2.13 and Fig 2.14.

Fig. 2.13 refers to a scenario when only T varies – between 0.5 s and 1.5 s (i.e. the corresponding heart rate varies between 40 beats/min and 120 beats/min) – which from a physiological point of view is a large range. Notice that the trajectories of the averaged system follow relatively close the real moving averages of the original system as the modulation period changes. Without a weighted averaged approach as the one presented here, i.e. through a standard averaging approach, the averaged system would have been invariant in respect with the modulation period, and thus the trajectories would remain constant during the entire scenario.

Fig. 2.14 refers to a scenario where the transient responses are due to consecutive step changes of the slow varying inputs E_s, R_1 and x_T. It can be observed that although there is a certain offset error dependent on the inputs, the error remains in certain acceptable limits even for relatively large variations of the inputs (from a physiological point of view).

As a last remark, the spikes of P_{lv} are due to numerical errors ([61]), and have no physiological significance - thus not being of any importance in appreciating the averaging process.

Table 2.1 Parameter values of the cardiovascular model – open loop

Parameter	Value
R_0	0.01 mmHg ml^{-1} s
R_1	1.0 mmHg ml^{-1} s
R_2	0.03 mmHg ml^{-1} s
C_d	10 ml $mmHg^{-1}$
C_s	0.4 ml $mmHg^{-1}$
C_1	2.0 ml $mmHg^{-1}$
C_2	100.0 ml $mmHg^{-1}$
C_{0init}	0.4 ml $mmHg^{-1}$
$P_{lv,init}$	56 ml
$P_{sa,init}$	56 ml
$P_{v,init}$	16 ml
x_T	1734 ml

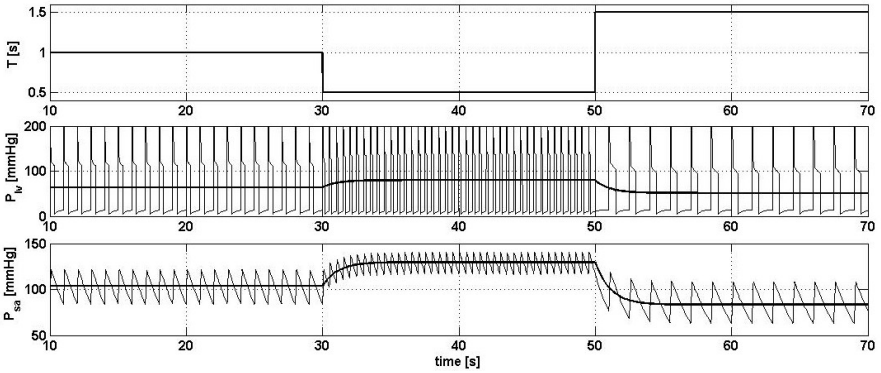

Fig.2.13. Transient response to changes in T (1 s→0.5 s at t=30s, 0.5 s→ 1.5 s at t=50s).

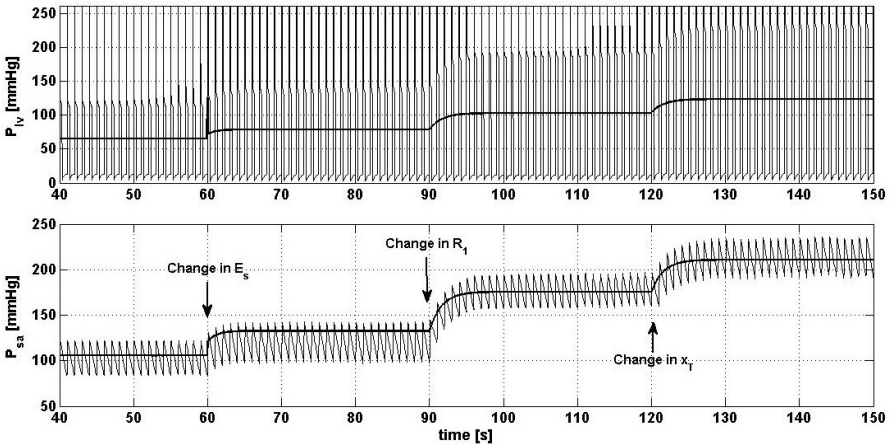

Fig.2.14. Transient response to changes in E_s (2.5→5, at t=60s), R_1 (1→2, at t=90s), and x_T (1734→2081, at t=120s).

2.6.2. Closed loop simulations

For the evaluation of the closed loop pulsatile model given by Fig. 2.12, we have calibrated the parameters of the simplified baroreflex model, based on the information from [39], [86], [87], [88], [89] and [90]. The obtained parameters are given in Table 2.2. For the closed loop averaged model (2.37), all the parameters remain the same, except those that set the slope of the sigmoids at central point (i.e. k_{iTp}, k_{iTs}, k_{iE}, k_{iR}, k_{iV}), which are adjusted in order to take into account the pulsatility effect on the baroreflex – because both experiments ([39]) and dither analysis ([80]) show a reduction of the baroreflex gains, we have considered a reduction by about one third of the central point slope for each sigmoid (i.e. the new parameters used for the averaged closed loop model are $k_{iTp}=0.7\cdot0.14$ mmHg^{-1}, $k_{iTs}=-0.7\cdot0.088$ mmHg^{-1}, $k_{iE}=-0.7\cdot0.088$ mmHg^{-1}, $k_{iR}=-0.7\cdot0.088$ mmHg^{-1}, $k_{iV}=-0.7\cdot0.088$ mmHg^{-1}).

Consider a pathological scenario involving an acute venous hemorrhage (10% total blood volume loss, i.e. about 500 ml). This can be regarded as a scenario where an additive disturbance acts on the control signal x_v, which in turn will influence the cardiovascular system. Fig. 2.15 illustrates the transient responses of the closed loop averaged model (2.37) and the original periodic closed loop model from Fig. 2.12, to a step variation of the disturbance at moment t=200 s. It can be noticed that the disturbance triggers a sudden drop in blood pressure (P_{sa}). The counteraction of the baroreflex control loop (through an increase in HR=1/T, E_s, R_1 and x_v) limits the drop in blood pressure, and further tries to bring it back as close as possible to its nominal value – a steady state control error does however remain (due to the lack of an integrator component).

Regarding the comparison between the response of the averaged model and the pulsatile model, it can be observed that the trajectory of the averaged model follows relatively close the average trajectory of the pulsatile model. Finally, it should be mentioned that the results are qualitatively in agreement with the data from [39] and [87], in respect with the same scenario – e.g. about 10% decrease in the average of P_{sa}, 15% increase in HR.

Table 2.2 Parameter values of simplified baroreflex model after calibration – closed loop pulsatile model

P_{san}= 100 mmHg				
T_d=6.37 s , T_p=2.08 s				
T_{Tp}=0.5 s	T_{Ts}=1.5 s	T_E=1.5 s	T_R=1.5 s	T_V=10 s
τ_{Tp}=0.2 s	τ_{Ts}=2 s	τ_E=2 s	τ_R=2 s	τ_V=5 s
x_{Tp}^{min} = 0.88 s	x_{Ts}^{min} = 0 s	x_E^{min} = 1.91 mmHg/ml	x_R^{min} = 0.6 mmHg s/ml	x_V^{min} =1385 ml
x_{Tp}^{max} = 1.44 s	x_{Ts}^{max} = 0.33 s	x_E^{max} = 3.10 mmHg/ml	x_R^{max} = 1.4 mmHg s/ml	x_V^{max} = 2085 ml
k_{iTp}=0.14 mmHg^{-1}	k_{iTs}=-0.088 mmHg^{-1}	k_{iE}=-0.088 mmHg^{-1}	k_{iR}=-0.088 mmHg^{-1}	k_{iV}=-0.088 mmHg^{-1}

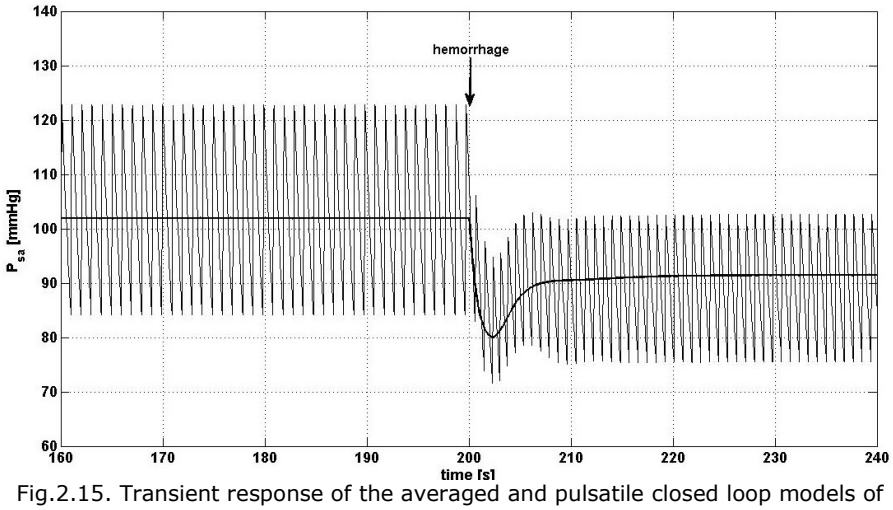

Fig.2.15. Transient response of the averaged and pulsatile closed loop models of cardiovascular regulation during an acute hemorrhage scenario.

2.7. Conclusions

In this chapter a closed-loop averaged model for the cardiovascular system, along with its corresponding nervous control, has been developed.

First, a classical model of the cardiovascular system is brought to the form of a switched system. An averaging methodology for the cardiovascular system is proposed, with a general applicability to pulse-frequency modulated switched systems. Through averaging, a simpler model is obtained, which approximates the original periodic model. Although an upper bound for the approximation error is not guaranteed, like in the case of other approximation methods for nonlinear systems (e.g. the describing function method), practice shows that the approximation is usually good enough, providing answers (solutions) where none existed before ([91]-pp. 13).

Second, a simplified model for the nervous control (baroreflex mechanism) is derived, starting from a well known model from the literature.

Finally, a closed loop simplified model of cardiovascular regulation is obtained, along with its corresponding averaged model. Simulation results show how the averaged cardiovascular model approximates the original pulsatile model, both in open loop and closed loop scenarios. The simplicity of the closed loop averaged model makes it suitable for further stability analyses of cardiovascular regulation.

3. THEORETICAL FRAMEWORK FOR AVERAGING A CLASS OF PULSE MODULATED SYSTEMS

3.1. Introduction

Averaging theory has been widely used for approximating nonlinear systems, and thus facilitating future analysis and control design approaches. Especially for the class of periodic (quasi-periodic) systems, averaging methods permit one to obtain a simpler non-periodic system, which approximates to a certain degree the original system. Applications of averaging can be found in power electronics ([91]), pneumatic systems ([92]), robotic manipulators ([93]), adaptive control ([94]), vibrational control ([3]-vol.3-ch.52), switched controllers ([69]), extremum seeking control ([96]), synchronization of oscillators ([97]), multi-agent systems ([98]) and congestion control ([99]).

Over the years, several averaging methods have been proposed, ranging from rather heuristic or application oriented methods to theoretical methods for specific classes of systems. In power electronics, the circuit averaging and state space averaging methods were among the first to be used in applications. The circuit averaging method involves averaging the waveforms of the signals and manipulations of the circuit diagram (different circuit parts are replaced with equivalent ones), which requires a physical insight of the system ([65]). The state space averaging method provides a more general framework, with a simpler a more straightforward methodology, by averaging directly the equations of the state space model associated to the system ([65]). The results obtained with the state space averaging method are equivalent with those obtained by averaging based on perturbation theory ([1]-ch. 10) or through the Krylov-Bogoliubov-Mitropolsky (KBM) averaging method of 1st order ([63]); however both of these methods provide additional theoretical guarantees on the approximation error involved in the averaging process. An increase in the accuracy of the approximation (with the price of increased complexity of the averaged model) is obtained either by using a KBM averaging method of 2nd order ([95]), or through a multifrequency averaging approach ([64]) and ([100]), which implies the use of a generalized average defined based on Fourier series. When the periodic behavior is induced by a relatively high-frequency signal at the input of a static nonlinearity, other approaches are that of the dithering technique – ([66]) and ([101]), or the incremental-input describing function (an extension of the describing function method) – ([67]), which both finally lead to replacing the original nonlinearity by an equivalent (averaged) nonlinearity. Finally, recent studies focus on developing averaging methods for hybrid systems ([68]) and ([102]), and systems with disturbances ([103]).

Pulse modulated systems are widely encountered in both technical control applications ([104]) and biological control mechanisms ([73]). Although many averaging methods have been proposed in conjunction with pulse modulated systems, most of them actually deal with pulse-width modulation (used especially in power electronics). However, some control applications use pulse-frequency

modulation (e.g. [85]), while many biological systems also exhibit pulse-frequency modulation (neural structures) – ([73]). As it will be shown through the case study presented in this chapter (referring to the cardiovascular system – regarded as a pulse-frequency modulated system[53] controlled by the nervous system), there are even some situations when the pulse-frequency modulation is with constant duty ratios and the moving-averages of the system's trajectories are dependent on the modulation frequency (or period). In such a context, conventional averaging approaches usually lead to frequency independent averaged models, which can not properly approximate the original periodic system.

In addressing this issue, the current chapter[54] proposes a new period-weighted averaging approach, which leads to a period-dependent averaged model, while also maintaining the averaged model as simple as possible. In the first part of the chapter a theoretical framework is developed for the period-weighted averaging method using perturbation theory, in order to ensure an error bound for the approximation between the original systems and the averaged system, and also to relate the stability of the averaged system with that of the original system. In the second part of the chapter, a step-by-step description is provided, on how the proposed averaging method can be used in a case study referring to the cardiovascular system from chapter 2, while pointing out ways of copping with the practical issues that emerge.

3.2. Problem formulation

Consider the class of nonlinear systems

$$\dot{\boldsymbol{x}} = \boldsymbol{f}(t, \boldsymbol{x}) \tag{3.1}$$

characterized by a periodic regime of period T, such that $\mathbf{f}(t,\mathbf{x})=\mathbf{f}(t+T,\mathbf{x})$.

Assumption 3.1: **f** is piecewise continuous in t and locally Lipschitz in **x**.

Assumption 3.2: The system (3.1) can be approximated by a piecewise continuous system, with a finite number of points of discontinuity, and with the left hand side expressed as

$$\boldsymbol{f}(t,\boldsymbol{x}) = \begin{cases} \boldsymbol{f}_1(\boldsymbol{x}), & nT \le t < (n+d_1)T \\ \boldsymbol{f}_2(\boldsymbol{x}), & (n+d_1)T \le t < (n+d_1+d_2)T \\ \quad\vdots & \\ \boldsymbol{f}_m(\boldsymbol{x}), & (n+d_1+d_2\ldots+d_{m-1})T \le t < (n+1)T \end{cases}, \tag{3.2}$$

$$\sum_{i=1}^{m} d_i = 1,\ n \in \mathcal{N},$$

where the duty ratios d_i are considered to be constant.

In order to state the main problem addressed in this paper, the system (3.1) is rewritten- with the right hand side (3.2) - as

$$\dot{\boldsymbol{x}} = \tilde{\boldsymbol{f}}(\omega t, \boldsymbol{x}) \tag{3.3}$$

[53] See chapter 2.
[54] The results of this chapter have been published in [105].

with the angular frequency $\omega=2\pi/T$, and where

$$\tilde{\boldsymbol{f}}(\omega t,\boldsymbol{x})=\begin{cases}\boldsymbol{f}_1(\boldsymbol{x}), & 2\pi n\le\omega t<2\pi(n+d_1)\\ \boldsymbol{f}_2(\boldsymbol{x}), & 2\pi(n+d_1)\le\omega t<2\pi(n+d_1+d_2)\\ \vdots & \\ \boldsymbol{f}_m(\boldsymbol{x}), & 2\pi(n+d_1+d_2+\ldots d_{m-1})\le\omega t<2\pi(n+1)\end{cases}. \tag{3.4}$$

Moreover, in accordance with Assumption 3.2, the system can be recasted as a pulse-modulated switched system, with a switching function $q:[0,\infty)\to\{1,2,\ldots m\}$:

$$\dot{\boldsymbol{x}}=\tilde{\boldsymbol{f}}_{q(\omega t)}(\boldsymbol{x}),\ q(\omega t)=\begin{cases}1, & 2\pi n\le\omega t<2\pi(n+d_1)\\ 2, & 2\pi(n+d_1)\le\omega t<2\pi(n+d_1+d_2)\\ \vdots & \\ m, & 2\pi(n+d_1+d_2+\ldots d_{m-1})\le\omega t<2\pi(n+1)\end{cases}. \tag{3.5}$$

Next, through a time scaling of the form $\tau=\omega t$, system (3.3) becomes

$$\boldsymbol{x}'=\frac{1}{\omega}\tilde{\boldsymbol{f}}(\tau,\boldsymbol{x}) \tag{3.6}$$

where $\boldsymbol{x}'=d\boldsymbol{x}/d\tau$ and $\tilde{\boldsymbol{f}}(\tau,\boldsymbol{x})=\tilde{\boldsymbol{f}}(\tau+2\pi,\boldsymbol{x})$. Finally, by adopting the small positive parameter $\varepsilon=1/\omega$, (3.6) can be brought to the "standard" form

$$\boldsymbol{x}'=\varepsilon\,\tilde{\boldsymbol{f}}(\tau,\boldsymbol{x}),\quad \boldsymbol{x}(0)=\boldsymbol{x}_0. \tag{3.7}$$

The trajectories of (3.7) describe a periodic orbit Γ, which is dependent on the modulation period T. It will be further considered, as a working hypothesis, that the (geometric) center χ of the periodic orbit Γ is also dependent on the modulation period T (i.e. $\chi\overset{\Delta}{=}\chi(T)$); the center corresponds to an average operation point Λ of the periodic system.

In the above presented context, the problem addressed in the current study is as follows:

Problem statement: Determine an averaged system which approximates the original periodic system (3.7) within a certain error bound and which is dependent on the modulation period T.

The novelty of the current problem formulation consists in the fact that the averaged system has to be dependent on the modulation period T. Standard averaging approaches (like the one from [1]-ch. 10.4) fail in addressing this problem. In particular, for the periodic system (3.7), the standard averaging method associates the following averaged system

$$\boldsymbol{x}'_{av}=\varepsilon\,\tilde{\boldsymbol{f}}_{av}(\boldsymbol{x}_{av}) \tag{3.8}$$

with

$$\tilde{\boldsymbol{f}}_{av}(\boldsymbol{x})=\frac{1}{2\pi}\int_{\tau-2\pi}^{\tau}\tilde{\boldsymbol{f}}(s,\boldsymbol{x})\,ds \tag{3.9}$$

Returning to the absolute time ($t=\tau/\omega$), yields

$$\dot{\boldsymbol{x}}_{av} = \tilde{\boldsymbol{f}}_{av}(\boldsymbol{x}_{av}) \tag{3.10}$$

By taking into account that $\tilde{\boldsymbol{f}}$ was defined also through (3.4), one further obtains

$$\tilde{\boldsymbol{f}}_{av}(\boldsymbol{x}) = \sum_{i=1}^{m} d_i \, \tilde{\boldsymbol{f}}_i(\boldsymbol{x}) \tag{3.11}$$

Therefore, the averaged system (3.10) is independent of the modulation period T, and can not properly approximate the original periodic system (3.3) when the average operation point Λ changes as function of the period T.

Remark 3.1 Even though the study deals with pulse-frequency modulated systems, in which the period T actually varies in time, it is considered that these variations are relatively slow in respect with the duration of a period T, and as a consequence the averaging approach considers T to be constant ($T=T_{max}$). However, the emphasis is that the resulting averaged model should be T dependent, such that T becomes a new slow-varying input of the averaged system.

3.3. Theoretical framework

In addressing the problem stated in the previous section, a period-weighting averaging approach for system (3.7) will be considered. First, an additional simplifying assumption is imposed.

Assumption 3.3: Suppose $\tilde{\boldsymbol{f}}$ can be decomposed as $\tilde{\boldsymbol{f}}(\tau,\boldsymbol{x}) = \tilde{\boldsymbol{f}}_0(\tau,\boldsymbol{x}) + \tilde{\boldsymbol{g}}(\tau)$, where the piecewise continuous functions $\tilde{\boldsymbol{f}}_0$ and $\tilde{\boldsymbol{g}}$ are also periodic, and defined in a similar manner as $\boldsymbol{f}$.

Next, the following time averaged functions are defined:

$$\begin{aligned} \tilde{\boldsymbol{f}}_{0,av}(\boldsymbol{x}) &= \frac{1}{2\pi} \int_{\tau-2\pi}^{\tau} \tilde{\boldsymbol{f}}_0(s,\boldsymbol{x})\, ds \\ \tilde{\boldsymbol{g}}_{av}(T) &= \frac{1}{2\pi} \int_{\tau-2\pi}^{\tau} \tilde{\boldsymbol{g}}(s)\, m(s,T)\, ds \end{aligned} \tag{3.12}$$

where m(s,T) is a weighting function with the (fixed) parameter T, on the interval $s\in(\tau-2\pi,\tau)$; e.g. $m(s,T)=e^{aT(s-\tau+2\pi)/(2\pi)}$, with a as a tuning parameter. One can note that for a=0, the standard averaging approach can be recovered.

Remark 3.2: Although a weighted average directly for the function $\tilde{\boldsymbol{f}}$ could have been defined, i.e. without the decomposition given by Assumption 3.3, the mixed averaging approach given by (3.12) has been chosen instead because it leads to a simpler averaged model. Moreover, it is expected that the $\tilde{\boldsymbol{g}}$ component is the main cause for why the average operation point Λ changes as function of the period T.

Let us associate to (3.7) the following averaged system:

$$\boldsymbol{x}'_{av} = \varepsilon \, \tilde{\boldsymbol{f}}_{av}(\boldsymbol{x}_{av}, T), \quad \boldsymbol{x}_{av}(0) = \boldsymbol{x}_{av0}, \tag{3.13}$$

where the left hand side is obtained through (3.12) as $\tilde{\boldsymbol{f}}_{av}(\boldsymbol{x}_{av}, T) = \tilde{\boldsymbol{f}}_{0,av}(\boldsymbol{x}_{av}) + \tilde{\boldsymbol{g}}_{av}(T)$.

Finally, by returning to the absolute time, one obtains the averaged system associated to (3.1):

$$\dot{\boldsymbol{x}}_{av} = \boldsymbol{f}_{av}(\boldsymbol{x}_{av}, T) \tag{3.14}$$

Assumption 3.4: $\mathbf{f}_{av}$ is locally Lipschitz in respect with $\boldsymbol{x}_{av}$.

Remark 3.3 Considering the particular choice of the weighting function $m(s,T)=e^{aT(s-\tau+2\pi)/(2\pi)}$, and that the function $\tilde{\boldsymbol{g}}$ is defined in a similar piecewise manner as $\mathbf{f}$, it is sometimes useful to approximate de averaged function $\tilde{\boldsymbol{g}}_{av}$ from (3.12) as:

$$\begin{aligned}
\tilde{\boldsymbol{g}}_{av}(T) &= \frac{1}{2\pi} \int_{\tau-2\pi}^{\tau} \tilde{\boldsymbol{g}}(s)\, e^{aT(s-\tau+2\pi)/(2\pi)}\, ds \\
&= \frac{1}{2\pi} \sum_{i=1}^{m} \tilde{\boldsymbol{g}}_i \int_{\tau-2\pi+2\pi d_1+\ldots 2\pi d_{i-1}}^{\tau-2\pi+2\pi d_1+\ldots 2\pi d_i} e^{aT(s-\tau+2\pi)/(2\pi)}\, ds = \\
&= \sum_{i=1}^{m} \tilde{\boldsymbol{g}}_i \frac{1}{aT} e^{aT(s-\tau+2\pi)/(2\pi)} \Big|_{\tau-2\pi+2\pi d_1+\ldots 2\pi d_{i-1}}^{\tau-2\pi+2\pi d_1+\ldots 2\pi d_i} \approx \sum_{i=1}^{m} \tilde{\boldsymbol{g}}_i \underbrace{(\alpha_i + \beta_i T)}_{\theta_i}
\end{aligned} \tag{3.15}$$

where the coefficients of θ_i can be determined either through a first order Taylor series expansion or linear interpolation. Such an approximation further simplifies the resulting averaged model, and holds for a sufficiently small range of T. Moreover, the theoretical results further presented hold even when this approximation is used, instead of the original function $\tilde{\boldsymbol{g}}_{av}$ from (3.12).

Next, the following theorem provides a bound on the closeness between the trajectories of the averaged system and original system. The proof is inspired from [1]-ch. 10.4, and adapted for the weighted averaged case defined through (3.12).

Theorem 3.1: If the initial conditions for (3.7) and (3.13) are such that $\|\boldsymbol{x}(0) - \boldsymbol{x}_{av}(0)\| = O(\varepsilon)$, then for a sufficiently small ε, there exists a positive constant *b*, such that (3.13) represents an $O(\varepsilon)$ approximation of (3.7) on the time interval $[0,\ b/\varepsilon]$, i.e.:

$$\|\boldsymbol{x}(\tau/\omega) - \boldsymbol{x}_{av}(\tau/\omega)\| = O(\varepsilon), \quad \tau \in [0,\ b/\varepsilon]. \tag{3.16}$$

□

Proof: The following functions are defined:

$$\boldsymbol{h}(\tau, \boldsymbol{x}) = \tilde{\boldsymbol{f}}(\tau, \boldsymbol{x}) - \tilde{\boldsymbol{f}}_{av}(\boldsymbol{x}) - \varphi(T) \tag{3.17}$$

with the function φ adopted such that **h** has zero mean

$$\varphi(T)=\begin{cases}\dfrac{1}{2\pi}\displaystyle\int_{\tau-2\pi}^{\tau}\tilde{\boldsymbol{g}}(s)\,ds-\dfrac{1}{2\pi}\int_{\tau-2\pi}^{\tau}\tilde{\boldsymbol{g}}(s)\,m(s,T)\,ds\,, & T\neq 0\\ 0, & T=0\end{cases} \tag{3.18}$$

and

$$\boldsymbol{u}(\tau,\boldsymbol{x})=\int_{0}^{\tau}\boldsymbol{h}(s,\boldsymbol{x})\,ds\,. \tag{3.19}$$

Assumption 3.5 The function φ is locally Lipschitz in respect with T.

Remark 3.4 It can be shown that for the class of weighting functions $m(s,T)=e^{aT(s-\tau+2\pi)/(2\pi)}$, the function φ is of class C^1, and as a result it is also locally Lipschitz.

By taking into account how ε was defined, it can be noticed that φ is actually a function of ε: $\varphi(T)=\varphi(2\pi\varepsilon)$. Thus, φ is also Lipschitz in respect with ε.

The functions **u** and **h** are periodic in τ, and **u** is bounded. It can be shown that the partial derivatives of **u**

$$\frac{\partial\boldsymbol{u}}{\partial\tau}=\boldsymbol{h}(\tau,\boldsymbol{x}),\quad \frac{\partial\boldsymbol{u}}{\partial\boldsymbol{x}}=\int_{0}^{\tau}\frac{\partial\boldsymbol{h}}{\partial\boldsymbol{x}}(s,\boldsymbol{x})\,ds\,, \tag{3.20}$$

are also periodic in τ and bounded.

Next, consider the system (3.7), with the following change of variables:

$$\boldsymbol{x}=\boldsymbol{y}+\varepsilon\boldsymbol{u}(\tau,\boldsymbol{y})\,. \tag{3.21}$$

Differentiating both the left hand side and the right hand side in respects with τ leads to

$$\frac{d\boldsymbol{x}}{d\tau}=\frac{d\boldsymbol{y}}{d\tau}+\varepsilon\frac{\partial\boldsymbol{u}}{\partial\tau}+\varepsilon\frac{\partial\boldsymbol{u}}{\partial\boldsymbol{y}}\frac{d\boldsymbol{y}}{d\tau}\,. \tag{3.22}$$

Further using (3.7), (3.17) and (3.20), expression (3.22) becomes

$$\begin{aligned}\left[\boldsymbol{I}+\varepsilon\frac{\partial\boldsymbol{u}}{\partial\boldsymbol{y}}\right]\frac{d\boldsymbol{y}}{d\tau}&=\varepsilon\tilde{\boldsymbol{f}}(\tau,\boldsymbol{y}+\varepsilon\boldsymbol{u})-\varepsilon\frac{\partial\boldsymbol{u}}{\partial\tau}\\ &=\varepsilon\tilde{\boldsymbol{f}}(\tau,\boldsymbol{y}+\varepsilon\boldsymbol{u})-\varepsilon\tilde{\boldsymbol{f}}(\tau,\boldsymbol{y})+\varepsilon\tilde{\boldsymbol{f}}_{av}(\boldsymbol{y})+\varepsilon\varphi(2\pi\varepsilon)\\ &=\varepsilon\tilde{\boldsymbol{f}}_{av}(\boldsymbol{y})+\varepsilon\left[\tilde{\boldsymbol{f}}(\tau,\boldsymbol{y}+\varepsilon\boldsymbol{u})-\tilde{\boldsymbol{f}}(\tau,\boldsymbol{y})\right]+\varepsilon\left[\varphi(2\pi\varepsilon)-\varphi(0)\right]\end{aligned} \tag{3.23}$$

Because $\tilde{\boldsymbol{f}}$ is Lipschitz in $\boldsymbol{y}$ and φ is Lipschitz in ε, the differences of the right hand side can be expressed as $\left\|\tilde{\boldsymbol{f}}(\tau,\boldsymbol{y}+\varepsilon\boldsymbol{u})-\tilde{\boldsymbol{f}}(\tau,\boldsymbol{y})\right\|=O(\varepsilon)$ and $\left\|\varphi(2\pi\varepsilon)-\varphi(0)\right\|=O(\varepsilon)$. Also, because $\partial\boldsymbol{u}/\partial\boldsymbol{y}$ is bounded, the matrix $\boldsymbol{I}+\varepsilon\,\partial\boldsymbol{u}/\partial\boldsymbol{y}$

is nonsingular for sufficiently small ε, and its inverse can be written as

$$\left[\boldsymbol{I}+\varepsilon\frac{\partial \boldsymbol{u}}{\partial \boldsymbol{y}}\right]^{-1}=\boldsymbol{I}+O(\varepsilon) \tag{3.24}$$

As a result, (3.23) becomes

$$\boldsymbol{y}'=\varepsilon\tilde{\boldsymbol{f}}_{av}(\boldsymbol{y})+\varepsilon^2\,\boldsymbol{q}(\tau,\boldsymbol{y},\varepsilon)\,, \tag{3.25}$$

where $\boldsymbol{q}$ is a periodic function in τ, bounded, with first partial derivatives with respect to **y** and ε continuous and bounded.

Further on, (3.25) is compared with the averaged system (3.13). By integrating both sides and subtracting the resulting equations yields

$$\begin{aligned}&\boldsymbol{y}(\tau/\omega)-\boldsymbol{x}_{av}(\tau/\omega)=\boldsymbol{y}(0)-\boldsymbol{x}_{av}(0)+\\&+\varepsilon\int_0^{\tau}\left[\tilde{\boldsymbol{f}}_{av}(\boldsymbol{y}(s))-\tilde{\boldsymbol{f}}_{av}(\boldsymbol{x}_{av}(s),T)\right]ds+\varepsilon^2\int_0^{\tau}\boldsymbol{q}(s,\boldsymbol{y}(s),\varepsilon)\,ds\,.\end{aligned} \tag{3.26}$$

Taking the norm of the above expression and applying the triangle inequality leads to

$$\begin{aligned}&\left\|\boldsymbol{y}(\tau/\omega)-\boldsymbol{x}_{av}(\tau/\omega)\right\|\le\left\|\boldsymbol{y}(0)-\boldsymbol{x}_{av}(0)\right\|+\\&+\varepsilon\int_0^{\tau}\left\|\tilde{\boldsymbol{f}}_{av}(\boldsymbol{y}(s))-\tilde{\boldsymbol{f}}_{av}(\boldsymbol{x}_{av}(s),T)\right\|ds+\varepsilon^2\int_0^{\tau}\left\|\boldsymbol{q}(s,\boldsymbol{y}(s),\varepsilon)\right\|ds\,.\end{aligned} \tag{3.27}$$

The following notation can be introduced $\left\|\boldsymbol{y}(\tau/\omega)-\boldsymbol{x}_{av}(\tau/\omega)\right\|=\boldsymbol{\xi}(\tau/\omega)$. Using the fact that $\tilde{\boldsymbol{f}}_{av}$ is Lipschitz (with Lipschitz constant *L*) and that $\boldsymbol{q}$ is bounded (i.e. the norm is bounded by a positive constant μ), (3.27) becomes

$$\boldsymbol{\xi}(\tau/\omega)\le\boldsymbol{\xi}(0)+\varepsilon L\int_0^{\tau}\boldsymbol{\xi}(s)ds+\varepsilon^2\mu\,\tau\,. \tag{3.28}$$

The further use of Gronwall-Belman's inequality with respect to $\boldsymbol{\xi}$ yields

$$\boldsymbol{\xi}(\tau/\omega)\le\left[\boldsymbol{\xi}(0)+\frac{\varepsilon\mu}{L}\right]e^{\varepsilon L\tau} \tag{3.29}$$

Therefore, when $\left\|\boldsymbol{y}(0)-\boldsymbol{x}_{av}(0)\right\|=O(\varepsilon)$ one has $\left\|\boldsymbol{y}(\tau/\omega)-\boldsymbol{x}_{av}(\tau/\omega)\right\|=O(\varepsilon)$ for $\tau<1/(\varepsilon L)$. Through the change of variables (3.21) it result that $\left\|\boldsymbol{x}(\tau/\omega)-\boldsymbol{y}(\tau/\omega)\right\|=O(\varepsilon)$. By further using the triangle inequality one obtains

$$\left\|\boldsymbol{x}(\tau/\omega)-\boldsymbol{x}_{av}(\tau/\omega)\right\|\le\left\|\boldsymbol{x}(\tau/\omega)-\boldsymbol{y}(\tau/\omega)\right\|+\left\|\boldsymbol{y}(\tau/\omega)-\boldsymbol{x}_{av}(\tau/\omega)\right\| \tag{3.30}$$

thus finally reaching the result (3.16), with $b=1/L$.

■

In order to extend this result to the infinite time interval, one must add a stability condition.

Theorem 3.2: If the system (3.13) is exponentially stable and $\|\boldsymbol{x}(0)-\boldsymbol{x}_{av}(0)\|=O(\varepsilon)$, then for sufficiently small ε, (3.13) represents an $O(\varepsilon)$ approximation of (3.7):

$$\|\boldsymbol{x}(\tau/\omega)-\boldsymbol{x}_{av}(\tau/\omega)\|=O(\varepsilon),\quad \tau\in[0,\infty] \tag{3.31}$$

□

Proof: Through the change of variables $v=\varepsilon\tau$, (3.25) is brought the form of a perturbed system

$$\frac{d\boldsymbol{y}}{dv}=\tilde{\boldsymbol{f}}_{av}(\boldsymbol{y})+\varepsilon\boldsymbol{q}(v/\varepsilon,\boldsymbol{y},\varepsilon) \tag{3.32}$$

associated to the nominal system

$$\frac{d\boldsymbol{y}}{dv}=\tilde{\boldsymbol{f}}_{av}(\boldsymbol{y}). \tag{3.33}$$

This is now a standard perturbation problem. Therefore, Theorem 9.1 from [1]-ch. 9 can be used for proving the $O(\varepsilon)$ closeness between the solutions of (3.32) and (3.33), when the term $\varepsilon\mathbf{q}$ denotes a persistent perturbation, but bounded. The basic idea is to build a system given by the difference between (3.32) and (3.33), with the error between the two corresponding trajectories as state variable. Assuming that the corresponding unperturbed system is exponentially stable, and that the perturbation is bounded in a certain sense, the comparison method provides an upper bound for the solution of the perturbed system. Finally, this means that also the solutions in the τ time scale are $O(\varepsilon)$ close.

■

Finally, from the stability of the averaged system, the stability of the original (periodic) system can be inferred.

Theorem 3.3: If the system (3.13) is exponentially stable, then for sufficiently small ε, the system (3.7) is orbitally exponentially stable.

□

Proof: Again, one can make use of the system in perturbed form, given through (3.32), and its nominal version (3.33). This is now regarded as a periodic perturbation problem. In this case, Theorem 10.3 from [1]-ch. 10 provides the desired stability result. The basic idea is to regard the term $\varepsilon\mathbf{q}$ as a periodic perturbation. A change of variables of the form $\mathbf{z}=\mathbf{y}-\mathbf{y}^p$ ($\mathbf{y}^p$ is the periodic solution of (3.32)), and then a linearization at the origin, brings the system to a perturbed form (still linearized) with a vanishing perturbation. The stability is inferred from the stability of the unperturbed system. Moreover, because one deals with exponential stability, the stability of the linearized system finally implies that of the original nonlinear system.

■

3.4. Case study

Consider the averaging problem for the dynamics of the cardiovascular system, modelled as a pulse frequency modulated switched system as in chapter 2 (the cardiovascular system is regarded as a plant controlled through pulse modulation by the nervous system):

$$\dot{\boldsymbol{x}} = \boldsymbol{A}_{q(\omega t)}\boldsymbol{x} + \boldsymbol{b}_{q(\omega t)} \tag{3.34a}$$

$$\boldsymbol{y} = \boldsymbol{C}_{q(\omega t)}\boldsymbol{x} \tag{3.34b}$$

with the state and output vectors $\mathbf{x}=[x_0\ x_1]^T$ and $\mathbf{y}=[y_0\ y_1]^T$ (denoting ventricular and arterial stressed blood volume, respectively ventricular and arterial blood pressure), the T periodic switching signal $q:[0,\infty)\to\{0,1\}$ (mechanism of cardiac contraction), expressed as

$$q(\omega t) = \begin{cases} 0, & 2\pi n \le \omega t < 2\pi(n+d_0) \\ 1, & 2\pi(n+d_0) \le \omega t < 2\pi(n+1) \end{cases},$$

$$d_0 = \frac{\Delta t_0}{T}, d_1 = \frac{\Delta t_1}{T}, d_0 + d_1 = 1,$$

and where

$$\boldsymbol{A}_0 = \begin{bmatrix} -\frac{E_s}{R_0} & \frac{1}{R_0 C_1} \\ \frac{E_s}{R_0} - \frac{1}{R_1 C_2} & -\frac{1}{R_0 C_1} - \frac{1}{R_1 C_1} - \frac{1}{R_1 C_2} \end{bmatrix}, \boldsymbol{b}_0 = \begin{bmatrix} 0 \\ \frac{x_T}{R_1 C_2} \end{bmatrix},$$

$$\boldsymbol{A}_1 = \begin{bmatrix} -\frac{E_d}{R_2} - \frac{1}{R_2 C_2} & -\frac{1}{R_2 C_2} \\ -\frac{1}{R_1 C_2} & -\frac{1}{R_1 C_1} - \frac{1}{R_1 C_2} \end{bmatrix}, \boldsymbol{b}_1 = \begin{bmatrix} \frac{x_T}{R_2 C_2} \\ \frac{x_T}{R_1 C_2} \end{bmatrix},$$

$$\boldsymbol{C}_0 = diag\left(E_s, \frac{1}{C_1}\right), \boldsymbol{C}_1 = diag\left(E_d, \frac{1}{C_1}\right).$$

The parameters have the following interpretation: T represents the duration of the heart period (with the two subintervals denoting duration of systole and diastole); R_0, R_1 and R_2 represent hydraulic resistances; C_1, C_2 represent hydraulic capacitance (compliance), while E_s and E_d represent systolic and diastolic elastances (inverse of compliance); x_T represents total stressed blood volume.[55]

First, the averaged output equation (3.34b) is defined as

$$\boldsymbol{y}_{av} \overset{\Delta}{=} \frac{1}{T}\int_{t-T}^{T} \boldsymbol{C}_{q(t)}\boldsymbol{x}\, ds = \boldsymbol{C}_{av}\boldsymbol{x}_{av}, \quad \boldsymbol{C}_{av} = d_0\boldsymbol{C}_0 + d_1\boldsymbol{C}_1. \tag{3.35}$$

Next, the output equations are temporarily dropped, proceeding with the averaging method for the state equations, and ensuring an error bound for the

[55] Note that the model captures only the systemic circulation (large arteries, peripheral circulation, large veins), along with the left heart (left ventricle)

approximation in respect with the state variables. The stability inferred for the state equations will extend also to the final case when the output equations are reattached (i.e. in this particular case, internal stability implies external stability).

By time scaling the state equation (3.34a), one obtains

$$\boldsymbol{x}' = \frac{1}{\omega}\left[\boldsymbol{A}_{q(\tau)}\,\boldsymbol{x} + \boldsymbol{b}_{q(\tau)}\right]. \tag{3.36}$$

Adopting the small parameter $\varepsilon=1/\omega$ yields

$$\boldsymbol{x}' = \varepsilon\left[\boldsymbol{A}_{q(\tau)}\,\boldsymbol{x} + \boldsymbol{b}_{q(\tau)}\right]. \tag{3.37}$$

Obviously, (3.37) is a particular case of (3.7), and respects Assumption 3.3, by considering $\tilde{\boldsymbol{f}}_0(\tau,\boldsymbol{x}) = \boldsymbol{A}_{q(\tau)}\,\boldsymbol{x}$ and $\tilde{\boldsymbol{g}}(\tau) = \boldsymbol{b}_{q(\tau)}$. The averages of these components, according to (3.12) are:

$$\begin{aligned}\tilde{\boldsymbol{f}}_{0,av}(x) &\overset{\Delta}{=} \frac{1}{2\pi}\int_{\tau-2\pi}^{\tau}\boldsymbol{A}_{q(\tau)}\,\boldsymbol{x}\,ds = \frac{1}{2\pi}\int_{\tau-2\pi}^{\tau-2\pi+2\pi d_0}\boldsymbol{A}_0\,\boldsymbol{x}\,ds + \\ &+\frac{1}{2\pi}\int_{\tau-2\pi+2\pi d_0}^{\tau}\boldsymbol{A}_1\,\boldsymbol{x}\,ds = (d_0\boldsymbol{A}_0 + d_1\boldsymbol{A}_1)\boldsymbol{x}\end{aligned}$$

$$\begin{aligned}\tilde{\boldsymbol{g}}_{av}(T) &\overset{\Delta}{=} \frac{1}{2\pi}\int_{\tau-2\pi}^{\tau}\boldsymbol{b}_{q(\tau)}m(s,T)\,ds = \frac{1}{2\pi}\int_{\tau-2\pi}^{\tau-2\pi+2\pi d_0}\boldsymbol{b}_0\,m(s,T)\,ds + \\ &+\frac{1}{2\pi}\int_{\tau-2\pi+2\pi d_0}^{\tau}\boldsymbol{b}_1\,m(s,T)\,ds = \theta_0(T)\,\boldsymbol{b}_0 + \theta_1(T)\,\boldsymbol{b}_1\end{aligned} \tag{3.38}$$

with $\theta_0(T) = \left(e^{aTd_0} - 1\right)/(aT)$, $\theta_1 = \left(e^{aT} - e^{aTd_0}\right)/(aT)$.

The weighting terms θ_0 and θ_1 can be further approximated through linear interpolation:

$$\theta_0(T) \approx \alpha_0 + \beta_0 T, \qquad \theta_1 \approx \alpha_1 + \beta_1 T, \tag{3.39}$$

which are now affine functions of the period T.

The averaged system is

$$\boldsymbol{x}'_{av} = \varepsilon\left[\boldsymbol{A}_{av}\boldsymbol{x}_{av} + \boldsymbol{b}_{av}(T)\right], \tag{3.40}$$

where $\boldsymbol{A}_{av} = d_0\boldsymbol{A}_0 + d_1\boldsymbol{A}_1$, $\boldsymbol{b}_{av}(T) = \theta_0(T)\,\boldsymbol{b}_0 + \theta_1(T)\,\boldsymbol{b}_1$.

Finally, by scaling back, one obtains the weighted averaged system associated to the original system (3.34a):

$$\dot{\boldsymbol{x}}_{av} = \boldsymbol{A}_{av}\boldsymbol{x}_{av} + \boldsymbol{b}_{av}(T). \tag{3.41}$$

According to Theorem 3.1, for a constant nominal value of T, the error between the original and the averaged systems is $O(\varepsilon)$ on a finite time interval. To extend this to the infinite time interval, one needs to check the stability of (3.40).

By making use of aproximation (3.39), the system (3.40) can be written as

$$\boldsymbol{x}'_{av} = \varepsilon\, \boldsymbol{A}_{av}\boldsymbol{x}_{av} + \varepsilon\left[\alpha_0\boldsymbol{b}_0 + \alpha_1\boldsymbol{b}_1\right] + \varepsilon\left[\beta_0\boldsymbol{b}_0 + \beta_1\boldsymbol{b}_1\right]T\,, \tag{3.42}$$

which is now a linear system with two constant input terms. This means that exponential stability follows if and only if the matrix $\varepsilon\, \boldsymbol{A}_{av}$ is Hurwitz. Additionally, the system would be stable even as T varies (slowly), and thus T could be further regarded as the new input of the averaged system.

For the cardiovascular model parameters given in Table 3.1, a=-0.7 (adopted such that the averaged system's trajectories follow the variations of the moving averages of the original system's trajectories to step changes in T), d_0=1/3, d_1=2/3, T=1 s (nominal value), and $\theta_0(T) \approx 0.33 - 0.03T, \quad \theta_1 \approx 0.61 - 0.18T$ (on the physiological domain $T \in [0.3,2]$ s), it can be easily checked that $\varepsilon\, \boldsymbol{A}_{av}$ is Hurwitz. Hence, the averaged system is exponentially stable, and as a result of Theorem 3.2, the error between the original system and the averaged system is $O(\varepsilon)$ on an infinite time interval. Moreover, according to Theorem 3.3, also the original system is orbitally exponentially stable. Lastly, it should be mentioned that the results are conserved even when taking the maximal value of T (i.e. T=2s), instead of the nominal value.

Remark 3.5 In this particular case, the stability of the original system (3.34a) can be alternatively investigated using Floquet Theory ([106]), adapted to switched linear systems. Thus, by using the results from [107], it can be proved that system (3.34a), rearranged as

$$\begin{bmatrix} \dot{\boldsymbol{x}} \\ \dot{x}_a \end{bmatrix} = \begin{bmatrix} \boldsymbol{A}_{q(\omega t)} & \boldsymbol{b}_{q(\omega t)} \\ \boldsymbol{0} & 0 \end{bmatrix} \begin{bmatrix} \boldsymbol{x} \\ x_a \end{bmatrix}, \begin{bmatrix} \boldsymbol{x}(0) \\ x_a(0) \end{bmatrix} = \begin{bmatrix} \boldsymbol{x}_0 \\ 1 \end{bmatrix}, \tag{3.43}$$

is in fact orbitally exponentially stable. Here x_a is a support state variable.

In many practical applications an offset steady state error was observed between the signals of the averaged system, and the (real) moving averages of the signals of the original system (see examples in power electronics – [63], [64], [108]. This is a generic issue, specific to most averaging methods (including the one presented here), and usually attributed to a large ripple of the signal of interest, for a relatively low frequency range. While in some applications this error can be neglected, in our particular application this is not the case. Moreover, because this error can not be expressed analytically, there are no systematic methods to correct it without substantially increasing the complexity of the averaged model.[56] Consequently, in an attempt to minimize the error as much as possible, a multiplicative type correction is considered for the system matrix by introducing the corrector matrix - $\mathbf{M}_c$= diag (ρ_0, ρ_1), with ρ_0>0 and ρ_1>0. Hence, (3.42) becomes

$$\boldsymbol{x}'_{av} = \varepsilon\, \boldsymbol{A}_{av}\boldsymbol{M}_c\boldsymbol{x}_{av} + \varepsilon\left[\alpha_0\boldsymbol{b}_0 + \alpha_1\boldsymbol{b}_1\right] + \varepsilon\left[\beta_0\boldsymbol{b}_0 + \beta_1\boldsymbol{b}_1\right]T\,. \tag{3.44}$$

[56] See also the discussion on averaging from chapter 2.

In the numerical context stated above, these tuning parameters were adopted as ρ_0=0.6 and ρ_1=1.0, so as to ensure that the equilibrium point of (3.44) is as close as possible to the moving average of (3.37) in a nominal steady state scenario. For a more detailed discussion on how to determine the set of tuning parameters $\{a, \rho_0, \rho_1\}$ see chapter 2.

Remark 3.6 Note that, despite the correction that transforms the system (3.42) into (3.44), the stability is preserved: because the main diagonal elements of $\varepsilon \boldsymbol{A}_{av}$ are always negative (from a physiological interpretation) and the elements of $\mathbf{M}_c$ are positive, the Hurwitz determinants of $\varepsilon \boldsymbol{A}_{av}$ and $\varepsilon \boldsymbol{A}_{av}\boldsymbol{M}_c$ have the same signs. In other words, for this particular application (2^{nd} order system), (3.42) is stable if and only if (3.44) is stable. This result can be generalized for higher order systems by further taking into account the fact that we are actually dealing with a positive linear system (most models of the cardiovascular system have as state variables either volumes or pressure, which can not take negative values). By considering the correction matrix $\mathbf{M}_c$ as a known multiplicative perturbation, it can be shown through the D-stability theorem[57] that the nominal system – given here by (3.42) – is stable if and only if the perturbed system – given here by (3.44) – is stable. Furthermore, one can intuitively expect that the correction would lower the error bound $O(\varepsilon)$ between the trajectory of the averaged system and the original system.

Finally, a scenario for the resulting averaged system is considered - with the output equation (3.35) reattached

$$\begin{aligned} \dot{\boldsymbol{x}}_{av} &= \boldsymbol{A}_{av}\boldsymbol{M}_c\boldsymbol{x}_{av} + \left[\alpha_0\boldsymbol{b}_0 + \alpha_1\boldsymbol{b}_1\right] + \left[\beta_0\boldsymbol{b}_0 + \beta_1\boldsymbol{b}_1\right]T \\ \boldsymbol{y}_{av} &= \boldsymbol{C}_{av}\,\boldsymbol{x}_{av} \end{aligned}, \qquad (3.45)$$

when the input T varies as in Fig. 3.1.[58] The trajectories of the averaged system follow relatively close the real moving averages of the original system as the modulation period changes[59]. Without a weighted averaging approach as the one presented here, i.e. through a standard averaging approach, the averaged system would have been invariant in respect with the modulation period, and thus the trajectories would remain constant during the entire scenario[60].

Table 3.1. Parameter values of the cardiovascular model (adapted from [61])

Parameter	Value	Measure unit
R_0	0.01	mmHg ml^{-1} s
R_1	1.0	mmHg ml^{-1} s
R_2	0.03	mmHg ml^{-1} s
E_d	0.1	mmHg ml^{-1}
E_s	2.5	mmHg ml^{-1}
C_1	2.0	ml $mmHg^{-1}$
C_2	100.0	ml $mmHg^{-1}$
x_T	1734	ml
$x_0(0)$	22.4	ml
$x_1(0)$	112	ml

[57] See Theorem 16 from [109].
[58] This variations are considered large from a physiological point of view.
[59] The spikes of y_0 are due to numerical errors, and do not influence the averaging process – see chapter 2.
[60] See also chapter 2.

Remark 3.7 As shown in chapter 2, the averaged system (3.45) can be obtained more straightforwardly through a state space weighted averaging approach, but without any theoretical guarantees for the result.

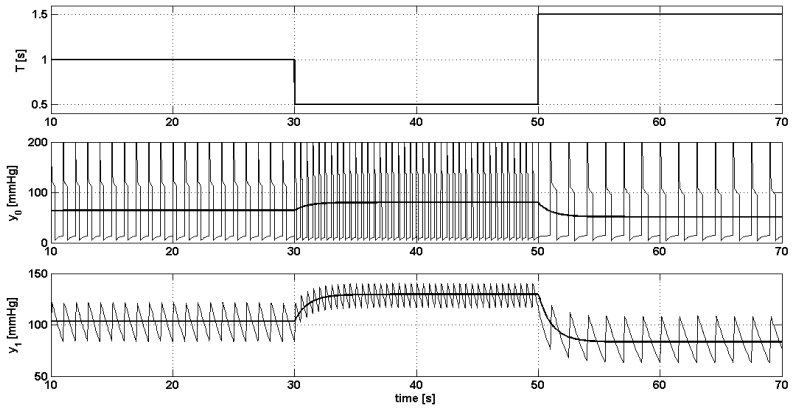

Fig.3.1. Trajectories of the averaged system and the original system as T varies from 1 s to 0.5 s, and from 0.5 s to 1.5 s.

3.5. Conclusions

The current chapter has presented a novel averaging approach for pulse-frequency modulated systems with constant duty ratios. The approach involves a period-weighting component that makes the resultant averaged system dependent on the modulation period, which is important for situations when the average operating point of the original periodic system is also dependent on the modulation period. In such cases the standard averaging approach fails because it leads to a period-independent averaged model, which can not provide a suitable approximation for the original system. A theoretical framework was developed for the period-weighted averaging method, which ensures an error bound for the approximation between the original systems and the averaged system, and which relates the stability of the averaged system with that of the original system. Finally, the new averaging method is used for a case study involving a model of the cardiovascular system. Simulation results show that the period-dependent average model of the cardiovascular system represents a good approximation of the original periodic systems. Because the averaged model is simpler than the original periodic one, it could be further used for closed-loop analysis of cardiovascular regulation - the cardiovascular model coupled with a model for the nervous control loop (among which the most important is the baroreflex feedback mechanism). Such a coupling would be straightforward because, as in the case of many technical control systems, the (nervous) feedback control loop actually regulates the time-averages of key state variables of the plant (cardiovascular system), instead of instantaneous values ([61]).

4. STABILITY ANALYSIS OF CARDIOVASCULAR REGULATION

4.1. Introduction

Systems analysis of biomedical systems represents a very active area of research, not only due to the link between biomedical systems and healthcare, but also because only recently have tools provided by Systems Theory begun to be considered in medicine. One topic of high interest is the analysis of the cardiovascular system, along with its possible control mechanisms, mainly due to the high mortality of cardiovascular diseases. On the other hand, another topic of recent interest is that of time delays, which have a yet an undetermined role in many control mechanisms of biological systems. The nervous control of the cardiovascular system (or shortly referred to as cardiovascular regulation) is of no exception – multiple delays act on the feedback loops involved (see Fig. 4.1); the delays refer to propagation processes of the control signals from the central nervous system to the cardiovascular system. Due to the complexity of most models from the literature (large scale, multiple strong nonlinearities, periodic behavior), there are very few systematic studies which involve quasi-analytical or numerical systems analysis results (like stability for example, or the effect of delays). Most studies resort to an empirical analysis only through numerical simulations (e.g. [89], [110]).

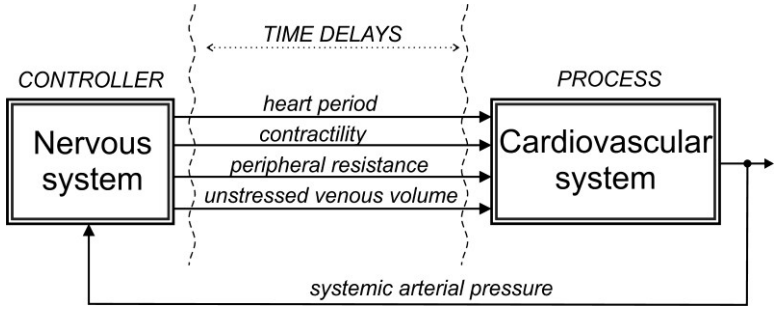

Fig.4.1. Cardiovascular regulation as a nonlinear control system, with the cardiovascular system as the controlled process and the nervous system as the controller[61].

The present study analyses the stability of cardiovascular regulation, along with the effect of multiple time delays. Our systems analysis approach is focused on three steps: simple model, local analysis, global analysis. The first step, undergone in chapter 2, was to derive a model a simple as possible (control engineering

[61] The measured signal is the systemic arterial pressure, while the control signals are the heart period, cardiac contractility, systemic peripheral resistance and systemic venous unstressed volume. Time delays appear on each control path.

approach) - in this case an averaged model – which still preserves the main dynamic features of cardiovascular regulation. In the second step, we will analyze the system locally via linearization around the nominal-physiological equilibrium point. This is the classical approach in biomathematics because global methods for biological systems are rarely employed due to the non-standard features (nonlinearities) of such models (which are hard to pin-point into conventional classes of nonlinear systems). However, this step is non-trivial if one takes into consideration the multiple time delays involved in cardiovascular regulation, as it will be shown in chapter 4.2. The third step, global analysis (chapter 4.3), is motivated not only by the need to have a global perspective of the systems dynamics, at least at the level of certain global properties witch complement the local analysis results, but also by the issue of robustness. Robustness is probably one of the most important and intriguing aspects of biological systems in general (*robustness despite noise and uncertainty*). So, besides the fact that an equilibrium point is stable or not, or that the system exhibits oscillations or not, we are interested to see if the systems exhibits some form of '*globally stable behavior*'. For example, Fig. 4.2 shows a scenarios involving a acute hemorrhage (1000 ml drop at t=200s) when all time delays of cardiovascular regulation are increased by 4s. It is interesting to see that when the operating domain or regime (the domain around an equilibrium point) is changed – due to an external disturbance for example or uncertainty in the systems parameters, the systems' behavior can change from oscillatory to aperiodic (with the same time delays). What we are interested in the global analysis is to certify the fact that the trajectories of the systems - with oscillations or not – remain somehow bounded and even exhibit stable behavior in respect with their imposed functional regime. Finally, is should be noted that our entire study based on the approach - simple model, local analysis, global analysis – actually undergoes the first steps in the area of robustness, and facilitates further robustness studies of cardiovascular regulation for different pathological scenarios; which can eventually lead to better diagnostics or treatments.

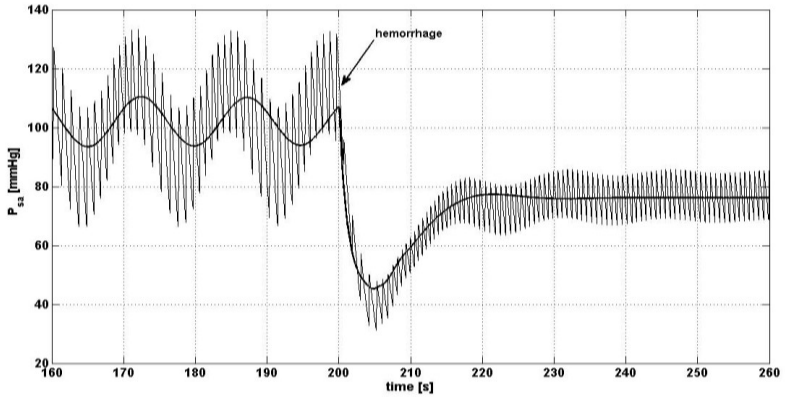

Fig.4.2. Transient response of the averaged and pulsatile closed loop models of cardiovascular regulation during an acute hemorrhage scenario when all delays are increased by 4s

For the subsequent subchapters, we define that state vectors as $\boldsymbol{x_c}(t)=[x_{wa0}(t)\ x_{wa1}(t)\ x_{Tp}(t)\ x_{Ts}(t)\ x_E(t)\ x_R(t)\ x_V(t)]^T$, $\boldsymbol{x_c}(t-\tau_i)=[x_{wa0}(t-\tau_i)\ x_{wa1}(t-\tau_i)\ x_{Tp}(t-\tau_i)\ x_{Ts}(t-\tau_i)\ x_E(t-\tau_i)\ x_R(t-\tau_i)\ x_V(t-\tau_i)]^T, i \in \{Tp,Ts,E,R,V\}$, and the output vector

as $\boldsymbol{y_c}(t)=[y_{wa0}(t)\ \ y_{wa1}(t)]^T$. The closed loop model of cardiovascular regulation (2.37)-(2.38) from chapter 2 can be rewritten in condensed form as

$$\begin{cases}\dot{\boldsymbol{x}}_C(t)=\boldsymbol{f}_C(\boldsymbol{x}_C(t),\boldsymbol{x}_C(t-\tau_{Tp}),\boldsymbol{x}_C(t-\tau_{Ts}),\boldsymbol{x}_C(t-\tau_E),\boldsymbol{x}_C(t-\tau_R),\boldsymbol{x}_C(t-\tau_V))\\ \boldsymbol{y}_C=\boldsymbol{g}_C(\boldsymbol{x}_C)\end{cases} \tag{4.1}$$

Note that the averaged model of cardiovascular regulation (4.1) can qualitatively reproduce (approximate) the basic hemodynamic behavior of the original (pulsatile) model both in nominal (physiological) and perturbed (pathological) conditions (e.g. like in Fig. 4.2), while both models are in agreement with the results (experiments) shown in the literature (e.g. [39])[62].

4.2. Local stability analysis

In the local stability analysis of cardiovascular regulation we will focus on the role of time delays in generating stability or instability[63].

Time delays lead to complex dynamics in nonlinear and linear systems, and are subject to intensive research, especially in the last three decades. The research interest is motivated also by the large number of applications which involve time delays (either constant, time varying or multiple delays). In particular, in biomedical systems, time delays emerge frequently, and are crucial for understanding the systems dynamics.

Cardiovascular regulation, as mentioned in chapter 4.1 and illustrated in Fig. 4.1, implies multiple delays that act on the feedback loops involved. However, due to the complexity of most models from the literature there are few systematic studies on the effect of these delays which involve quasi-analytical or numerical systems analysis results (e.g. stability). The few studies which analyze the effect of delays make use of particular results only through numerical simulations ([89], [110]).

In this context, the current section[64] analyses the effect of multiple time delays on the stability of cardiovascular regulation. With a focus on qualitative aspects, an averaged model of cardiovascular regulation is derived (with the aim of working with a model as simple as possible- as done in control engineering), and a frequency sweeping stability method for multiple delays systems is adopted in conjunction with the linearized model (the feasibility – both theoretical and computational – of the stability analysis problem in respect with multiple delays was taken into consideration). The local stability analysis provides new insights into the role of multiple time delays in generating stability or instability (based on delay stability maps), and on the interactions between time delays along with their possible physiological implications (with the aid of delay stability margins). The results show that there is still a lot to learn about the role of time delays in physiological systems: whether they play a role of stabilization in the presence of multiple feedback loops acting on different time scales in the presence of noise and

[62] See chapter 2 for results and discussions.
[63] Throughout chapter 4.2, the term *unstable* will refer to a system whose equilibrium point is *not asymptotically stable*.
[64] The results of this section have been published in [130].

uncertainty, or they play a role of destabilization for certain large absolute values or certain change in the magnitude order between the delays. Implications of such nature show how systems analysis can improve the understanding of physiological systems and possibly lead to better diagnosis methods.

4.2.1. Stability analysis for multiple time delays

Stability of time delay systems is a very active area of research. Time varying delays and/or multiple delays can induce complex dynamic behavior ([44]), and as a result the analysis of such system is also complex. For nonlinear systems, there are no general methods of study, and even for particular cases there are relatively few stability methods reported in the literature (most of them based of Lyapunov functionals- see [45], [111]). Most methods are very restrictive, conservative, and complex (e.g. the sum of squares based method from [49] provides a stability framework for polynomial delay systems, but the results may be conservative and the method is very complex). Because of this, most studies address linearization in deriving local results. Linear time delays systems have been intensively studies over the last three decades, and a wide range of methods have been proposed ([46]). However, when delaying with time delays that are not constant, and/or multiple delays, the problem becomes nontrivial even here, if one wants to obtain necessary and sufficient conditions.

In our present study we are dealing with multiple constant delays. As far as we know, the only general method available in the literature, for the case when the number of delays is larger than 3, which is computationally tractable, and can provide necessary and sufficient conditions, is the method proposed by [48]. Note that although many Lyapunov based methods were proposed in the literature (see e.g. [111], [43]), where the problem leads to solving an LMI using convex optimizations, these methods derive sufficient conditions only, and are usually very conservative. In this context, the current section addresses the local stability problem for cardiovascular regulation in respect with multiple constant delays by making used of this method.

4.2.1.1 The linearized system

The nonlinear autonomous system (4.1) has a unique equilibrium point $\mathbf{x}_e$. Before linearization around this equilibrium point, the following notations are introduced for reasons of simplicity:

$$\tau_{Tp} \overset{not}{=} \tau_1, \tau_{Ts} \overset{not}{=} \tau_2, \tau_E \overset{not}{=} \tau_3, \tau_R \overset{not}{=} \tau_4, \tau_V \overset{not}{=} \tau_5, \boldsymbol{x}_C(t) \overset{not}{=} \boldsymbol{x}_C, \boldsymbol{x}_C(t-\tau_1) \overset{not}{=} \boldsymbol{x}_{C,\tau_1},$$

$$\boldsymbol{x}_C(t-\tau_2) \overset{not}{=} \boldsymbol{x}_{C,\tau_2}, \boldsymbol{x}_C(t-\tau_3) \overset{not}{=} \boldsymbol{x}_{C,\tau_3}, \boldsymbol{x}_C(t-\tau_4) \overset{not}{=} \boldsymbol{x}_{C,\tau_4}, \boldsymbol{x}_C(t-\tau_5) \overset{not}{=} \boldsymbol{x}_{C,\tau_5}.$$

Using these notations, the following linearized system can be obtained:

$$\begin{cases} \dot{\boldsymbol{x}}_\ell(t) = \boldsymbol{A}\boldsymbol{x}_\ell(t) + \sum_{i=1}^{5} \boldsymbol{A}_i \boldsymbol{x}_\ell(t-\tau_i) \\ \boldsymbol{y}_\ell(t) = \boldsymbol{C}\boldsymbol{x}_\ell(t) \end{cases} \tag{4.2}$$

where

$$\boldsymbol{A}=\left.\frac{\partial \boldsymbol{f}_C}{\partial \boldsymbol{x}_C}\right|_{\boldsymbol{x}_e},\ \boldsymbol{A}_i=\left.\frac{\partial \boldsymbol{f}_C}{\partial \boldsymbol{x}_{C,\tau_i}}\right|_{\boldsymbol{x}_e},\ \boldsymbol{C}=\left.\frac{\partial \boldsymbol{g}_C}{\partial \boldsymbol{x}_C}\right|_{\boldsymbol{x}_e},$$

and with $\boldsymbol{x}_\ell(t)=\boldsymbol{x}_C(t)-\boldsymbol{x}_e$ and $\boldsymbol{x}_\ell(t-\tau_i)=\boldsymbol{x}_C(t-\tau_i)-\boldsymbol{x}_e$ (i=1,…,5). The matrices **A**, $\mathbf{A}_i$ and **C** are given explicitly in Appendix 2.

The system (4.2) is linear time invariant, of order N=7, with multiple (constant) delays (number of delays L=5).

4.2.1.2 Stability analysis method

For the stability analysis, the ACFS (advanced clustering with frequency sweeping) method proposed by [48] will be further used, which provides a general methodology for deriving necessary and sufficient stability conditions for linear system with multiple delays. The essence of the method is as follows.

First, the characteristic equation associated to the state equation of (4.2) is written under the general form

$$f(s,\boldsymbol{\tau})=\sum_{k=0}^{K}P_k(s)e^{-s\sum_{l=1}^{L}v_{kl}\tau_l}=0 \tag{4.3}$$

where $\boldsymbol{\tau}=[\tau_1\ \tau_2\ \tau_3\ \tau_4\ \tau_5]^T$, P_k are polynomials in s with real coefficients, $K\in Z_+$ and $v\in N$. It is known that the system is asymptotically stable when sup{Re(s)|f(s,**τ**)=0} is negative. Assuming that there are no roots on the imaginary axis when τ_l=0, the focus is on investigating the stability transitions in the delay parameter space, and as consequence the imaginary roots s=jω of (4.3) are of prime interest ($\omega\in R_{0+}$).

Second, the following *crossing frequency set* (CFS) of (4.3) is defined:

$$\Omega=\{\omega\in R_{0+}\mid f(j\omega,\boldsymbol{\tau})=0,\ for\ \ \boldsymbol{\tau}\in R_{0+}^{L}\} \tag{4.4}$$

For all $\omega\in\Omega$, the delay solutions from (4.3) form L-dimensional *potential stability switching hypersurfaces* (PSSHs)

$$\wp=\{\boldsymbol{\tau}\in R_{0+}^{L}\mid f(j\omega,\boldsymbol{\tau})=0,\forall\omega\in\Omega\} \tag{4.5}$$

The PSSHs give the boundaries which decompose the delay space into stable and unstable regions (see the τ – decomposition theorem [112]). If L=2 we have *curves* instead of *hypersurfaces* (PSSCs).

Third, in addressing this infinite-dimensional problem, a common approach is to use the so called Rekasius transformation ([113])

$$e^{-\tau_l s}=\frac{1-T_l s}{1+T_l s},\ s=j\omega,\ T_l\in R,\ l=\overline{1,L} \tag{4.6}$$

which leads to a finite dimensional characteristic equation in ω and T_l. Note that the

transformation holds exactly for

$$\tau_l = \frac{2}{\omega}\left(arctan(\omega T_l) \mp \eta_l \pi\right),\ \eta_l = 0,\ 1,\ 2\ldots \tag{4.7}$$

By substituting (4.6) in (4.3), one finally arrives to the transformed characteristic function

$$g(s,\boldsymbol{T}) = \left(f(s,\boldsymbol{\tau})\,|_{e^{-\tau_l s}=(1-T_l s)/(1+T_l s),\,l=\overline{1,L}}\right)\prod_{l=1}^{L}(1+T_l s)^{c_l} = \sum_{m=0}^{M} Q_m(\boldsymbol{T})s^m \tag{4.8}$$

where Q_m are multinomials in $\boldsymbol{T} = [T_1 \ldots T_L]^T$, c_l=rank(A_l), and $M = N + \sum_{l=1}^{L} c_l$. In particular for the current study, because of the special form of each matrix $\mathbf{A}_i$ from (4.2) we have c_l=1 (l=1,...,L). It has been shown in [48] that by finding the set

$$\overline{\Omega} = \{\omega \in R_{0+} \mid g(j\omega,\boldsymbol{T}) = 0, for\ \boldsymbol{T} \in R^L\} \tag{4.9}$$

one immediately obtains Ω because $\Omega \equiv \overline{\Omega}$.

Fourth, for avoiding exponential computation times needed for extracting an L-dimensional PSSH, one seeks to determine 2-D projections of the PSSH directly, by considering some of the delays constant a priori. For example, for the 2-D projection in the τ_1-τ_2 delay space, with τ_l (l=3,4,…,L) fixed a priori (given values $\tau_l = \tilde{\tau}_l$), the characteristic function becomes

$$h(j\omega,T_1,T_2) = \left(f(j\omega,\boldsymbol{\tau})\,|_{e^{-j\omega\eta}=(1-j\omega T_l)/(1+j\omega T_l),\,l=1,2.}\right)\prod_{l=1}^{2}(1+j\omega T_l)^{c_l} \tag{4.10}$$

which can be decomposed into a real part and an imaginary part

$$h(j\omega,T_1,T_2) = h_{re}(\omega,T_1,T_2) + j\,h_{im}(\omega,T_1,T_2) \tag{4.11}$$

with h_{re}=Re(h) and h_{im}=Im(h). Note that the crossing set of (4.11), denoted as $\overline{\overline{\Omega}}$ is a subset of $\overline{\Omega}$.

Fifth, the notions of resultant[65] (R) and discriminant (D) from algebraic geometry are further used (see [114]). It is shown in [48] that instead of studying the zeroes of $h(j\omega,T_1,T_2)$, one can study the zeroes of the resultant R_{T2} with respect with ω and T_1 (i.e. the resultant of h_{re} and h_{im} by eliminating T_2). Moreover, the minimum and maximum positive real roots of the discriminant D of R_{T2} (i.e. the resultant of R_{T2} and $\partial R_{T2}/\partial T_1$ with respect with ω by eliminating T_1), that correspond to real (T_1, T_2) solutions give the lower and upper bounds of $\overline{\overline{\Omega}}$ - ω_{min} and ω_{max} ([48]). This leads to the following Theorem given in [48]:

[65] See the Appendix 2 for an explicit and formal definition of the notion of resultant.

Theorem 4.1: The linear system with multiple delays (4.2) is (weak) delay independent stable on the τ_1-τ_2 delay domain if and only if:

i) System (4.2) is asymptotically stable for $\tau_1=\tau_2=0$.

ii) The discriminant $D(\omega)$ has no positive real roots corresponding to real (T_1,T_2) solutions of h.

Sixth, if the discriminant D has positive real roots corresponding to real (T_1,T_2) solutions of *h*, i.e. Theorem 4.1 does not hold and we can find ω_{min} and ω_{max}, the PSSC is constructed based on the following frequency sweeping algorithm ([48]) - run iteratively for each $\omega \in [\omega_{min}, \omega_{max}]$, with an appropriate step size:

Algorithm 4.1

Step 1. Solve $R_{T2}=0$ for T_1 real.

Step 2. For each real T_1 solution found, if there exist real T_2 solution such that $h_{re}=0$ and $h_{im}=0$, go the next step, otherwise increment ω and go to Step 1.

Step 3. Determine the delay values (τ_1, τ_2) corresponding to each (T_1,T_2) solution, then increment ω and go to Step 1.

Note that in practice some degenerate cases can emerge, which were omitted in this presentation. For more details see [48].

Seventh, the regions delimited by the PSSCs are identified as stable or unstable either by the method suggested in [115], or by simply using a numerical approximation tool which plots the rightmost characteristic roots for a chosen delay point from each region.

4.2.2. Results of stability analysis

We will focus the analysis on the delays acting on the heart period $\{\tau_1, \tau_2\}$, on how they can influence stability for different fixed values of $\{\tau_3, \tau_4, \tau_5\}$. Our goal is not that of obtaining an exhaustive picture, but that of revealing certain important aspects which are counterintuitive, like the fact that the system may become unstable if some of the delays actually decrease.

A particular goal is also to capture the effect of the delays of the vascular system $\{\tau_4, \tau_5\}$ – vascular delays - on the robust stability of cardiovascular regulation, for uncertain delays acting on the heart $\{\tau_1, \tau_2, \tau_3\}$ – cardiac delays.

In the results further presented, for the calculation of the resultants and discriminants needed by the stability method from section 4.2.1.2., the Maple symbolic algebra package was used. For completeness, the parameters of the model are given in Table 4.1.

Table 4.1. Parameter values for the model of cardiovascular regulation (adapted from [61],[39],[89],[74])

Param.	Value	Param.	Value
R_0	0.01 mmHg ml^{-1} s	T_V	10 s
R_1	1.0 mmHg ml^{-1} s	k_{iTp}	0.098 mmHg^{-1}
R_2	0.03 mmHg ml^{-1} s	k_{iTs}	-0.0616 mmHg^{-1}
E_d	0.1 mmHg ml^{-1}	k_{iE}	-0.0616 mmHg^{-1}
E_s	2.5 mmHg ml^{-1}	k_{iR}	-0.0616 mmHg^{-1}
C_1	2.0 ml mmHg^{-1}	k_{iV}	-0.0616 mmHg^{-1}
C_2	100.0 ml mmHg^{-1}	$x_{Tp}^{\min}$	0.88 s
x_T	1734 ml	$x_{Tp}^{\max}$	1.44 s
d_0	1/3	$x_{Ts}^{\min}$	0 s
d_1	2/3	$x_{Ts}^{\max}$	0.33 s
a	-0.7	$x_E^{\min}$	1.91 mmHg/ml
ρ_0	0.6	$x_E^{\max}$	3.10 mmHg/ml
ρ_1	1.0	$x_R^{\min}$	0.6 mmHg s/ml
α_0	0.33	$x_R^{\max}$	1.4 mmHg s/ml
β_0	-0.03	$x_V^{\min}$	1385 ml
α_1	0.61	$x_V^{\max}$	2085 ml
β_1	-0.18	τ_{Tp}	0.2 s
P_{san}	100 mmHg	τ_{Ts}	2 s
T_{Tp}	0.5s	τ_E	2 s
T_{Ts}	1.5 s	τ_R	2 s
T_E	1.5 s	τ_V	5 s
T_R	1.5s		

4.2.2.1 Stability for nominal physiological values of the delays

According to [89], the nominal (physiological) values of the delays are τ_1=0.2 s, τ_2=2 s, τ_3=2 s, τ_4=2 s, τ_5=5 s. We next construct the discriminant D in respect with ω, according to section 4.2.1.2. We find that the discriminant has no positive real roots - condition ii) from Theorem 4.1. For τ_1=τ_2=0 s, by using the characteristic root computing tool provided by [116], which calculates the rightmost characteristic roots λ of the system, we obtain that there are no right-half plane roots (see Fig. 4.3), which means that the system is asymptotically stable – condition i) from Theorem 4.1. Consequently, according to Theorem 4.1, for these fixed values of $\{\tau_3, \tau_4, \tau_5\}$ the system is asymptotically stable independent of $\{\tau_1, \tau_2\}$.

This result, for nominal delay values, was kind of obvious – we expected the system in (nominal) physiological conditions to be stable. However, the fact that the system is asymptotically stable independent of $\{\tau_1, \tau_2\}$, which means that an

increase in the delays acting on the heart period alone is not sufficient to induce instability for nominal values of the other delays $\{\tau_3, \tau_4, \tau_5\}$, was not obvious at all.

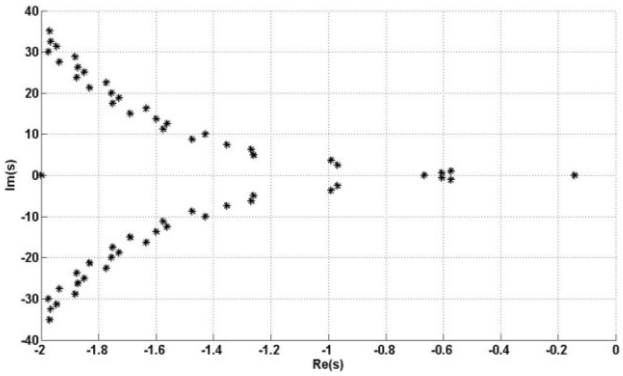

Fig.4.3. Characteristic roots λ with Re(s)>=-2, for $\tau_1=\tau_2=0$ s, $\tau_3=2$ s, $\tau_4=2$ s, $\tau_5=5$ s.

4.2.2.2 Stability for pathological values of the delays

The analysis for pathological delay values is conducted starting from the (nominal) physiological delay values from the previous section.

First, let us consider here an additive increase α for all delays. One can easily determine the value of α (starting from an initial value $\alpha_0=0.5$ s) for which the system begins to show instability – with approximation α=4 s in our case. Now we are interested to see how uncertainties in $\{\tau_1, \tau_2\}$ can influence the stability of the system. For this we fix the delays $\{\tau_3, \tau_4, \tau_5\}$ to $\tau_3=6$ s, $\tau_4=6$ s, $\tau_5=9$ s, and investigate the stability on the τ_1-τ_2 domain by means of the method from section 4.2.1.2. We compute the discriminant D in respect with ω, and obtain $\omega_{min}=0.2406$ and $\omega_{max}=0.4461$. Then, the Algorithm 4.1 produces the stability map from Fig. 4.4. The shaded regions are identified to be unstable by means of [116].

The result shows that the system has a relatively large stability margin (from a physiological perspective) for additive synchronous increase in all delay values, i.e. when the *magnitude difference* between delays is conserved. Also, it should be noticed that, for a small enough τ_1, the system can remain stable even for absurdly large values of τ_2.

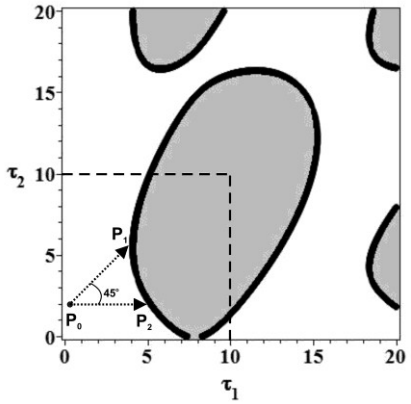

Fig.4.4. Stability map for τ_1-τ_2 [s] with $\tau_3=6$ s, $\tau_4=6$ s, $\tau_5=9$ s. Shaded regions are unstable.

Second, let us consider all the delay to take the same value β. Again, it is trivial to determine the value of β (starting from an initial value $\beta_0=\min\{\tau_1, \tau_2, \tau_3, \tau_4, \tau_5\}=0.2$ s) for which the system begins to show instability – with approximation β=3 s in our case. Because we are again interested to see how uncertainties in $\{\tau_1, \tau_2\}$ can influence the stability of the system, we fix the delays $\{\tau_3, \tau_4, \tau_5\}$ to τ_3=3 s, τ_4=3 s, τ_5=3 s, and investigate the stability on the τ_1-τ_2 domain by means of the method from section 4.2.1.2. We compute the discriminant in respect with ω and obtain ω_{min}=0.4504 and ω_{max}=0.6938. Algorithm 4.1 produces the stability map from Fig. 4.5, with the shaded regions identified as unstable by means of [116].

The result shows that the system can have a relative lower stability margin (from a physiological perspective) when the magnitude difference between the delays is no longer preserved (instability occurs for considerably lower overall delay values). Also, it should be noticed that, for a small enough τ_2 (or τ_1), the system can remain stable even for absurdly large values of τ_1 (or τ_2).

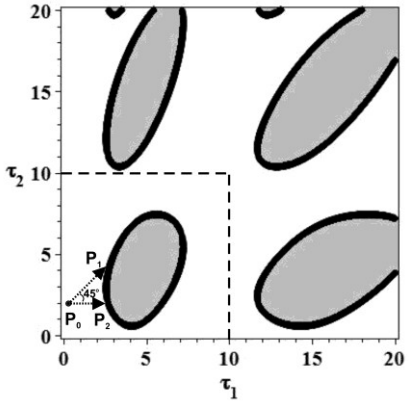

Fig.4.5. Stability map for τ_1-τ_2 [s] with τ_3=3 s, τ_4=3 s, τ_5=3 s. Shaded regions are unstable.

Finally, we analyze the oscillations of the system in the time domain (see Fig. 4.6), when we have increased all delays by α=4 s (τ_1=4.2 s, τ_2=6 s, τ_3=6 s, τ_4=6 s, τ_5=9 s), i.e. for a given point in the delay space of the case depicted by Fig. 4.4; and when all delays have the value β=3 s ($\tau_1=\tau_2=\tau_3=\tau_4=\tau_5$=3 s), i.e. for a point in the delay space of the case depicted by Fig. 4.5. It is interesting to notice here that the amplitude of the oscillations is actually larger for smaller delay values.

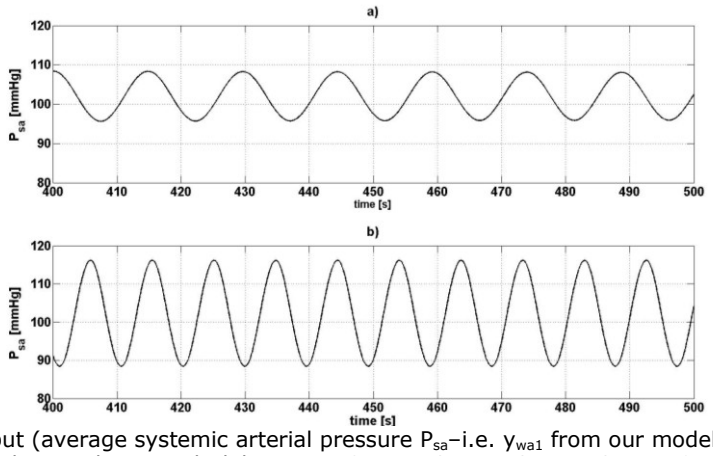

Fig.4.6. Output (average systemic arterial pressure P_{sa}–i.e. y_{wa1} from our model) trajectories for cardiovascular regulation with delays τ_1=4.2 s, τ_2=6 s, τ_3=6 s, τ_4=6 s, τ_5=9 s - a); and with delays $\tau_1=\tau_2=\tau_3=\tau_4=\tau_5$=3 s – b).

4.2.3. Discussion

For the scenarios from section 4.2.2.2 illustrated by Fig. 4.4 and Fig. 4.5, although we have a delay space from 0 s to 20 s for a more complete overall perspective, the square windows of 0s-10s (marked with dashed lines) are of interest from a physiological and pathophysiological point of view.

For a comparative discussion, consider the starting point P_0 which sets the nominal values for $\{\tau_1, \tau_2\}$ to {0.2, 2} in both Fig. 4.4 and Fig. 4.5. If we increase both delays $\{\tau_1, \tau_2\}$ by an equal amount, we follow the path set by vector $\overrightarrow{P_0P_1}$ which leads to the most nearest instability region on the 0-10 s delay space window. A similar thing happens if we increase only the smallest delay τ_1 (parasympathetic component of T), but now we have the path set by the vector $\overrightarrow{P_0P_2}$. The lengths of the two vectors can be regarded as *T delay stability radii* (parasympathetic and sympathetic, or only parasympathetic components). In either case, what is important to notice is that the system reaches instability faster in Fig. 4.5 than in Fig. 4.4, i.e. for a smaller additive increase in the delay(s) $\{\tau_1, \tau_2\}$ (*a smaller stability radius*), when we actually have smaller delay values for the set $\{\tau_3, \tau_4, \tau_5\}$. Moreover, for the case illustrated in Fig. 4.5 the delay τ_5 (which acts on the venous vascular subsystem) was actually decreased below its nominal value; i.e. the system is relatively more unstable for smaller values of this delay.

Two conclusions can be drawn based on the above analysis and discussion:

i) Instability may be more dependent on the magnitude difference between delays, rather than on their absolute values. As consequence stability can be theoretically maintained even for an absurdly large independent delay τ_i (*i* is 1 or 2 in our case study).

ii) If the vascular ("large") delays $\{\tau_4, \tau_5\}$ become smaller, instability may occur for smaller values of the cardiac ("small") delays $\{\tau_1, \tau_2, \tau_3\}$. As a consequence instability can emerge even by decreasing some independent delay τ_i (*i* is 5 in our case study)

As an overall conclusion, it may be more important and revealing to study the interaction between multiple delays (see also [117]) – in terms of *delay magnitude differences* and *delay stability radii*, than to analyze absolute values of a single overall/partial "lumped" delay (like in [110]). Finally, from a physiological point of view, one can conclude that an abnormal fast vascular response can actually make cardiovascular regulation more unstable or less robust.

4.3. Global stability analysis

In this part of the study the focus will be on deriving some global properties for the model of cardiovascular regulation[66]. As an anticipation, we will show that when the system is not asymptotically stable in respect with a specific equilibrium point, it can exhibit bounded oscillatory behavior (limit cycles) – due to large time delays for example.

Global analysis results like trajectory convergence and boundedness are derived using contraction theory, which appeals to a differential approach. This approach – based on contraction theory – is less complex and conservative than those based on Lyapunov methods, while it is also more suitable for studies of robustness because the results hold even for a certain amount of parameter uncertainty which can change the position of the equilibrium point (or limit cycle).

4.3.1. Problem formulation

Consider the following state space form of the cardiovascular regulation model (2.37)-(2.38) from chapter 2:

$$\begin{cases} \dot{\boldsymbol{x}}_a = \boldsymbol{A}_a\ \boldsymbol{x}_a + \boldsymbol{g}_{ab}(\boldsymbol{x}_a, \boldsymbol{x}_b) + \boldsymbol{g}_b(\boldsymbol{x}_b) \\ \dot{\boldsymbol{x}}_b = \boldsymbol{A}_b\ \boldsymbol{x}_b + \boldsymbol{h}(\boldsymbol{x}_{a,\tau}) \end{cases} \tag{4.12}$$

$$y = \boldsymbol{C}_a \boldsymbol{x}_a \tag{4.13}$$

where

$$\boldsymbol{x}_a = [x_0\ \ x_1]^T,\ \boldsymbol{x}_b = [x_2\ \ x_3\ \ x_4\ \ x_5\ \ x_6]^T$$

$$\boldsymbol{A}_a = \begin{bmatrix} a_1 & a_2 \\ 0 & a_5 \end{bmatrix},\ \boldsymbol{A}_b = diag\left(-\frac{1}{T_{Tp}}, -\frac{1}{T_{Ts}}, -\frac{1}{T_E}, -\frac{1}{T_R}, -\frac{1}{T_V}\right),\ \boldsymbol{C}_a = [0\ \ a_{13}],$$

$$\boldsymbol{g}_{ab}(\boldsymbol{x}_a, \boldsymbol{x}_b) = \begin{bmatrix} a_0 x_4 x_0 \\ a_3 x_4 x_0 + a_4 x_0 / x_5 + a_6 x_1 / x_5 \end{bmatrix},$$

$$\boldsymbol{g}_b(\boldsymbol{x}_b) = \begin{bmatrix} a_7 x_6 - a_8 x_6 x_3 + a_8 x_6 x_2 \\ a_9 x_6 / x_5 - a_{10} x_6 x_3 / x_5 + a_{10} x_6 x_2 / x_5 \end{bmatrix},$$

$$\boldsymbol{h}(\boldsymbol{x}_{a,\tau}) = \left[\frac{1}{T_{Tp}} f_{sig,Tp}\left(a_{13} x_{1\tau_{Tp}}\right) \frac{1}{T_{Ts}} f_{sig,Ts}\left(a_{13} x_{1\tau_{Ts}}\right) \frac{1}{T_E} f_{sig,E}\left(a_{13} x_{1\tau_E}\right) \frac{1}{T_R} f_{sig,R}\left(a_{13} x_{1\tau_R}\right) \frac{1}{T_V} f_{sig,V}\left(a_{13} x_{1\tau_V}\right)\right]^T$$

and with the new notations: $y=y_{wa1}, x_1(t-\tau_i) = x_{1\tau_i}, x_0 = x_{wa0}, x_1 = x_{wa1}, x_2 = x_{Tp}$, $x_3 = x_{Ts}, x_4 = x_E,\ \ x_5 = x_R, x_6 = x_V$. The constant coefficients a_i can be identified

[66] The results of this section have been published in [131].

from (2.37)-(2.38), and are give explicitly in the Appendix 2.

Due to the bounded functions **h** (sigmoids) and the diagonal structure of the matrix $\mathbf{A}_b$ (low pass filters), the states $\mathbf{x}_b$ are also bounded, with maximum and minimum values imposed by the sigmoids. As a consequence, the bounds of function $\mathbf{g}_b$ can also be easily determined. Finally, note that the subsystem associated to the states $\mathbf{x}_b$ is always stable because it can be regarded as a linear system with the input vector given by **h**.[67]

In respect with the subsystem associated with the state vector $\mathbf{x}_a$, we regard $\mathbf{x}_b$ as an unknown bounded disturbance vector **w** ($w_1=x_2,\ldots,w_5=x_6$):

$$\dot{\boldsymbol{x}}_a = \boldsymbol{A}_a\ \boldsymbol{x}_a + \boldsymbol{g}_{ab}(\boldsymbol{x}_a,\boldsymbol{w}) + \boldsymbol{g}_b(\boldsymbol{w}) \tag{4.14}$$

Then, subsystem (4.14) can be rewritten as

$$\dot{\boldsymbol{x}}_a = \boldsymbol{A}(\boldsymbol{w})\ \boldsymbol{x}_a + \boldsymbol{g}_b(\boldsymbol{w}) \tag{4.15}$$

with

$$\boldsymbol{A}(\boldsymbol{w}) = \begin{bmatrix} a_1 + a_0 w_3 & a_2 \\ a_3 w_3 + a_4 / w_4 & a_5 + a_6 / w_4 \end{bmatrix}.$$

More compactly, we have

$$\dot{\boldsymbol{x}}_a = \boldsymbol{f}(\ \boldsymbol{x}_a,\boldsymbol{w}) \tag{4.16}$$

with

$$\boldsymbol{f}(\ \boldsymbol{x}_a,\boldsymbol{w}) = \boldsymbol{A}(\boldsymbol{w})\ \boldsymbol{x}_a + \boldsymbol{g}_b(\boldsymbol{w})\,.$$

Next, we want to show that no matter how the bounded disturbance **w** varies in time, the states of system (4.16) - $\mathbf{x}_a$ - remain bounded. Moreover, we want to show that no matter how **w** varies in its bounded domain, if it reaches steady state – imposing an equilibrium point, or if it exhibits sustained oscillations (periodic signal) – imposing a limit cycle, the trajectory $\mathbf{x}_a(t)$ is stable. The interpretation behind this is that in closed loop (i.e. when the two subsystems of (4.12) are interconnected), the system reaches steady state for certain values of the time delays, while for other (relatively large) delay values oscillations may emerge. In other words, we want to show that the closed loop systems may oscillate due to pathological values of the time delays, but can never exhibit finite escape time behavior or other type of unbounded growth.

4.3.2. Analysis via contraction theory

A direct approach to stability of (4.16) is infeasible in terms of Lyapunov functions and input-to-state stability[68] for example, due to the large bounds of **w**. Instead, we turn to the alternative notion of *convergence*, as part of the theoretical framework given by contraction theory – [118], [128]. The idea is to analyze the system *differentially*, in terms of distance between a given state trajectory and some nominal trajectory (which can describe a limit cycle or a path converging

[67] The matrix $\mathbf{A}_b$ is Hurwitz.
[68] See the classical approach from [1] - ch. 4.9, or the recent results from [121].

towards an equilibrium point). The nominal trajectory does not have to be known, only the fact that any given trajectory eventually converges to the nominal one is of interest[69]. Obviously, such convergence is a form of stability (incremental stability – see [119])[70]. Additionally, it is shown in [120] that for convergent systems the nominal solution (trajectory) exists, is unique and bounded; because all other solutions (trajectories) converge asymptotically to it, the boundedness of all solutions is imposed by the set encompassing the initial conditions.[71]

First, note that for system (4.16), because **w** is actually time varying - **w**(t), the right hand side can be written as **f**($\mathbf{x}_a$,t). As working hypothesis, **f** is continuous in *t*, continuous differentiable in $\mathbf{x}_a$, and $\|\boldsymbol{f}(0,t)\| \le c < +\infty$ for all *t* (this last condition is needed for precluding a finite escape time – [120]). The differential relations corresponding to (4.16) is

$$\delta\dot{\boldsymbol{x}}_a = \frac{\partial \boldsymbol{f}}{\partial \boldsymbol{x}_a}(\boldsymbol{x}_a, t)\,\delta\boldsymbol{x}_a \tag{4.17}$$

where $\delta\boldsymbol{x}_a$ represents an infinitesimal displacement at a fixed time (virtual displacement), while $\delta\boldsymbol{x}_a^T\delta\boldsymbol{x}_a$ represents the squared distances between two trajectories. It is shown in [118] that this distance converges to zero if the Jacobian is uniformly negative definite, i.e.

$$\frac{1}{2}\left(\frac{\partial \boldsymbol{f}}{\partial \boldsymbol{x}_a} + \frac{\partial \boldsymbol{f}}{\partial \boldsymbol{x}_a}^T\right) \le -\beta\boldsymbol{I} < 0, \qquad \exists\beta > 0, \forall \boldsymbol{x}_a, t. \tag{4.18}$$

More generally, one can define a length $\delta\boldsymbol{x}_a^T\boldsymbol{M}(\boldsymbol{x}_a,t)\delta\boldsymbol{x}_a$, where the metric **M**($\mathbf{x}_a$,t) is symmetric, uniformly positive definite and continuously differentiable, i.e.

$$\boldsymbol{M}(\boldsymbol{x}_a,t) \ge \mu\boldsymbol{I} > 0, \qquad \mu > 0, \forall \boldsymbol{x}_a, t. \tag{4.19}$$

In this case, the system is contracting – the distance converges to zero – if

$$\frac{\partial \boldsymbol{f}}{\partial \boldsymbol{x}_a}^T \boldsymbol{M} + \boldsymbol{M}\frac{\partial \boldsymbol{f}}{\partial \boldsymbol{x}_a} + \dot{\boldsymbol{M}} \le -\beta_M \boldsymbol{M} \quad , \beta_M > 0, \forall \boldsymbol{x}_a, t. \tag{4.20}$$

The state space region in which (4.20) holds is called a contraction region with respect to the metric **M**. If (4.20) holds globally then the contraction region is the whole state space. All of this leads to the following theorems [118][72]:

Theorem 4.2a: If system (4.16) is contracting with a certain contraction region, then *any trajectory starting in a ball* of constant radius and contained in the contraction region – both with respect to the metric **M,** centered at another given

[69] This means that initial conditions or vanishing disturbances are eventually "forgotten".
[70] See also [120] and [122] for a more detailed discussion on convergent systems and [123] for a Lyapunov approach to incremental stability.
[71] In our case study we are dealing with physiological systems, so the initial conditions are in a bounded set.
[72] Note that the theorems invoke sufficient only conditions.

(nominal) trajectory, *will remain in that ball and converge exponentially to the nominal trajectory*.

Theorem 4.2b: If system (4.16) is globally contracting, i.e. the contraction region is the whole state space, *then any trajectory will globally converge exponentially to the nominal trajectory*.[73]

Remark 4.1: Through convergence of a perturbed trajectory $\boldsymbol{x}_p(t)$ to a nominal trajectory $\boldsymbol{x}_n(t)$ we mean that: i. when the nominal trajectory is trivially periodic, i.e. it eventually reduces to an equilibrium point, we have $\boldsymbol{x}_p(t) \to \boldsymbol{x}_n(t)$ ([118]); ii. when the nominal trajectory is periodic, i.e. it eventually reduces to a limit cycle , there exists a fixed η such that $\boldsymbol{x}_p(t) \to \boldsymbol{x}_n(t+\eta)$ ([124]).

4.3.3. Results using contraction theory

By calculating the Jacobian for system (4.16), and adopting a constant metric $\mathbf{M}$=diag(m_0,m_1) - m_0>0 and m_1>0, we obtain the following matrix inequality:

$$\begin{bmatrix} a_1 + a_0 w_3 & a_2 \\ a_3 w_3 + a_4 / w_4 & a_5 + a_6 / w_4 \end{bmatrix}^T \boldsymbol{M} + \boldsymbol{M} \begin{bmatrix} a_1 + a_0 w_3 & a_2 \\ a_3 w_3 + a_4 / w_4 & a_5 + a_6 / w_4 \end{bmatrix} + \beta_M \boldsymbol{M} < 0 \quad , \forall t. \tag{4.21}$$

If we define the left hand side of inequality (4.21) as a matrix $\boldsymbol{\Lambda}(w_3,w_4)$, then we need to prove that there exists a matrix $\mathbf{M}$ for which $\boldsymbol{\Lambda}(w_3,w_4)$ has eigenvalues only in the open left half plane for any values of w_3 and w_4 (in their corresponding domain). The characteristic polynomial of $\boldsymbol{\Lambda}$, after some calculations, is determined as:

$$p(s) = s^2 + q_1(w_3,w_4)s + q_0(w_3,w_4). \tag{4.22}$$

with

$$q_1(w_3,w_4) = -2m_0a_1 - 2m_0a_0w_3 - m_0\beta_M - 2m_1a_5 - 2m_1a_6/w_4 - m_1\beta_M$$

$$q_0(w_3,w_4) = -(m_0a_2 + m_1a_3w_3 + m_1a_4/w_4)^2 + (2m_0a_1 + 2m_0a_0w_3 + m_0\beta_M)(2m_1a_5 + 2m_1a_6/w_4 + m_1\beta_M)$$

Additionally, we know the interval of the two polynomials q_1 and q_0, according to the bounds on w_3 and w_4: $q_1 \in [q_1^-, q_1^+], q_0 \in [q_0^-, q_0^+]$. According to Kharitonov's Theorem (see [3]-vol.3-ch.7), the interval polynomial (4.22) is stable (all eigenvalues are in the open left half plane) *if and only if* the following four fixed polynomials are stable:

[73] The result of Theorem 4.2b practically states that if the system is globally contracting, then the solution is bounded and globally asymptotically stable ([120]).

$$\begin{aligned} p_1(s) &= s^2 + q_1^{+} s + q_0^{+} \\ p_2(s) &= s^2 + q_1^{-} s + q_0^{-} \\ p_3(s) &= s^2 + q_1^{-} s + q_0^{+} \\ p_4(s) &= s^2 + q_1^{+} s + q_0^{-}. \end{aligned} \tag{4.23}$$

Let us further adopt the values m_0=1 and m_1=0.3 for the metric **M**, with $\beta_M = 0.1$[74]. By calculating the characteristic polynomial *p* of matrix **Λ**, and then the four fixed polynomials p_1-p_4 according to the bounds on q_1 and q_0[75], we obtain that all four polynomials of (4.23) are stable. Thus, by Kharitonov's Theorem the interval polynomial *p* from (4.22) is stable for any values of w_3 and w_4, which means that condition (4.21) holds. Consequently, system (4.16) is globally contracting, and the results of Theorem 4.2b hold.

Finally, we will show how system (4.12)-(4.13) behaves in numerical simulations for two scenarios: a) Nominal (physiological) values for the delays (see section 4.2.2.1) – when an equilibrium point is attained – with a vanishing perturbation acting at a given moment; b) Large (pathological) values for the delays (3 s increase in all delays except τ_V) – when a limit cycle is attained – with a vanishing perturbation acting at a given moment. The perturbation acts on the heart period T– i.e. on the both states x_2 and x_3 – which means that it acts practically at the level of function $\mathbf{g}_b$ from (4.12). For each of the two scenarios, Fig. 4.7 illustrates that the perturbed trajectory converges towards the nominal one (contraction) - once the perturbation vanishes.[76] Note that for scenario b), in accordance with Remark 4.1, the duration of the perturbation was chosen approximately equal to the period of the oscillations of the nominal trajectory (η=0), in order to better illustrate the convergence. Moreover, it is important to note that generally speaking, the results state that our system is actually *contracting independent of delays*.

[74] Note that all the parameters which give the coefficients a_i are taken from Table 4.1.

[75] For the present case study we have: $q_0^{-} = 28.681, q_0^{+} = 100.338, q_1^{-} = 89.445, q_1^{+} = 137.382$.

[76] Contraction is illustrated in simulations – Fig. 4.7– at the level of the output y (average systemic blood pressure P_{sa}), and not the states $\mathbf{x}_a$, because this is more important (relevant) from a physiological prespective. Moreover, the baroreflex feedback control loop uses only this signal (y / average P_{sa}) as input.

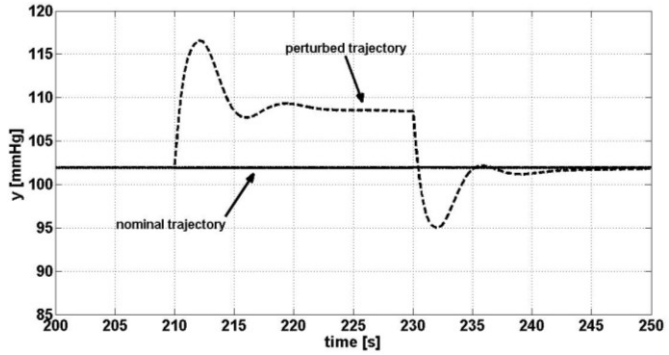

a) nominal delays

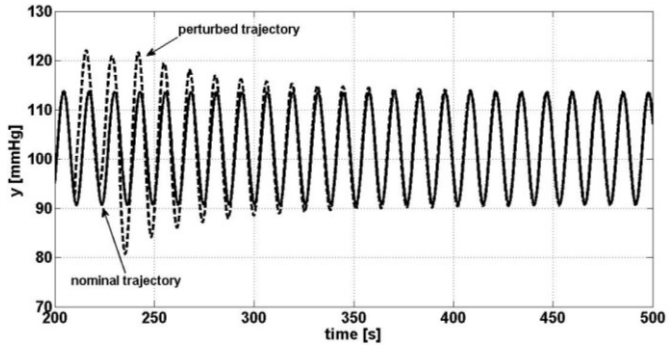

b) large delays

Fig.4.7. System response (output *y* represents average systemic arterial pressure) to a vanishing perturbation.

4.3.4. Robustness analysis

In the case of parameter uncertainty, one approach is to use the same (nominal) contraction metric **M** in order to see how much uncertainty can the systems face such that it is still contracting. Consider an additive uncertainty of the type $\mathbf{f}_u(\mathbf{x}_a,t) = \mathbf{f}(\mathbf{x}_a,t)+\mathbf{f}_\delta(\mathbf{x}_a,t)$, and in particular when the uncertain dynamic component is $\mathbf{f}_\delta(\mathbf{x}_a,t)=[\delta_0 x_0+\delta_1 x_1+\Delta \quad 0]^T$, with δ_0 and δ_1 as unknown positive constants, and Δ an unknown constant[77]. The new condition for contraction is

$$\begin{bmatrix} a_1 + a_0 w_3 + \delta_0 & a_2 + \delta_1 \\ a_3 w_3 + a_4 / w_4 & a_5 + a_6 / w_4 \end{bmatrix}^T \boldsymbol{M} + \boldsymbol{M} \begin{bmatrix} a_1 + a_0 w_3 + \delta_0 & a_2 + \delta_1 \\ a_3 w_3 + a_4 / w_4 & a_5 + a_6 / w_4 \end{bmatrix} + \beta_M \boldsymbol{M} < 0 \quad , \forall t. \tag{4.24}$$

Using the same constant metric **M** from the nominal case (see section 4.3.3), we can determine the uncertainty bounds, i.e. bounds on δ_0 and δ_1, for which the system is still contracting. Through a point-wise sweeping of these bounds[78], and using Kharitonov's Theorem as in the previous section, we obtain the

[77] The adopted class of uncertain dynamics is for exemplification purposes. The robustness analysis can be conducted in a similar manner for other types of uncertain dynamics – like for example where the second element (row) of $\mathbf{f}_\delta$ is non-null.

[78] The point-wise sweeping was done in the following manner: starting from the maximum feasible value of δ_0 (for which δ_1 is 0), with each decrease of δ_0 the maximum feasible value of

uncertainty region for which the systems is still contracting given in Fig. 4.8. Note that the region can be determined as precise as needed by reducing the step size of the sweeping (here Fig. 4.8, for illustrative purposes, gives only a rough approximation).

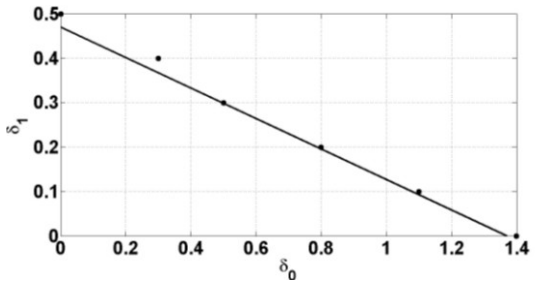

Fig.4.8. Uncertainty region for which the system is still contracting in respect with the nominal contraction metric.

The results can be interpreted in the following manner: if there exists an uncertainty in the systems parameters, and this parameter uncertainty can be characterized in terms of an additional additive component $\mathbf{f}_\delta$, then the system is robustly contracting in respect with the nominal metric **M** in the presence of such uncertainties only if the uncertainty finally expressed through the parameters δ_0 and δ_1 is inside the a priori computed uncertainty region. For example an increase of the venous resistance parameter R_2 (which modifies the coefficients a_1, a_2, a_7 and a_8) by 100% leads to δ_0=0.73 and δ_1=0.11, which in our case is inside the uncertainty region.[79]

Finally, an alternative to this approach is to search directly for a contraction metric $\mathbf{M}_u$ which provides the largest uncertainty region for which the system is contracting ([125])[80].

4.3.5. Discussion

Global properties for models of cardiovascular regulation are hard to determine due to multiple nonlinearities and multiple time delays. In the current chapter, we have tried to derive some global properties for a simple model of cardiovascular regulation using contraction theory, which appeals to a differential approach. The results show that the system is contracting (convergent), which leads to state boundedness and stability of the nominal solution $\mathbf{x}_a$ of the cardiovascular subsystem.

δ_1 was determined, until δ_0 equals 0 is reached (for which we have the maximum feasible value of δ_1). In respect with the maximum feasible (δ_0, δ_1) points obtained, a geometric region can be set (in our case with the aid of a simple line) which roughly delimitates the uncertainty region.

[79] Note that the results of the analysis are independent of Δ, which in this case is given by the change in a_7 and a_8.

[80] For certain classes of autonomous nonlinear systems, the contraction metrics can be obtained through numerical methods based on convex optimization involving linear matrix inequalities ([54]) or sum of squares programming ([126], [127])- see [125] for details.

Although one would have expected that cardiovascular regulation to exhibit stable dynamic behavior in a nominal-physiological regime, besides the fact that we have attested this through systems analysis (and not empirically for particular cases), along with an extension to robustness (in respect with possible pathological scenarios),of interest is also the fact that according to our studies cardiovascular regulation, at least at the level of nervous feedback control, can not exhibit finite escape time behavior – i.e. systems trajectory can not escape towards infinity in finite time. This can be explained partially by the fact that the nervous feedback control loop (baroreflex feedback control loop) presents strong limitations (upper and lower saturation) on all control signals acting on the cardiovascular system, with no integrator component. This means the control systems presents a non-null steady state error (in respect with a certain reference signal imposed by higher nervous centers), but it does present the advantage of increasing the stability of the system in respect with large disturbances, by precluding possible wind-up scenarios (actuator saturation for integral feedback control).

Another interesting fact worth discussing is that the baroreflex feedback control loop is with one input (measured signal) and with multiple outputs (control signals). Conventionally, this represents and output feedback control systems. However, the presence of different time constants and time delays on each feedback control loop, lead to control loops acting on different time scales. As an interpretation, different time constants and time delays on each feedback control loop can virtually represent additional states variables, thus making the control resemble more like a state feedback control one. So the time delays can to a certain degree actually help to better control the cardiovascular system.

Finally, it should be noted that although in our study the cardiovascular system is reduced to a minimal model (i.e. as simple as possible), in reality the cardiovascular system represents a large-scale system, and with this in mind, the feedback control structure would not seem over-actuated any more, and the complexity and robustness of the nonlinear control involved become highly justified.

4.4. Conclusions

The stability analysis of cardiovascular regulation reveals and generalizes certain features of the dynamic behavior which could have only been noticed empirically, through simulations. The *local analysis* shows that the asymptotic stability of the equilibrium point is dependent on the delays values. Moreover, it may be more important and revealing to study the interaction between multiple delays than to analyze absolute values of a single overall/partial "lumped" delay. The *global analysis* shows that the states of the system are always bounded, and that the nominal solution $\mathbf{x}_a$ of the cardiovascular subsystem is stable independent of delays (whether the solution is trivially periodic or not). So, although the system is *not delay independent stable*, it proves to be *convergent independent of delays*.

Finally, from a physiological and pathophysiological point of view, the results state that cardiovascular regulation is not only a stable process in nominal conditions, but it also presents boundedness for a wide category of scenarios, stable limit cycles in pathological conditions (e.g. large delays), and robustness in respect with uncertainty.

5. CONCLUSIONS AND FUTURE RESEARCH

Before we present the thesis summary with its main contributions, along with future research directions, we need to express some final conclusions regarding the entire research study which was the object of this PhD thesis.

The study started from the well known idea in control engineering that one needs to work with mathematical models as simple as possible, but not simpler. Despite a wide range of mathematical models with capture the cardiovascular system and cardiovascular regulation, we adopted and adjusted the models which seem to fall best into this category – simple as possible, but which conserve the main dynamic behavior of the biomedical systems involved.

Once the modeling phase was surpassed, we addressed the main goal of the thesis: systems analysis of cardiovascular regulation.

The local stability analysis reveals how the system can become unstable in respect with an equilibrium point due to multiple time delays. The problem of how time delays interact in order to produce oscillations is a nontrivial problem, into which we managed to provide some new and we think useful insights. Because there are pathologies which affect these time delays (like the Guillain–Barré syndrome or Diabetic Autonomic Peripheral Neuropathy), we think that our results will be of use for improving diagnosis practices in the future.

The global analysis has revealed that although cardiovascular regulation can exhibit oscillatory behavior (for example due to time delays), it presents a stable behavior in respect with specific regimes imposed by (the lack or presence of) disturbances. Robustness in respect with uncertainty is an important characteristic revealed also by our analysis. This can be viewed as a paradox: while biomedical systems are seen from one point as fragile, with high variability, and predisposed to all kinds of pathological disturbances, from another point of view, living organisms show complex and hierarchical control mechanisms, with precise function for each organ and cell, which actually shows high robustness and reliability in the sense that its subsystems maintain their critical functional role on the long term as best as possible without consuming to much additional resources from the organism as a whole (limits on energy, complexity, and so on). The best example is the heart, which may be predisposed to all sort of illnesses, but is one of the best functioning hydraulic pumps on long term known to man. It can be said that control mechanisms of living organisms are in some way optimal. So, finally, although we haven't tackled cases of global instability, our results provide insight into aspects like trajectory convergence and robustness, which can be of use for understanding how a pathological agent can influence cardiovascular regulation, and what this means from a control point of view.

As a general conclusion, our study reveals once more that biomedical systems represent an important challenge to control theorists, because these kind of studies present a unique opportunity to study control structure and control mechanisms which were not built by man. Such interdisciplinary research studies

not only help scientists and clinicians in the field of medicine, but give new ideas to engineers in the design of technical systems. All for the good of mankind.

5.1. Summary and Contributions

The main scientific contributions of the current thesis are the following:

- Development of a simplified averaged model for cardiovascular regulation starting from models of the cardiovascular system and the baroreflex system from the literature (Chapter 2);
- Development of a new averaging method - along with its theoretical framework, which can be applied not only for the cardiovascular system, but for an entire class of nonlinear systems (Chapter 2 and Chapter 3);
- A local stability analysis of cardiovascular regulation which reveals the role of multiple time delays in generating stability or instability, along with insights into possible physiological implications (Chapter 4);
- A global stability analysis of cardiovascular regulation which reveals properties like trajectory convergence and boundedness, with a study of robustness in respect with disturbances and parameter uncertainty, and an interpretation on how physiological systems (in particular cardiovascular regulation) behave as control systems (Chapter 4).

The thesis begins with a short introduction (Chapter 1) which contains the motivation of the entire study, preliminary notions on biomedical systems in general and on cardiovascular regulation in particular, and preliminary notions on nonlinear systems, classes of nonlinear systems and analysis approaches.

Chapter 2 contains all that is related to mathematical modeling, model simplification and averaging, and finally model validation. After a short motivation on the need to work with models as simple as possible, the model of the cardiovascular systems adopted from the literature is presented and explained. Then, the model is brought to the form of a switched linear system. As a second step in the modeling phase, a model of the baroreflex control loop is adopted from the literature, which is then brought to a simplified form. The closed loop (pulsatile) model of cardiovascular regulation is further derived by coupling the cardiovascular and the baroreflex models, and by also taking in account the interactions which appear on both the direct and feedback paths. Finally, after adapting the conventional averaging method so that it can handle pulse frequency modulated systems – as it the case for cardiovascular regulation – an averaged closed loop model of cardiovascular regulation is obtained. Simulations results, both in open loop and closed loop, show that the averaged model captures the basic dynamics of the original (periodic) system. Model validations are done also through simulations, by comparing the results obtained for a pathological scenario – hemorrhage – with experimental results from the literature.

Chapter 3 provides a theoretical framework for the averaging method developed in the previous chapter. The chapter starts with a short survey on averaging methods developed in the literature along the years. Next, the problem formulation defines the class of systems taken into consideration – pulse frequency modulated systems with constant duty ratios – and defines the goal: to derive an

averaging method which approximates the original system within a certain error bound and which is dependent on the modulation period. The theoretical framework further presented consists in three theorems adapted from the literature (which make use of perturbation theory) to this new class of systems. In the last part of the study, a step-by-step description is provided, on how the proposed averaging method can be used in the case study referring to the cardiovascular system, while pointing out ways of copping with the practical issues that emerge. Finally, numerical results obtained through simulations illustrate the effectiveness of the proposed averaging method.

The most elaborate part of the thesis is Chapter 4, which addresses the systems analysis of cardiovascular regulation – the actual goal of this study, both locally and globally. The local stability analysis works with the linearized model around its equilibrium point. The focus is on the role of multiple time delays on generating stability or instability. After highlighting the fact that the issue of multiple delays is of recent date, with few methods found in the literature, the most suitable stability method from the literature is presented – which provides necessary and sufficient conditions for stability. The numerical results consist in stability maps in terms of specific a priori imposed delay coordinates for two pathological scenarios. A discussion is done on the interpretation of these results, concluding that it may be more import to focus on the interaction between multiple delays, and not on the delay absolute value (taken independently). This means that a decrease in a specific delay value does not necessary improve stability, on the contrary - it may deteriorate stability. The global analysis makes use of contraction theory – with reference to convergent systems – which views the systems in terms of a nominal trajectory (solution) to which all other trajectories (solutions) converge to. The conditions requires for a system to be contracting are presented, along with a case study for cardiovascular regulation. Simulation scenarios confirm the results regarding convergence. As an extension, the issue of robustness is raised and addressed in the last part, showing that the system is robust to parameter uncertainties or certain types of disturbances (numerical results make possible the delimitation of a specific uncertainty region in which the systems maintains its properties). A short discussion points out the main characteristics of cardiovascular regulation as a control system. Finally, the conclusions state that the system is not delay independent stable, but it is convergent independent of delays.

Chapter 5 draws the final conclusions, highlights the main contributions of the present study, and points out possible directions for future research.

5.2. Future research directions

The directions for future research, set forth by the current research study – which falls into the category of applied theory, can be divided into two types: applied and theoretical.

A future theoretical development can refer to further robustness studies, in respect to a multitude of pathological scenarios (disturbances, parameter uncertainties). Thus, one can search for specific types of disturbances for which the system starts to show signs of instability, and then connect them to pathological scenarios.

Systems analysis studies set the path towards future research concerning design, which in the case of biomedical systems can refer to state observers for example, or even specific technical devices which assist the human organism (e.g. left ventricle assist devices). The design of state observers for the cardiovascular system is of high interest because it can inform clinicians about certain physiological signals which are non-measureable (at least non-invasive), and the convergence issue for observers (between the estimated state and the actual state signals) can be formulated as a stability problem – thus the analysis part becomes of real and direct help here. Moreover, some physiological signals which act on the cardiovascular signal can be regarded as unknown external disturbances, and thus can be estimated through unknown input observers.

A more applied research direction is the one in which more developed and complex models of the cardiovascular system are employed - the analysis approaches from the current study permit the extensions to larger systems – and the study focuses on specific physiological or/and pathological scenarios. The complexity and uncertainty (high variability) of biomedical systems impose that for (quasi-)quantitative studies one should focus on specific scenarios. Thus, such an approach can make possible thorough experimental validations in respect with a specific scenario and a priori imposed category of test subjects, which can eventually lead to better diagnosis or treatment methods.

APPENDIX 1

In determining how relay-hysteresis models can behave as Pulse Modulators, a piecewise analysis approach is conducted.

First, consider the relay-hysteresis model proposed by Tsypkin (Fig. 2.10) for PFMs. On the first modulation interval (t_1, t_2), the output of the integrator is

$$f_0 = e(t) = 0 + k_d \int_{t_1}^{t_2} f \, dt = k_d (t_2 - t_1) f \,, \tag{a1.1}$$

where the input *f* was considered constant on the given interval. The interval can be thus calculated as t_2-t_1=f_0/(k_d·x). On the second modulation interval (t_2, t_1'), the output of the integrator is

$$0 = e(t) = f_0 + k_d \int_{t_2}^{t_1'} (f - k_f) \, dt = k_d (t_1' - t_2)(f - k_f) + f_0 \,, \tag{a1.2}$$

where again *f* is constant on the given interval. The interval is now calculated as t_1'-t_2=f_0/[k_d·(k_f-f)]. The entire modulation period is the sum of these two intervals, which would have to be equal to the inverse of the input *f*, i.e.

$$\frac{1}{f} \cong \frac{f_0 \, k_f}{f \, k_d (k_f - f)} \,. \tag{a1.3}$$

Condition (a1.3) does not hold in general, because it would imply an equality of the form $k_d(k_f-f)=f_0k_f$, with *f* as an only variable. However, for certain values of the parameters and for a certain range of *f*, condition (a1.3) could approximately be met. To illustrate this better, we will exemplify for the case when the input is the prescribed heart frequency $f=f_T$, which is defined in the physiological domain [0.3, 4] Hz. We will adopt k_d=1 and f_0=1. Fig. A1.1 further shows the graphs of the right-hand side and left-hand side functions of (a1.3) in respect with the variable *f,* and we can see that the increase in the value of k_f means moving the singularity point of the right-hand side function out of the considered domain of interest, while the overall approximation gets better and better. Consequently, the relays-hysteresis model from Fig. 2.10 can approximately capture the dynamic behavior of a PFM in certain conditions (like k_f sufficiently large for a given domain of the input).

Second, consider the relay-hysteresis model that we proposed - Fig. 2.11 - for CPMs. Suppose that the duration of the modulated pulse varies proportional with the modulation period (constant duty ratio case) - i.e. $\tau = T/\alpha_k$. Let the feedback gain vary with the input modulation frequency *f* through the law $k_f = \alpha_k \cdot f$. The calculation based on (a1.1) and (a1.2) remains the same, but in the final expression of (a1.3) we replace the value of k_f:

$$\frac{1}{f} = \frac{f_0 \, \alpha_k}{f \, k_d (\alpha_k - 1)} \,. \tag{a1.4}$$

Besides this condition, we also want to impose the duration of τ to equal the previously calculated duration of the interval (t_2,t_1'):

$$\tau = \frac{f_0}{f\, k_d(\alpha_k - 1)}. \qquad \text{(a1.5)}$$

After adopting k_d=1, both conditions (a1.4) and (a1.5) reduce to the single constraint: $f_0 \cdot \alpha_k = \alpha_k - 1$. Thus, for a given α_k (e.g. α_k=3), we immediately find also the last remaining parameter f_0 (e.g. f_0=2/3). Consequently, the conditions imposed by the desired type of pulse modulation (CPM) are satisfied exactly by our model.

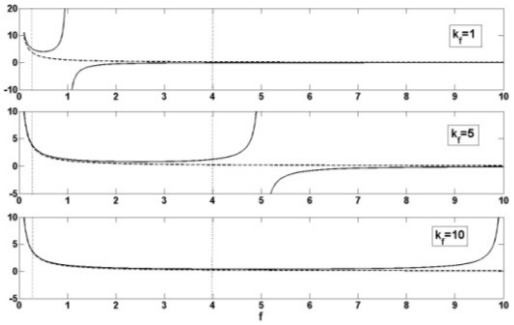

Fig. A1.1. Graphs of the right-hand side (continuous line) and left-hand side (dashed line) of (a1.3) in respect with *f,* for different values of k_f.

Last, we will show that a relay-hysteresis model can be equivalent to an IPFM (e.g. [57]), which is also referred in the literature as an "integrate and fire" (e.g. [39] or [92]) model. An IPFM generates at the output a saw-tooth signal[81] with the frequency given by the input signal, which is further used as a timer for coordinating the contractions of the heart (practically the elastance function is generated based on this signal) – [17]. Although several studies use a resetting integrator, or a fractional operation, and so on, we will show that a simple relay element can achieve the task. By rearranging the diagram from Fig. 2.10 and setting k_d=1 and f_0=1, we obtain the relay-hysteresis model from Fig. A1.2, which approximates an IPFM for sufficiently large values of k_f (e.g. k_f=1000 in our case). The advantage of the model is that it is more tractable from an analytical point of view. Finally, an additional "shaping" component was added which shows how an elastance signal like the one from Fig. 2.2 can be generated.

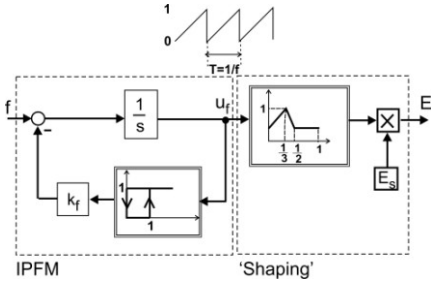

Fig. A1.2. Relay-hysteresis model for an IPFM.

[81] In some applications, the actual output of the IPFM used consists in a train of impulses, which are generated on the falling edge of the saw tooth signal. This can be accomplished by simply adding a bi-positional relay element.

APPENDIX 2

Equilibrium point (nominal-physiological conditions):

$\mathbf{x}_e$=[70.67 203.9 1.18 0.15 2.47 0.98 1714].

Matrices **A**, $\mathbf{A}_i$ and **C** from model (4.2):

$$\boldsymbol{A}=\begin{bmatrix} a_0x_E+a_1 & a_2 & a_8x_V & -a_8x_V & a_0x_{wa0} & 0 & a_7-a_8x_{Ts}+a_8x_{Tp} \\ a_3x_E+\frac{a_4}{x_R} & a_5+\frac{a_6}{x_R} & a_{10}\frac{x_V}{x_R} & -a_{10}\frac{x_V}{x_R} & a_3x_{wa0} & -\frac{a_4x_{wa0}+a_6x_{wa1}+a_9x_V-a_{10}x_V(x_{Ts}-x_{Tp})}{x_R^2} & \frac{a_9}{x_R}-a_{10}\frac{x_{Ts}-x_{Tp}}{x_R} \\ 0 & 0 & -\frac{1}{T_{Tp}} & 0 & 0 & 0 & 0 \\ 0 & 0 & 0 & -\frac{1}{T_{Ts}} & 0 & 0 & 0 \\ 0 & 0 & 0 & 0 & -\frac{1}{T_E} & 0 & 0 \\ 0 & 0 & 0 & 0 & 0 & -\frac{1}{T_R} & 0 \\ 0 & 0 & 0 & 0 & 0 & 0 & -\frac{1}{T_V} \end{bmatrix}_{\boldsymbol{x}_e}$$

$$\boldsymbol{A}_1=\begin{bmatrix} 0 & 0 & 0\,0\,0\,0\,0 \\ 0 & 0 & 0\,0\,0\,0\,0 \\ 0 & \frac{1}{T_{Tp}}\frac{d}{dx_{wa1,\tau_{Tp}}}f_{sig,Tp} & 0\,0\,0\,0\,0 \\ 0 & 0 & 0\,0\,0\,0\,0 \\ 0 & 0 & 0\,0\,0\,0\,0 \\ 0 & 0 & 0\,0\,0\,0\,0 \\ 0 & 0 & 0\,0\,0\,0\,0 \end{bmatrix}_{\boldsymbol{x}_e},$$

$$\boldsymbol{A}_2=\begin{bmatrix} 0 & 0 & 0\,0\,0\,0\,0 \\ 0 & 0 & 0\,0\,0\,0\,0 \\ 0 & 0 & 0\,0\,0\,0\,0 \\ 0 & \frac{1}{T_{Ts}}\frac{d}{dx_{wa1,\tau_{Ts}}}f_{sig,Ts} & 0\,0\,0\,0\,0 \\ 0 & 0 & 0\,0\,0\,0\,0 \\ 0 & 0 & 0\,0\,0\,0\,0 \\ 0 & 0 & 0\,0\,0\,0\,0 \end{bmatrix}_{\boldsymbol{x}_e},$$

$$\boldsymbol{A}_3=\begin{bmatrix} 0 & 0 & 0\,0\,0\,0\,0 \\ 0 & 0 & 0\,0\,0\,0\,0 \\ 0 & 0 & 0\,0\,0\,0\,0 \\ 0 & 0 & 0\,0\,0\,0\,0 \\ 0 & \frac{1}{T_E}\frac{d}{dx_{wa1,\tau_E}}f_{sig,E} & 0\,0\,0\,0\,0 \\ 0 & 0 & 0\,0\,0\,0\,0 \\ 0 & 0 & 0\,0\,0\,0\,0 \end{bmatrix}_{\boldsymbol{x}_e},$$

$$\boldsymbol{A}_4=\begin{bmatrix} 0 & 0 & 0\,0\,0\,0\,0 \\ 0 & 0 & 0\,0\,0\,0\,0 \\ 0 & 0 & 0\,0\,0\,0\,0 \\ 0 & 0 & 0\,0\,0\,0\,0 \\ 0 & 0 & 0\,0\,0\,0\,0 \\ 0 & \frac{1}{T_R}\frac{d}{dx_{wa1,\tau_R}}f_{sig,R} & 0\,0\,0\,0\,0 \\ 0 & 0 & 0\,0\,0\,0\,0 \end{bmatrix}_{\boldsymbol{x}_e},$$

$$\boldsymbol{A}_5 = \begin{bmatrix} 0 & 0 & 0\,0\,0\,0\,0 \\ 0 & 0 & 0\,0\,0\,0\,0 \\ 0 & 0 & 0\,0\,0\,0\,0 \\ 0 & 0 & 0\,0\,0\,0\,0 \\ 0 & 0 & 0\,0\,0\,0\,0 \\ 0 & 0 & 0\,0\,0\,0\,0 \\ 0 & \frac{1}{T_V}\frac{d}{dx_{wa1,\tau V}} f_{sig,V} & 0\,0\,0\,0\,0 \end{bmatrix}_{\boldsymbol{x}_e},$$

$$\boldsymbol{C} = \begin{bmatrix} a_{11}x_E + a_{12} & 0 & 0\,0 & a_{11}x_{wa0} & 0\,0 \\ 0 & a_{13} & 0\,0 & 0 & 0\,0 \end{bmatrix}_{\boldsymbol{x}_e}.$$

The non-null term in each matrix $\mathbf{A}_i$ (i=1,2,3,4,5) represents the derivative of the function $f_{sig,j}$ in respect with the variable $x_{wa1}(t-\tau_j)$; where $j \in \{T_{Tp}, T_{Ts}, E, R, V\}$. For example, for the matrix $\mathbf{A}_1$ we have:

$$\frac{d}{dx_{wa1,\tau Tp}} f_{sig,Tp} = -\frac{(x_{Tp}^{min} - x_{Tp}^{max})\gamma_{Tp} k_{iTp}}{C_1} \frac{exp(x_{wa1,\tau_{Tp}} k_{iTp} / C_1)}{\left(1 + \gamma_{Tp} exp(x_{wa1,\tau_{Tp}} k_{iTp} / C_1)\right)^2}.$$

.

Constant coefficients a_i from model (4.2) - matrices $\mathbf{A}$, $\mathbf{A_i}$, $\mathbf{C}$ - and model (4.12)-(4.13):

$a_0 = -\rho_0 d_0 / R_0,$
$a_1 = -\rho_0 d_1 E_d / R_2 - \rho_0 d_1 /(R_2 C_2),$
$a_2 = \rho_1 d_0 /(R_0 C_1) - \rho_1 d_1 /(R_2 C_2),$
$a_3 = \rho_0 d_0 / R_0,$
$a_4 = -\rho_0 / C_2,$
$a_5 = -\rho_1 d_0 /(R_0 C_1),$
$a_6 = -(\rho_1 C_1 + \rho_1 C_2)/(C_1 C_2),$
$a_7 = \alpha_1 /(R_2 C_2),$
$a_8 = \beta_1 /(R_2 C_2),$
$a_9 = (\alpha_0 + \alpha_1)/ C_2,$
$a_{10} = (\beta_0 + \beta_1)/ C_2,$
$a_{11} = d_0,$
$a_{12} = d_1 E_d,$
$a_{13} = 1/C_1.$

As defined in [129], the *resultant* of two multivariate polynomials with real coefficients,

$$p_1(\upsilon, \boldsymbol{\mu}) = \sum_{i=0}^{m} a_i(\upsilon, \mu_1, \ldots, \mu_{r-1})\mu_r^i = 0, \quad a_m \neq 0,$$

$$p_2(\upsilon, \boldsymbol{\mu}) = \sum_{i=0}^{n} b_i(\upsilon, \mu_1, \ldots, \mu_{r-1})\mu_r^i = 0, \quad b_n \neq 0,$$

with respect to μ_r is the determinant

$$R_{\mu_r}(p_1, p_2) = \begin{vmatrix} a_m & a_{m-1} & . & . & . & a_0 & 0 & 0 & 0 \\ 0 & a_m & a_{m-1} & . & . & a_1 & a_0 & 0 & 0 \\ . & . & . & . & . & . & . & . & . \\ . & . & . & . & . & . & . & a_1 & a_0 \\ b_n & b_{n-1} & . & . & . & b_0 & 0 & 0 & 0 \\ 0 & b_n & b_{n-1} & . & . & b_1 & b_0 & 0 & 0 \\ . & . & . & . & . & . & . & . & . \\ . & . & . & . & . & . & . & b_1 & b_0 \end{vmatrix}.$$

REFERENCES

[1] H.K. Khalil, *Nonlinear Systems*, 3rd Edition, Prentice-Hall, 2000.

[2] J.J. Slotine, W. Li, *Applied Nonlinear Control*, Prentice-Hall, 1991.

[3] W.S. Levine (Editor*), Control Handbook,* vol. 1-3, CRC Press, 2011.

[4] Guyton A. C., Hall J. E., *Textbook of Medical Physiology*, 11th Edition, Elsevier Saunders, 2006.

[5] S. Silbernagl, A. Despopoulos, *Color Atlas of Physiology*, Thieme; 6th Edition, 2008.

[6] R.M. Murray, *Control in an Information Rich World*, Report of the Panel on Future Directions in Control, Dynamics and Systems, SIAM, 2003.

[7] T. Samad and A.M. Annaswamy (eds.), *The Impact of Control Technology*, IEEE Control Systems Society, 2011, available online at: www.ieeecss.org."

[8] Berne R. M., Levy M. N., *Physiology*, C. V. Mosby, 2003.

[9] A Vision and Strategy for the VPH in 2010 and beyond, VPH Vision & Strategy, 2009, available online at: http://www.vph-institute.org/upload/vph-vision-strategy-submitted-141209-4_519244d49f91e.pdf .

[10] P.J. Hunter, "The IUPS Physiome Project: a framework for computational physiology", *Progress in Biophysics and Molecular Biology*, vol. 85, no. 2–3, June–July 2004, pp. 551–569.

[11] Khoo M. C.K., Physiological Control Systems: Analysis, Simulation, and Estimation, IEEE Press Series on Biomedical Engineering, 1999.

[12] Houk J.C., Control Strategies in physiological systems, The FASEB Journal, vol. 2, pp. 97-107, 1988.

[13] Pota A., Rienzo M.D., Wessel N., Kurths J., "Addressing the complexity of cardiovascular regulation", *Phil. Trans. R. Soc. A* 367, pp. 1215-1218, 2009.

[14] S.Y. Nof (Ed.), *Springer Handbook of Automation*, Springer-Verlag, 2009.

[15] T. Kailath, *Linear Systems,* Prentice Hall, 1980.

[16] T.-L. Dragomir, *Elemente de teoria sistemelor* (in Romanian), vol. I, Politehnica Publishing House, Timisoara, 2004.

[17] **A. Codrean**, "Modeling Physiological Control Mechanisms", *Bachelor Thesis*, Politehnica University of Timisioara, 2010.

[18] H. Kalmus (Ed*), Regulation and Control in Living Systems*, John Wiley & Sons, 1966.

[19] MATLAB version 7.14.0. Natick, Massachusetts: The MathWorks Inc., 2012.

[20] Maple version 15.01. Waterloo, Ontario: Maplesoft, a division of Waterloo Maple Inc., 2011.

[21] F.S. Grodins, *Control Theory and Biological Systems*. Columbia University Press, New York, 1963.

[22] V. Fuster and B.B. Kelly (Editors), Promoting Cardiovascular Health in the Developing World: A Critical Challenge to Achieve Global Health, The National Academies Press, Washington D.C., 2010.

[23] J.D. Bronzio (Ed.), *Biomedical Engineering Fundamentals*, 4th Edition, CRC Press, 2006.

[24] Y. Wu, P.E. Allaire, G. Tao, D. Olsen, „Modeling, Estimation, and Control of Human Circulatory System With a Left Ventricular Assist Device," *IEEE Trans. On Control Systems Technology*, vol. 15, no. 4, 2007, pp. 754-767.

[25] P. Valigi, „Parameter estimation based on a switched observer for the study of left ventricle contractility," *16th IFAC World Congress*, Prague, 2005, pp. 272-277.

[26] F. D. Ledezma, T. M. Laleg-Kirati, „Detection of Cardiovascular Anomalies: Hybrid Systems Approach," *4th IFAC Conference on Analysis and Design of Hybrid Systems*, Eindhoven, 2012, pp. 222-227.

[27] M.A. Simaan, A. Ferreira, S. Chen, J.F. Antaki, and D.G. Galati, "A Dynamical State Space Representation and Performance Analysis of a Feedback-Controlled Rotary Left Ventricular Assist Device*", IEEE Transactions on Control System Technology*, vol. 17, no. 1, pp. 15-28, 2009.

[28] U. an der Heiden, "Delays in Physiological Systems," *Journal of Mathematical Biology*, vol. 8, pp. 345-364, 1979.

[29] L. Glass, A. Beuter, D. Larocque, "Time Delays, Oscillations, and Chaos in Physiological Control Systems," *Mathematical Biosciences*, vol. 90, pp. 111-125, 1988.

[30] P. Ataee, J.-O. Hahn, G. A. Dumont, W. Thomas Boyce, „A Systematic Approach to Local Stability Analysis of Cardiovascular Baroreflex," *33rd Annual International Conference of the IEEE EMBS*, Boston, 2011, pp. 700-703.

[31] J. T. Ottesen, „Modelling of the baroreflex-feedback mechanism with time-delay," *Journal of Mathematical Biology*, vol. 36, 1997, pp. 41-63.

[32] J.J. Batzel, F. Kappel, "Time delay in physiological systems: Analyzing and modeling its impact," *Mathematical Biosciences*, vol. 234, pp. 61–74, 2011.

[33] G. D. Baura, System Theory and Practical Applications of Biomedical Signals, Wiley-IEEE Press, 2002.

[34] T. Heldt and G. C. Verghese, "Model-Based Data Integration in Clinical Environments," *32nd Annual International Conference of the IEEE EMBS*, Buenos Aires, Argentina, 2010, pp. 5209-5212.

[35] L. Gaohua and H. Kimura, A Control-Theoretical Approach to Model-Based Medicine, *17th World Congress The International Federation of Automatic Control*, Seoul, Korea, 2008, pp. 10810-10821.

[36] L. Kovács, "New principles and adequate control methods for insulin dosage in case of diabetes", *PhD Thesis* (in Hungarian), Budapest University of Technology and Economics, 2008.

[37] National Academy of Engineering, *Grand Challenges for Engineering*, 2008, available online at: http://www.engineeringchallanges.org/.

[38] R.A. Rhoades, G.A. Tanner, *Medical Physiology*, ch. 18, 2nd Edition, Lippincott Williams & Wilkins, 2003.

[39] M. Ursino, „Interaction between carotid baroregulation and the pulsating heart: a mathematical model," *Am. J. Physiol. Heart Circ. Physiol.*, vol. 275, 1998, pp. 1733-1747.

[40] P.H. Gordon, A.J. Wilbourn, "Early Electrodiagnostic Findings in Guillain-Barré Syndrome", *Archives of Neurology*, vol. 58, no. 6, pp. 913-917, 2001.

[41] R. Freeman,"Autonomic peripheral neuropathy," *The Lancet*, vol. 365, no. 9466, pp. 1259-1270, 2005.

[42] G. Said, "Diabetic neuropathy—a review", *Nature Clinical Practice Neurology*, vol. 3, pp. 331-340, 2007.

[43] E.-K. Boukas, Z.-K. Liu, *Deterministic and Stochastic Time Delay Systems*, Birkhauser, 2002.

[44] R. Sipahi, S.I. Niculescu, C.T. Abdallah, W. Michiels, and K. Gu, "Stability and Stabilization of Systems with Time Delay", *IEEE Control Systems Magazine*, pp. 38-65, 2011.

[45] J.P. Richard, "Time-delay systems: an overview of some recent advances and open problems", *Automatica*, vol. 39, pp. 1667-1694, 2003.

[46] S.I. Niculescu, *Delay Effects on Stability*, Springer-Verlag, 2001.

[47] Y. He, Q.-G. Wang, C. Lin, M. Wu, "Delay-range-dependent stability for systems with time-varying delay", *Automatica*, vol. 43, pp. 371–376, 2007.

[48] R Sipahi, II Delice, "Advanced clustering with frequency sweeping methodology for the stability analysis of multiple time-delay systems", *IEEE Transactions on Automatic Control*, vol. 56, no. 2, pp. 467-472, 2011.

[49] A. Papachristodoulou, M.M. Peet, and S. Lall, "Analysis of Polynomial Systems With Time Delays via the Sum of Squares Decomposition", *IEEE Transactions On Automatic Control*, vol. 54, no. 5, pp. 1058-1064, 2009.

[50] A. Papachristodoulou and S. Prajna, "On the construction of Lyapunov functions using the sum of squares decomposition," *IEEE Conference on Decision and Control*, pp. 3482–3487, 2002.

[51] W.E. Dixon, A. Behal, D.M. Dawson, S.P. Nagarkatti, *Nonlinear Control of Engineering Systems: A Lyapunov-Based Approach*, Birkhauser, 2003.

[52] R. Shorten, F. Wirth, O. Mason, K. Wulff, and C. King, "Stability Criteria for Switched and Hybrid Systems", SIAM Review, vol. 49, no. 4, pp. 545–592, 2007.

[53] D. Liberzon, *Switching in Systems and Control*, Birkhauser, 2003.

[54] S. Boyd, L.E. Ghaoui, E. Feron, and V. Balakrishnan, *Linear Matrix Inequalities in Systems and Control Theory*, SIAM, 1994.

[55] **A. Codrean**, A. Korodi, T.-L. Dragomir, and L. Kovács, "Up to Date Issues on Modeling the Nervous Control of the Cardiovascular System on Short-Term," in *Proc. of 18th IFAC World Congress*, Milano, 2011, pp. 3747- 3752.

[56] G.D. Thomas, "Neural control of circulation," *Advances in Physiology Education*, vol. 35, pp. 28-32, 2011.

[57] T. Heldt, "Computational models of Cardiovascular Response to Orthostatic Stress," *Ph.D. Thesis,* M.I.T, 2004.

[58] M.S. Olufsen, H.T. Tran, J.H. Ottesen, L.A. Lipsitz, and V. Novak, "Modeling baroreflex regulation of heart rate during orthostatic stress," *Am. J. Physiol. Regul. Integr. Comp. Physiol.*, vol. 291, pp. 1355-1368, 2006.

[59] V. Le Rolle, A.I. Hernandez, P.-Y. Richard, and G. Carrault, "An Autonomic Nervous System Model Applied to the Analysis of Orthostatic Tests," *Modeling and Simulation in Engineering*, vol. 2008, Art. ID 427926.

[60] J.J. Batzel, F. Kappel, D. Schneditz, and H.T. Tran, *Cardiovascular and Respiratory Systems: Modeling, Analysis, and Control*. Philadelphia: SIAM, 2007.

[61] T. Heldt, J.L. Chang, J.J.S. Chen, G.C. Verghese, and R.G. Mark, "Cycle-averaged dynamics of a periodically driven, closed-loop circulation model," *Control Engineering Practice,* Vol. 13, pp. 1163-1171, 2005.

[62] T.A. Parlikar, T. Heldt, and G.C. Verghese, "Cycle-Averaged Models of Cardiovascular Dynamics," *IEEE Transactions on Circuits and Systems I,* Vol. 53, No. 11, pp. 2459-2468, 2006.

[63] P.T. Krein, J. Bentsman, R. Bass, and B. Lesieutre, "On the Use of Averaging for the Analysis of Power Electronic Systems," *IEEE Transactions on Power Electronics*, vol. 5, no. 2, pp. 182-190, 1990.

[64] V. Caliskan, G.C. Verghese, and A.M. Stankovic, "Multifrequency Averaging of DC/DC Converters*," IEEE Transactions on Power Electronics*, vol. 14, no. 1, pp. 124-133, 1999.

[65] R.W. Erickson and D. Maksimovic, *Fundamentals of Power Electronics*. New York: Springer, 2001, ch. 7.

[66] L. Iannelli, K.H. Johansson, U.T. Jonsson, and F. Vasca, "Averaging of nonsmooth systems using dither," *Automatica*, vol. 42, pp. 669-676, 2006.

[67] A. Gelb, W.E. Vander Velde, *Multiple-input describing functions and nonlinear system design*. McGraw-Hill, 1968, ch. 6.

[68] C. Pedicini, F. Vasca, L. Iannelli, and U. Jonsson, "An Overview on Averaging for Pulse-modulated Switched Systems," in Proc. of *50th IEEE Conference on*

Decision and Control and European Control Conference, Orlando, 2011, pp. 1860-1865.

[69] B. Sedghi, Control design of hybrid systems via dehybridization, *Ph.D. dissertation*, École Polytechnique Federale de Lausanne, 2003.

[70] A.K. Gelig, A.N. Churilov, *Stability and Oscillations of Nonlinear Pulse-Modulated Systems*, Birkhauser, Boston, 1998.

[71] M. A. Simaan, "Rotary Heart Assist Devices," in *Springer Handbook of Automation*, Ed. S.Y. Nof, Part H, pp. 1409-1422, Springer Berlin Heidelberg, 2009.

[72] F.D. Ledezma and T.M. Laleg-Kirati, "Detection of Cardiovascular Anomalies: Hybrid Systems Approach," in Proc. of *4th IFAC Conference on Analysis and Design of Hybrid Systems*, Eindhoven, 2012, pp. 222-227.

[73] R.W. Jones, C.C. Li, A.U. Meyer, and R.B. Pinter, "Pulse Modulation in Physiological Systems, Phenomenological Aspects," *IRE Transactions in Bio-Medical Electronics*, vol. 8, no. 1, pp. 59-67, 1961.

[74] **A. Codrean**, T.-L. Dragomir, "Averaged modeling of the cardiovascular system", IEEE 52nd Annual Conference on Decision and Control (CDC), Florence, Italy, 2013, pp. 2066-2071.

[75] Y. Wu, P.E. Allaire, G. Tao, and D. Olsen, "Modeling, Estimation, and Control of Human Circulatory System with a Left Ventricular Assist Device," *IEEE Transactions on Control Systems Technology*, vol. 15, no. 4, pp. 754-767, 2007.

[76] J.T. Ottesen, M. Danielsen, "Modeling ventricular contraction with heart rate changes," *Journal of Theoretical Biology*, Vol. 222, pp. 337-346, 2003.

[77] W.C. Rose, and J.S. Schwaber, "Analysis of heart rate-based control of arterial pressure," *Am. J. Physiol. Heart Circ. Physiol.*, Vol. 271, pp. H812-H822, 1996.

[78] T.A. Parlikar, "Modeling and Monitoring of Cardiovascular Dynamics for Patients in Critical Care," *Ph.D. Thesis,* M.I.T, 2007.

[79] S.H. Chen, "Baroreflex-based physiological control of a left ventricular assist device", *Ph.D. Thesis,* University of Pittsburgh, 2006.

[80] J. Ringwood, F. Taussi, and A.M. de Paor, "The effect of pulsatile blood flow on blood pressure regulatory mechanisms," in Proc. of *IEEE International Conference on Control Applications*, Dubrovnik, 2012, pp. 609-614.

[81] Ya.Z. Tsypkin, *Relay Control Systems*, Cambridge University Press, 1984.

[82] R.V. Monopoli, and J.F. Fitzgerald, "A describing function analysis in closed loop systems with pulse frequency modulators," *Southwest IEEE Conference*, Houston, Texas, 1967.

[83] H.C. Lee, "Integral Pulse Frequency Modulation with Technological and Biological Applications," *Ph.D. Thesis*, McGill University, Montreal, 1969.

[84] T. Pavlidis, and E.I. Jury, "Analysis of a New Class of Pulse-Frequency Modulated Feedback Systems," *IEEE Transactions on Automatic Control*, vol. 10, no. 1, pp. 35-43, 1965.

[85] T. Todo, K. Selvaratnam, T. Mori, and Y. Kuroe, "Analysis of hybrid feedback systems with PFM mechanisms," *IEE Proc.-Control Theory Appl.*, vol. 146, no. 3, 1999.

[86] M. Ursino, and E. Magosso, "Role of short-term cardiovascular regulation in heart period variability: a modeling study," *Am. J. Physiol. Heart Circ. Physiol.*, Vol. 284, pp. 1479-1493, 2003.

[87] M. Ursino, "A Mathematical Model of the Carotid Baroregulation in Pulsating Conditions," *IEEE Transactions on Biomedical Engineering*, vol. 46, no. 4, 1999, pp. 382-392.

[88] M. Ursino, "Role of active changes in venous capacity by the carotid baroreflex: analysis with a mathematical mode," *American Journal of Physiology Heart and Circulatory Physiology*, Vol. 267, No. 6, 1994, pp. 2531-2546.

[89] E. Magosso, V. Biavati and M. Ursino, "Role of the Baroreflex in Cardiovascular Instability: A Modeling Study," *Cardiovascular Engineering*, vol. 1, no. 2, 2001, pp. 101-115.

[90] K. Lu, J. W. Clark Jr., F. H. Ghorbel, D.L. Ware and A. Bidani, "A human cardiopulmonary system model applied to the analysis of the Valsalva maneuver," *American Journal of Physiology Heart and Circulatory Physiology*, Vol. 281, 2001, pp. 2661-2679.

[91] J.C. West, *Analytical techniques for non-linear control systems,* London: The English Universities Press, 1960.

[92] M.S. Olufsen, A.V. Alston, H.T. Tran, J.T. Ottesen, and V. Novak, "Modeling Heart Rate Regulation – Part I: Sit-to-stand Versus Head-up Tilt," *Cardiovascular Engineering*, vol. 8, pp. 73-87, 2008.

[91] C. Pedicini, L. Iannelli, F. Vasca, and U. Jönsson, "Averaging for Power Converters", in F. Vasca and L. Iannelli (Eds.), *Dynamics and Control of Switched Electronic Systems*, ch. 5, Springer-Verlag, 2012.

[92] X. Shen, J. Zhang, "Nonlinear Model-Based Control of Pulse Width Modulated Pneumatic Servos Systems", *Journal of Dynamic Systems, Measurements, and Control,* vol. 128, pp. 663-669, 2006.

[93] H. Sira-Ramirez, M. Zribi, and S. Ahmad, "Pulse width modulated control of robotic manipulators", International Journal of Systems Science, vol. 24 no. 8, pp. 1423-1437, 1993.

[94] S. Sastry and M. Bodson, *Adaptive Control: Stability, Convergence and Robustness*, ch. 4, Dover Publications, 2011.

[95] R.M. Bass, J. Sun, "Large-Signal Averaging Methods under Large Ripple Conditions", *29th Annual IEEE Power Electronics Specialists Conference*, pp. 630-632, 1998.

[96] S.J. Moura and Y.A. Chang, "Lyapunov-based switched extremum seeking for pothovoltaic power maximization", *Control Engineering Practice*, vol. 21, pp. 971-980, 2013.

[97] D.J. Stilwell, E.M. Bollt, and D.G. Roberson, "Sufficient conditions for fast switching synchronization in time-varying network topologies", *SIAM Journal on Applied Dynamical Systems*, vol. 5, pp. 140-156, 2006.

[98] M. Porfiri, D.G. Roberson, and D.J. Stilwell, "Tracking and formation control of multiple autonomous agents: a two level consensus approach", Automatica, vol. 43, no. 8, pp. 1318-1328, 2007.

[99] R. Marquez, E. Altman, and S. Solé-Álvarez, "Time-averaging of high-speed data transfer protocol", *IEEE Transactions on Automatic Control*, vol. 50, no. 12, pp. 2065-2069, 2005.

[100] S. Almér, S. Mariéthoz, and M. Morari, "Robust tracking control of pulse-width modulated systems through multi-frequency averaging", *American Control Conference*, Montreal, pp. 4558-4563, 2012.

[101] L. Iannelli, K. H. Johansson, U.T. Jönsson, F. Vasca, "Subtleties in the averaging of a class of hybrid systems with applications to power converters", *Control Engineering Practice*, vol. 16, pp. 961-975, 2008.

[102] W. Wang and D. Nešić, "Input-to-state Stability and Averaging of Linear Fast Switching Systems", *IEEE Transactions on Automatic Control*, vol. 55, no. 5, pp. 1274-1279, 2010.

[103] W. Wang, A. R. Teel, and D. Nešić, "Analysis for a class of singularly perturbed hybrid systems via averaging", *Automatica*, vol. 48, pp. 1057-1068, 2012.

[104] A. Kh. Gelig and A. N. Churilov, "Frequency Methods in the Theory of Pulse-Modulated Control Systems", *Automation and Remote Control*, vol. 67, no. 11, pp. 1752-1767, 2006.

[105] **A. Codrean**, T.-L. Dragomir, "Period dependent averaging of a class of pulse modulated systems. Application to the cardiovascular system", *Journal of Control Engineering an Applied Informatics*, vol. 17, no. 1, pp. 91-98, 2015.

[106] J. A. Richards, *Analysis of Periodically Time-Varying Systems*, Springer-Verlag, 1983.

[107] C. Gökçek, "Stability analysis of periodically switched linear systems using Floquet theory", *Mathematical Problems in Engineering*, vol. 1, pp. 1-10, 2004.

[108] B. Lehman and R. M. Bass, "Switching Frequency Dependent Averaged Models for PWM DC-DC Converters.", *IEEE Transactions on Power Electronics*, vol. 11, no. 1, pp. 89-98, 1996.

[109] L. Farina and S. Rinaldi, *Positive Linear Systems*, ch. 5. John Wiley & Sons, 2000.

[110] S. Cavalcanti and E. Belardinelli, "Modeling of Cardiovascular Variability Using a Differential Delay Equation", *IEEE Transactions on Biomedical Engineering*, vol. 43, no. 10, 1, pp. 982-989,1996.

[111] K. Gu , V. L. Kharitonov, J. Chen, *Stability of Time-Delay Systems*, Birkhäuser, 2003.

[112] M.S. Lee and C.S. Hsu, "On the τ-decomposition method of stability analysis for retarted dynamical systems," *SIAM Journal of Control*, vol. 7, no.2, pp. 242-259, 1969.

[113] Z.V. Rekasius, "A stability test for systems with delays," *Proc. Joint Automatic Control Conference*, San Francisco, 1980.

[114] I.M. Gelfand, M.M. Kapranov, and A.V. Zelevinsky, *Discriminants, Resultants, and Multidimensional Determinants*, Birkhauser, 1994.

[115] R. Sipahi, N. Olgac, "Complete Stability Robustness of Third-order LTI Multiple Time-Delay Systems", *Automatica*, vol. 41, no. 8, pp. 1413-1422, 2005.

[116] Z. Wu, W. Michiels, "Reliably computing all characteristic roots of delay differential equations in a given right half plane using a spectral method", *Journal of Computational and Applied Mathematics*, vol. 236, no. 9, 2012, pp. 2499–2514.

[117] S.I. Niculescu, P.S. Kim, K. Gu, P.P. Lee, D. Levy, "Stability crossing boundaries of delays systems modeling immune dynamics in leukemia," *Discrete and continuous dynamical systems Series B*, vol. 13, no. 1, 2010, pp. 129-156.

[118] W. Lohmiller and J.J. Slotine, "On contraction analysis for non-linear systems," *Automatica*, vol. 34, no. 6, 1998, pp. 683-696.

[119] F. Forni and R. Sepulchre, "A Differential Lyapunov Framework for Contraction Analysis," *IEEE Transaction on Automatic Control*, vol. 59, no. 3, pp. 614-628, 2014.

[120] A. Pavlov, A. Pogromsky, N. van de Wouw, H. Nijmeijer, "Convergent dynamics, a tribute to Boris Pavlovich," *Systems & Control Letters*, vol. 52, pp. 257-261, 2004.

[121] A. Chaillet, D. Angeli, H. Ito, "Combining iISS and ISS With Respect to Small Inputs: The Strong iISS Property," *," IEEE Transactions on Automatic Control*, vol. 59, no. 9, pp. 2518-2524, 2014.

[122] B.S. Rüffer, N. van de Wouw, M. Mueller, "Convergent systems vs. incremental stability*," Systems & Control Letters*, vol. 62, pp. 277-285, 2013.

[123] D. Angeli, "A Lyapunov Approach to Incremental Stability Properties," *IEEE Transactions on Automatic Control*, vol. 47, no. 3, pp. 410-421, 2002.

[124] I.R. Manchester, J.J. Slotine, "Transverse contraction criteria for existence, stability, and robustness of a limit cycle," *Systems & Control Letters*, vol. 63, pp. 32-38, 2014.

[125] E.M. Aylward, P.A. Parrilo, J.J. Slotine, "Stability and robustness analysis of nonlinear systems via contraction metrics and SOS programming," *Automatica*, vol. 44, no. 8, pp. 2163–2170, 2008.

[126] S Prajna, A. Papachristodoulou, P. Seiler, P.A. Parrilo, *Sum of Squares Optimization Toolbox for MATLAB–User's Guide*. Online: www.cds.caltech.edu/sostools/sostools/pdf.

[127] A Papachristodoulou, S Prajna, "A tutorial on sum of squares techniques for systems analysis," *American Control Conference*, pp. 2686-2700, 2005.

[128] W. Lohmiller, *Contraction Analysis of Nonlinear Systems*, Ph.D. Thesis, Massachusetts Institute of Technology, 1999.

[129] I.I. Delice and R. Sipahi, "Delay-Independent Stability Test for Systems With Multiple Time-Delays," *IEEE Transactions on Automatic Control*, vol. 57, no. 4, pp. 963-972, 2012.

[130] **A. Codrean**, T.-L. Dragomir, "Delay effect on cardiovascular regulation - a systems analysis approach", *European Control Conference*, Linz, Austria, 2015, in press.

[131] **A. Codrean**, T.-L. Dragomir, "Stability analysis of cardiovascular regulation", *23rd Mediterranean Conference on Control and Automation*, Torremolinos, Spain, 2015, accepted.